MISCELLANEOUS PAPER M-76-17

PERFORMANCE OF TOWED WHEELS OPERATING IN TURNED MODE ON SOFT SOILS--A PILOT STUDY

by

Klaus-J. Melzer

Mobility and Environmental Systems Laboratory
U. S. Army Engineer Waterways Experiment Station
P. O. Box 631, Vicksburg, Miss. 39180

August 1976
Final Report

Prepared for U. S. Army Materiel Development and Readiness Command
Alexandria, Virginia 22333

Under Project 1T062103A046, Task 03

Destroy this report when no longer needed. Do not return
it to the originator.

Unclassified

SECURITY CLASSIFICATION OF THIS PAGE (When Data Entered)

REPORT DOCUMENTATION PAGE

READ INSTRUCTIONS BEFORE COMPLETING FORM

1. REPORT NUMBER: Miscellaneous Paper M-76-17

2. GOVT ACCESSION NO.

3. RECIPIENT'S CATALOG NUMBER

4. TITLE (and Subtitle): PERFORMANCE OF TOWED WHEELS OPERATING IN TURNED MODE ON SOFT SOILS--A PILOT STUDY.

5. TYPE OF REPORT & PERIOD COVERED: Final report.

6. PERFORMING ORG. REPORT NUMBER

7. AUTHOR(s): Klaus-J. Melzer

8. CONTRACT OR GRANT NUMBER(s): WES-MP-M-76-17

9. PERFORMING ORGANIZATION NAME AND ADDRESS
U. S. Army Engineer Waterways Experiment Station
Mobility and Environmental Systems Laboratory
P. O. Box 631, Vicksburg, Miss. 39180

10. PROGRAM ELEMENT, PROJECT, TASK AREA & WORK UNIT NUMBERS
Project 1T062103A046
Task 03

11. CONTROLLING OFFICE NAME AND ADDRESS
U. S. Army Materiel Development and Readiness Command
Alexandria, Virginia 22333

12. REPORT DATE: August 1976

13. NUMBER OF PAGES: 94

98 p.

14. MONITORING AGENCY NAME & ADDRESS(if different from Controlling Office)

DA-1-T-062103-A-046

15. SECURITY CLASS. (of this report): Unclassified

15a. DECLASSIFICATION/DOWNGRADING SCHEDULE

16. DISTRIBUTION STATEMENT (of this Report)

Approved for public release; distribution unlimited.

1-T-062103-A-04603

17. DISTRIBUTION STATEMENT (of the abstract entered in Block 20, if different from Report)

18. SUPPLEMENTARY NOTES

19. KEY WORDS (Continue on reverse side if necessary and identify by block number)

Clays	Towed wheels
One-pass performance	Traffic tests
Pneumatic tires	Wheels
Sands	

20. ABSTRACT (Continue on reverse side if necessary and identify by block number)

The performance of single, pneumatic-tired, towed wheels operating in turned mode was investigated in a pilot study. Ninety-nine one-pass tests were conducted in the laboratory on one clay and two air-dry sands with 8.50-10, 7.00-6, and 6.00-9 tires. Turn angles were 0, 5, 10, 15, and 20 deg; wheel loads were varied from about 1000 to 7000 N; and tire deflections were 0.15, 0.25, 0.35, and 0.40 of the undeflected tire section heights. Clay consistencies ranged from soft to medium stiff, with corresponding cone penetration

(Continued)

next page

DD FORM 1 JAN 73 1473 EDITION OF 1 NOV 65 IS OBSOLETE

Unclassified

SECURITY CLASSIFICATION OF THIS PAGE (When Data Entered)

038100

20. ABSTRACT (Continued).

resistances between 255 and 543 kPa. Relative densities of the sands ranged from medium dense to very dense, with corresponding cone penetration resistance gradients ranging from 0.7 to 4.6 MPa/m.

Performance expressed in terms of towed force coefficient, side force coefficient, resultant coefficient, lateral force/drag, sinkage coefficient, and slip is influenced by the following independent variables: turn angle, soil strength, tire deflection, wheel load, and the product of tire width and diameter. Trail moment and eccentricity of the resultant are influenced more or less similarly.

For the ranges of the variables tested, the U. S. Army Engineer Waterways Experiment Station system of dimensionless parameters for predicting performance of towed wheels operating at zero turn angle on clay and on sand is extended to treat turn angles larger than zero. For this purpose, turn angle and mobility numbers for sand and clay, combined with additional independent dimensionless variables, are correlated with the aforementioned six performance parameters. For clay, towed force coefficient (P_T/W) decreases with increasing clay mobility number (N_c), but does not show a very well defined dependency on turn angle (α). In sand, P_T/W decreases with increasing sand mobility number (N_s); but for a given N_s, P_T/W increases with increasing α. Side force coefficient (S/W) for clay and sand increases with increasing mobility number for a given α and also with α if the mobility number is constant. Resultant coefficient (R/W) and lateral force/drag (S'/P_T') follow either the trend of P_T/W or of S/W, depending on which of the two latter parameters has the dominant influence. Sinkage coefficient (z_T/d) and slip for clay and for sand follow the same trend as for P_T/W in sand.

THE CONTENTS OF THIS REPORT ARE NOT TO BE USED FOR ADVERTISING, PUBLICATION, OR PROMOTIONAL PURPOSES. CITATION OF TRADE NAMES DOES NOT CONSTITUTE AN OFFICIAL ENDORSEMENT OR APPROVAL OF THE USE OF SUCH COMMERCIAL PRODUCTS.

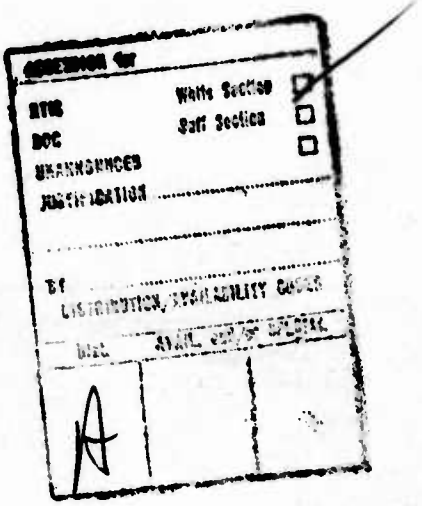

PREFACE

The study reported herein was conducted in 1973 as part of the U. S. Army Engineer Waterways Experiment Station (WES) vehicle mobility research program under former DA Project 1T062103A046, "Trafficability and Mobility Research," Task 03, "Mobility Fundamentals and Model Studies," under the sponsorship and guidance of the Research, Development and Engineering Directorate, U. S. Army Materiel Command.*

The tests were performed by personnel of the Mobility Investigations Branch, Mobility Systems Division (MSD), Mobility and Environmental Systems Laboratory (MESL), WES, under the general supervision of Messrs. W. G. Shockley, Chief, MESL; A. A. Rula, Chief, MSD; and C. J. Nuttall, Jr., Chief, Mobility Research and Methodology Branch (MRMB), MSD; and under the direct supervision of Dr. K.-J. Melzer, formerly of MRMB, who also prepared this report.

BG E. D. Peixotto, CE, COL G. H. Hilt, CE, and COL J. L. Cannon, CE, were Directors of the WES during the conduct of this study and preparation and publication of the report. Mr. F. R. Brown was Technical Director.

---

* Now designated the U. S. Army Materiel Development and Readiness Command.

CONTENTS

CONVERSION FACTORS, METRIC (SI) TO U. S. CUSTOMARY AND U. S. CUSTOMARY TO METRIC (SI) UNITS OF MEASUREMENT

Units of measurement used in this report can be converted as follows:

Multiply	By	To Obtain
	Metric (SI) to U. S. Customary	
millimetres	0.03937007	inches
centimetres	0.3937007	inches
metres	3.280839	feet
square centimetres	0.1550	square inches
newtons	0.2248089	pounds (force)
newtons per square centimetre	1.450377	pounds (force) per square inch
kilopascals	0.1450377	pounds (force) per square inch
megapascals per metre	3.684598	pounds (force) per cubic inch
metres per second	3.280839	feet per second
metre-newtons	0.7375621	foot-pounds
	U. S. Customary to Metric (SI)	
inches	25.4	millimetres
degrees (angular)	0.01745329	radians

PERFORMANCE OF TOWED WHEELS OPERATING IN TURNED MODE ON SOFT SOILS--A PILOT STUDY

PART I: INTRODUCTION

Background

1. In recent years, the U. S. Army Tank-Automotive Command, the U. S. Army Engineer Waterways Experiment Station (WES), and the U. S. Army Cold Regions Research and Engineering Laboratory, under the auspices of the U. S. Army Materiel Command (AMC), undertook the task of developing, from existing research and engineering knowledge of terrain-vehicle-man interactions, a comprehensive, computerized simulation of a vehicle moving across terrain. A major result of this joint effort is a comprehensive model for the prediction of ground vehicle mobility. The first generation of this model, known as the AMC Mobility Model (AMC-71), was completed in 1971 and published in 1973.[1]

2. The main output of the mobility model is maximum feasible straight-line vehicle speed as limited by one or a combination of the following factors:

a. Traction available to overcome the combined resistances of soil, slope, obstacles, and vegetation.

b. Driver discomfort in negotiating rough terrain (ride comfort) and his tolerance to vegetation and obstacle impacts.

c. Driver reluctance to proceed faster than the speed at which the vehicle could decelerate to a stop within the, possibly limited, visibility distance prevailing in the areal unit (braking-visibility limit).

d. Maneuvering to avoid trees or obstacles.

e. Acceleration and deceleration between obstacles if they are to be overridden.

f. Traction, interference, or swimming problems during vehicular crossing of significant linear features, such as rivers or embankments, that limit vehicle-terrain-driver interactions to determine the maximum feasible speed in a suitably quantified terrain situation.

3. The model has already proven useful in important studies whose objectives were, to name a few, the evaluation of concepts for a new main battle tank, the assessment of the off-road/on-road performance of a group of standard and modified wheeled vehicles, and the mobility performance of a wide range of towed and self-propelled artillery. These successful applications have led to requirements for still broader predictive capabilities, some of which were perceived even before the first-generation model was completed. In particular, potential need was identified for reliable engineering bases to predict performance limits for vehicles maneuvering in off-road terrain, as might be required in combat. The maneuvering submodel incorporated in AMC-71 is a simple empirical relation that does not address the problem in fundamental engineering terms. One important limit to vehicle maneuvering capability in off-road terrain derives from the steering forces that the vehicle running gear can generate in soils. In response to this perceived need, a pilot laboratory study was initiated to examine the performance in soils of simple, pneumatic-tired wheels operating in the turned mode. These forces influence not only the stability of the vehicle but also its power requirements and ability to develop net traction for slope negotiation.

4. Extensive research has been performed, especially in the automotive industry, in evaluating the side or cornering forces acting on free-rolling pneumatic tires operating in turned mode on unyielding surfaces,[2-5] and test procedures are being standardized.[6] Also, test devices for braked or driven wheels have been designed for hard-surface conditions; however, most of these have been fitted to stationary test drums,[7-9] and only a few have been built to use on the road.[9] Although the necessity for studying the influence of side forces on a wheel operating in soft soil has been emphasized often,[10] relatively few cases have been reported, and these are related mainly to towed wheels.[11-15] To be especially noted is the systematic research conducted at the Technical University of Munich, which essentially contributed to the clarification of the principles involved, first with regard to towed wheels equipped with pneumatic tires,[11,13] and later with regard to powered

wheels.[16] These efforts were limited, however, to a few special tire sizes and primarily to one specific soil type that exhibited, at most, two strength levels. The pilot program initiated at the WES was to study the performance of towed and powered wheels equipped with pneumatic tires of various sizes operating in turned mode on fine- and coarse-grained soils at various strength levels, with a view to developing general relations suitable for use in a comprehensive engineering model for studying total vehicle maneuvering behavior. The results of the first part of the study related to the performance of towed wheels are presented in this report.

Purpose and Scope

5. The purpose of this study was twofold:

   a. To investigate how the performance of single, pneumatic-tired, towed wheels is affected when the wheels are operating in turned mode in fine- and coarse-grained soils.

   b. To determine whether it is possible to describe the performance of the turned wheels in general terms by using techniques that had been developed by dimensional analysis to predict the performance of pneumatic-tired wheels operating in a straight path.[17,18]

6. Ninety-nine one-pass tests were conducted in the laboratory on soft soils with single, towed wheels equipped with 8.50-10, 7.00-6, and 6.00-9 tires and operating at turn angles ranging from 0 to 20 deg.* Wheel loads were varied from approximately 1000 to 7000 N; tire deflections were 0.15, 0.25, 0.35, and 0.40 of the undeflected tire section heights. Performance of the towed wheels was expressed in terms of towed force, side force, resultant force, lateral force/drag, sinkage, and slip. Forty-seven of these tests were conducted on a fat clay with consistencies ranging from soft to medium-stiff, with corresponding cone penetration resistances between 255 and 543 kPa. Fifty-two of the tests were conducted on two medium-dense to very dense air-dry sands, with

---

* A table of factors for converting metric (SI) units of measurement to U. S. customary units, and U. S. customary units to metric (SI) units is presented on page 4.

corresponding cone penetration resistance gradients ranging from 0.7 to 4.6 MPa/m. Forty-four of the 99 tests were conducted in a separate program for the U. S. Air Force,[19] but their results are included in this study.

PART II: RESEARCH RELATED TO THIS STUDY

7. Of the investigations conducted on the performance of towed wheels operating in turned mode, the studies conducted at Munich[13] have resulted in the most advanced state of knowledge. These studies are described briefly herein because they influenced the design of the program at the WES. Also discussed are trends observed during a study conducted by the WES in connection with the Lunar Roving Vehicle (LRV) program.[15] In addition, the WES method developed by dimensional analysis to predict the performance of towed pneumatic-tired wheels operating in a straight path[17,18] will be described briefly.

Tests at the Technical University of Munich

8. Tests were conducted with towed single wheels equipped with various sizes of agricultural tractor tires, using a laboratory dynamometer system. The following parameters were measured: drag P_T' in the direction of travel (Figure 1), lateral force S', sinkage z, and wheel slip s. The following test parameters were controlled: wheel load (1000-4000 N), inflation pressure (100-200 kPa), tire width (11.5-24.3 cm), tire diameter (42.0-113.5 cm), and turn angle (0-28 deg). A sandy loam prepared in a stationary soil bin to a moisture content of 14.5 percent was used. The angle of internal friction was between 30 and 36 deg, and cohesion was reported to be nearly zero. Only this one soil condition was investigated; however, for comparison, one tire was also tested on a concrete surface.

9. Results used in this study were from tests conducted with tires having the same tire deflection (0.16 of the unloaded tire section height*). Performance was expressed mainly in the same terms as those used in interpreting the test results herein (paragraph 33): towed force coefficient (P_T/W), side force coefficient (S/W), resultant

---

* Load-deflection characteristics were obtained from Reference 16.

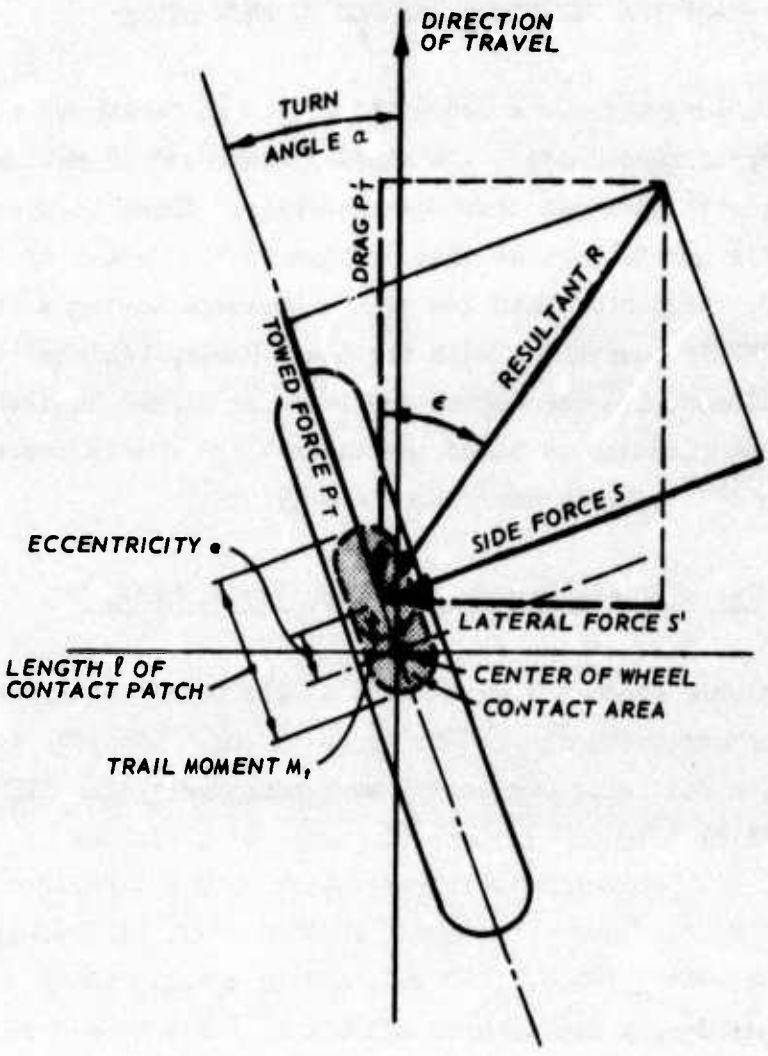

Figure 1. Scheme of forces and moments acting on towed wheel operating in turned mode

coefficient (R/W), and the ratio of lateral force/drag (S'/P'_T)* (Figure 1). It was found that, in addition to the effects of the turn angles on performance of the tires, the following influences could be studied: the type of surface traveled, the width of the tire, and the

---

* To follow the general convention that has been established in this subject area,[14,15,16] the forces acting in the plane of the wheel and perpendicular to it were chosen instead of the forces acting in the direction of travel and perpendicular to it (P_T and S instead of P'_T and S' in Figure 1).

wheel load. The influence of deflection on performance could not be checked because of the way the load-inflation pressure combinations were chosen by the original investigators.

Influence of travel surface and turn angle

10. The following can be concluded, at least qualitatively, concerning the influence of the type of travel surface and turn angle on the performance of the wheels (Figure 2). On an unyielding surface (concrete), the towed force coefficient is more or less independent of the turn angle α (Figure 2a), whereas the side force coefficient increases steeply with turn angle (Figure 2b), reaches a maximum at about $\alpha = 15$ deg, and then decreases again when a transition from adhesive to sliding friction takes place in a continuously increasing portion of the contact area.[13] Because the towed force coefficient is constant, the relation of resultant coefficient to turn angle (Figure 2c) takes the same general shape as that for side force coefficient. The ratio S'/P_T'* shows a similar, but even more pronounced, trend (Figure 2d) with the variation of turn angle, because it is influenced, at least indirectly, by the forces acting in the plane of the wheel (Figure 2a), which are much smaller than the forces acting perpendicular to it (Figure 2b).

11. For the same tire tested under the same conditions, but on sandy loam instead of concrete, the following results are noted. Towed force coefficient increases with increasing turn angle (Figure 2a); rate of increase is larger for turn angles of more than 15 deg than it is for smaller turn angles. The overall increase of towed force coefficient is accompanied by a similar increase in sinkage and slip with increasing turn angle (not shown in Figure 2). Naturally, the towed force coefficients are larger for the compressible sandy loam than for the concrete at a given turn angle.

---

* The ratio S'/P_T' is equivalent to the term "lift/drag" used in aeronautics. It is the tangent of the angle ε (Figure 1) under which the resultant of S and P_T and S' and P_T', respectively, is inclined to the direction of travel.

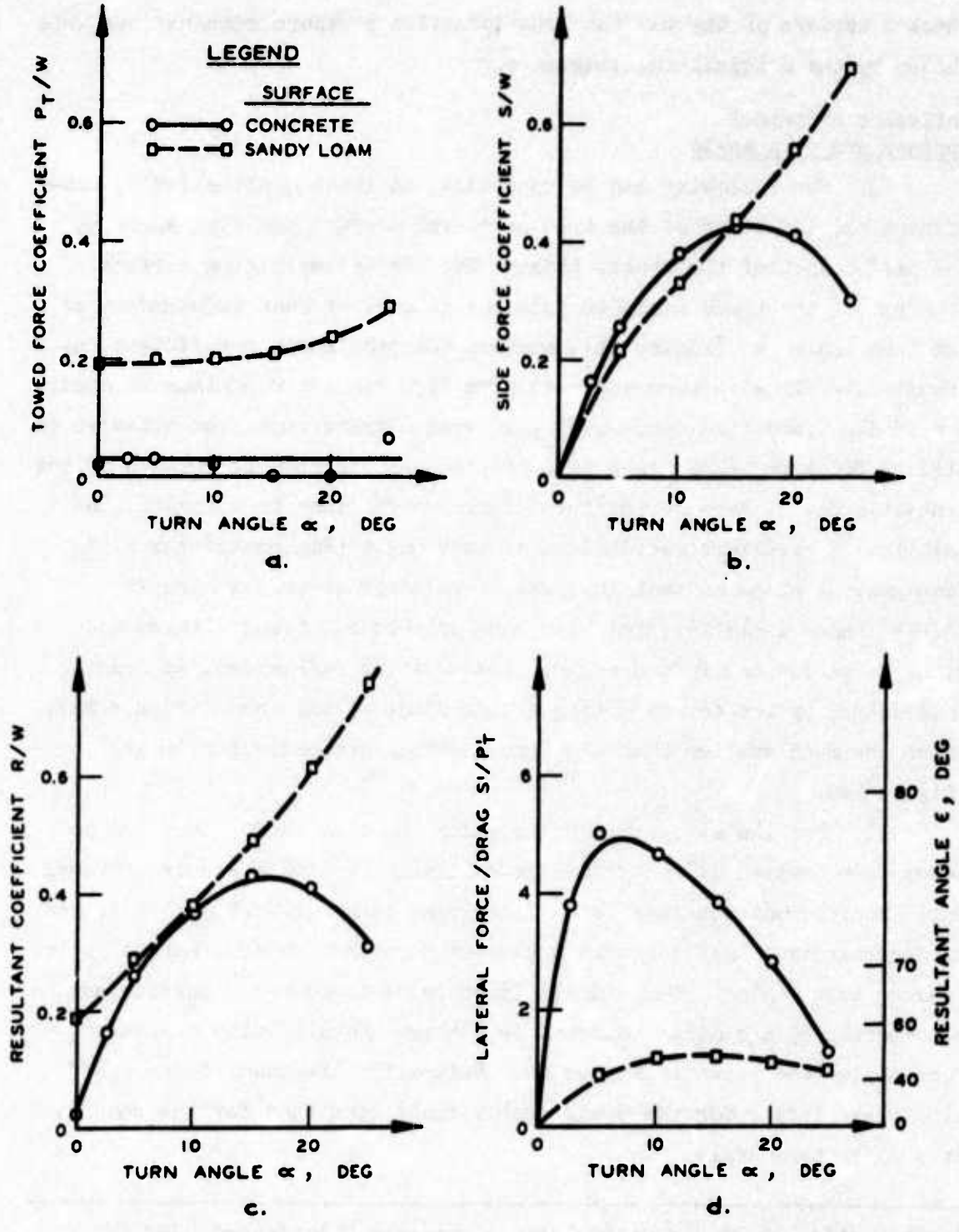

Figure 2. Influence of travel surface and turn angle on performance parameters for 5.50-16 tire with tire deflection $\delta/h = 0.16$ and design wheel load $W' = 3600$ N (from Reference 13)

12. Contrary to the behavior on concrete, side force coefficient for sandy loam does not reach a maximum but increases continuously with increasing turn angle (Figure 2b). This trend occurs not only because of the increase in sinkage with increasing turn angle but also because of the increase in the length of the contact area of the tire (Figure 1) with increasing turn angle and with sinkage. Thus, besides sinkage, contact length determines the magnitude of the side force for a given soil condition, as in a classical earth pressure case. Also, it must be pointed out that for turn angles equal to or smaller than 15 deg, side force coefficient for the compressible material (sandy loam) is smaller than for the concrete, although the difference is not large.

13. The above-mentioned trend does not occur in the relations between resultant coefficients and turn angles (Figure 2c), mainly because the towed force, by far larger in sandy loam than on concrete, contributes greatly to the resultant coefficient, which, in turn, is larger in sandy loam than on concrete at a given turn angle. From this, it is concluded that data of this type should be interpreted first in terms of towed force and side force coefficients before relations in terms of resultant coefficient relations are analyzed. Finally, the relation of lateral force/drag to turn angles for sandy loam does not show the same pronounced maximum as the one for concrete (Figure 2d), indicating that the ratio for the former surface does not change as drastically with turn angles as it does for the latter surface. Also, this relation indicates a larger drag force for sandy loam than for concrete, at a given turn angle, when compared with the lateral force caused by the larger towed force or sinkage.

Influence of tire width and turn angle

14. Two tires of about the same diameter, but different widths, were tested at the same deflection under the same load and on the same soil condition (Figure 3). Differences in towed force coefficients for a given turn angle are small, but the relations (Figure 3a) show an unusual trend. For a given turn angle, the towed force coefficient is larger for the wider tire, which, under these conditions, has the lower

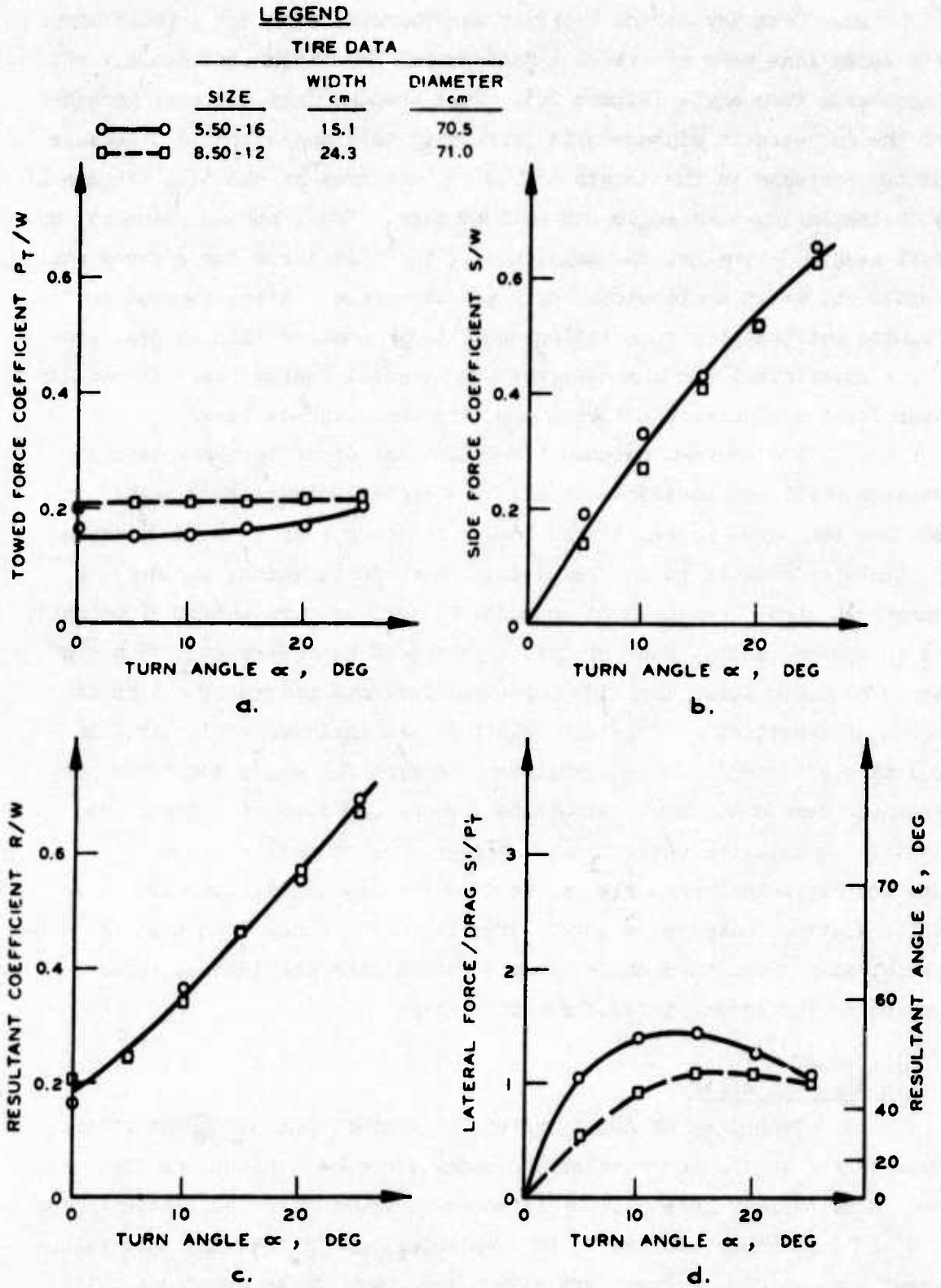

Figure 3. Influence of tire width and turn angle on performance parameters for 8.50-12 and 5.50-16 tires on sandy loam with tire deflection $\delta/h = 0.16$ and design wheel load $W' = 4300$ N[13]

contact pressure. Practically no separation by tire width can be noted in the relations of side force to turn angles (Figure 3b). This is not too surprising because the influence of the tire width is overshadowed by the influence of the length of the contact area (paragraph 12), which for a given turn angle was constant (tire diameter and deflection were constant for both tires). As a consequence of the relations shown in Figures 3a and 3b, no influence of tire width can be noted in the relations of resultant coefficients to turn angles (Figure 3c). However, for a given turn angle, lateral force/drag is larger for the narrower tire (Figure 3d) than for the wider one. The difference seems to decrease with increasing turn angles larger than 15 deg.

Influence of design
wheel load* and turn angle

15. The influence of wheel load on the various performance parameters is illustrated in Figure 4. For the three wheel loads used in this test program, the towed force coefficient was always lower for wheel loads at 4300 N; towed force coefficients at 2500 and 3600 N were essentially equal with the possibility that the towed force coefficient at 2500 N may be slightly lower at high wheel turn angle. A similar trend was observed for the relations between side force coefficients and turn angles (Figure 4b). There was very little difference between the results for loads of 2500 and 3600 N, and the results for a load of 4300 N separated slightly from the former. For a given turn angle, side force coefficient seemed to increase with decreasing load. Towed force and side force coefficients having developed this particular trend, resultant coefficients (Figure 4c) and lateral force/drag (Figure 4d) followed the same trend.

Previous Research at the WES

LRV wheel operating in turned mode

16. One of the wheels of the LRV was tested in the turned mode in

---

* Normally, design wheel load W' and actual wheel load W measured during a test differ only slightly. It is assumed that the investigator[13] used design wheel loads for comparison.

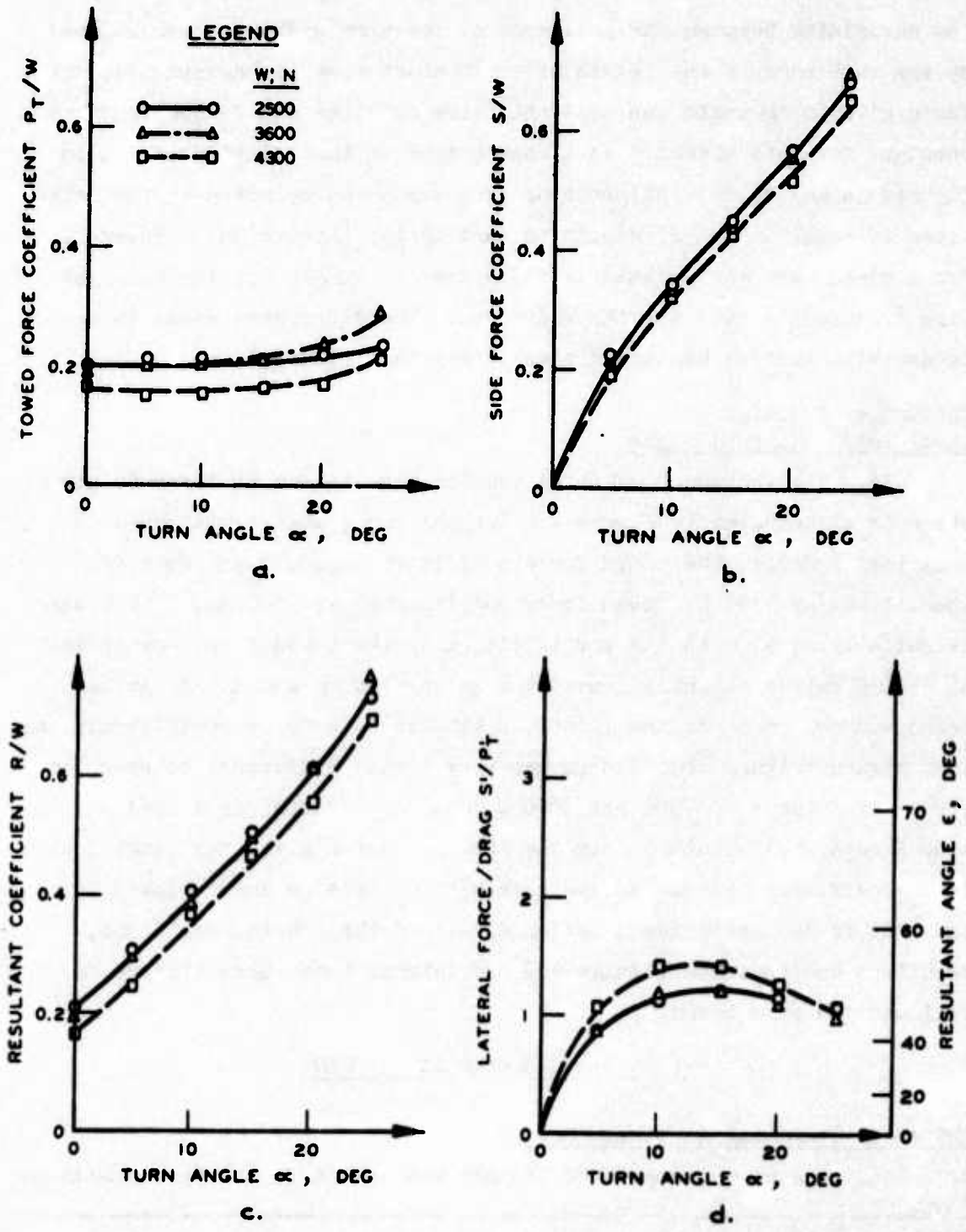

Figure 4. Influence of design wheel load and turn angle on performance parameters for 5.50-16 tire on sandy loam with tire deflection $\delta/h = 0.16$[13]

a lunar soil simulation.[15] The turn angle of the wheel was varied from -5 to +90 deg; in the latter case, the plane of the wheel was perpendicular to the travel direction. Test loads ranged from 187 to 276 N, and wheel velocities were varied from 1.1 to 3.1 m/sec. Although the LRV wheel is constructed of wire mesh and is not equipped with a pneumatic tire, the results of this study are believed pertinent and are summarized briefly.

17. Side force coefficient (Figure 5), sinkage, and slip

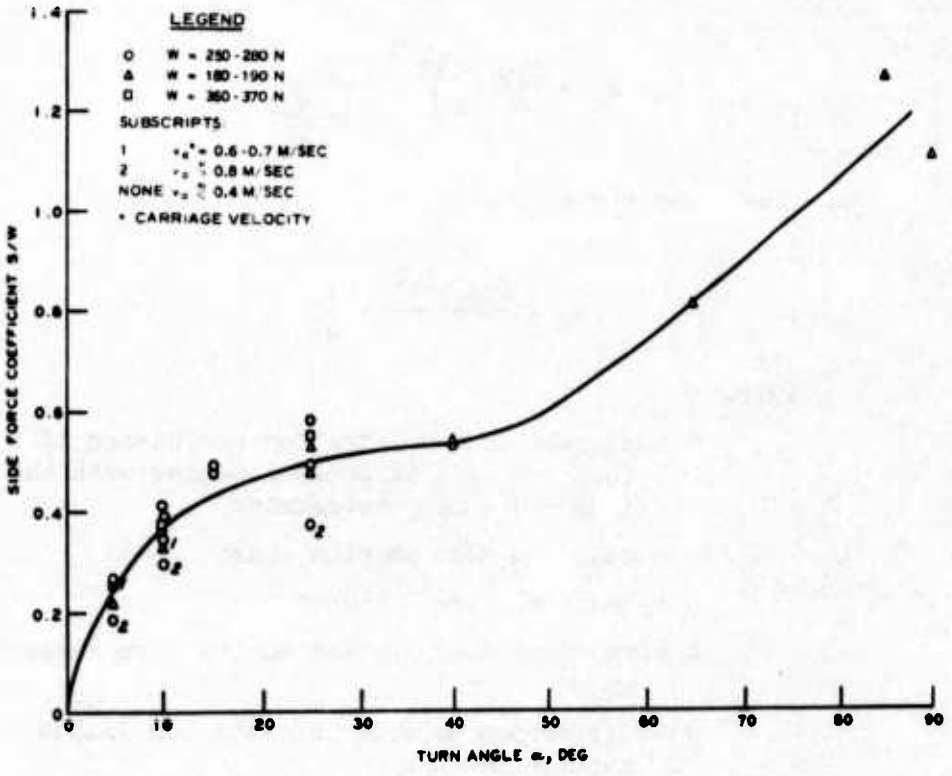

Figure 5. Turn angle versus side force coefficient for the LRV wheel[15]

increased with increasing turn angle for a given test condition; towed force coefficient was more or less constant, although there seemed to be a decreasing trend for turn angles larger than about 40 deg. Velocity had a slight effect on side force. The effects of wheel load on towed force coefficient, side force coefficient, and sinkage were not significant, a fact that had been found earlier for this particular wheel tested under these extremely light loads.[20]

WES numeric prediction system

18. A system has been developed by the WES[17,18,21] that allows the prediction of certain performance parameters of pneumatic tires if tire geometry, loading condition, soil strength, and soil type are known. This system was established from one-pass single-tire tests conducted at zero turn angle on a fat clay (Vicksburg clay) and on a dune sand (Yuma sand). The independent variables were combined by dimensional analysis into so-called mobility numbers for the two soils tested:

a. Clay mobility number N_c :

$$N_c = \frac{Cbd}{W}\left(\frac{\delta}{h}\right)^{1/2} \frac{1}{1 + \frac{b}{2d}} \tag{1}$$

b. Sand mobility number N_s :

$$N_s = \frac{G(bd)^{3/2}}{W} \cdot \frac{\delta}{h} \tag{2}$$

where

C = average cone penetration resistance of the 0- to 15-cm soil layer as measured with the WES standard cone penetrometer

b = unloaded tire section width

d = unloaded tire diameter

W = vertical load applied to the tire through the axle

δ = difference between unloaded and loaded tire section heights

h = unloaded tire section height

G = average cone penetration resistance gradient of the 0- to 15-cm soil layer as measured with the WES standard cone penetrometer

19. Relations were established between each of the following performance parameters and the sand and clay mobility numbers, respectively: pull coefficient P/W , torque coefficient M/Wr_a , and sinkage coefficient z/d , all at 20 percent slip; and towed force coefficient

P_T/W .* These relations (Figure 6 for clay and Figure 7 for sand) describe the performance for the lower limit (towed point) and, for all practical purposes, the upper limit (20 percent slip) of the operational range of a wheel being driven on these two specific soils. Additional

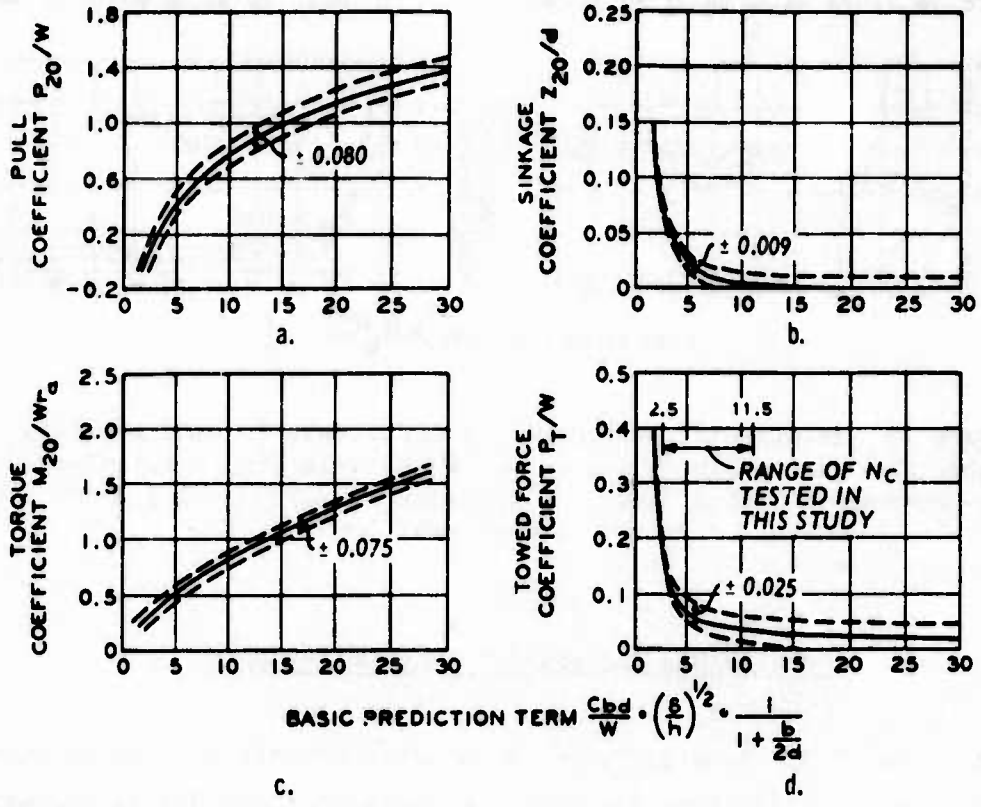

Figure 6. Relation of performance coefficients to clay mobility number for turn angle $\alpha = 0$, v_w (wheel velocity) = 1.5 m/sec for powered condition, and v_a (carriage velocity) = 1.5 m/sec $\approx v_w$ for towed condition[21]

research[22,23,24] has shown that performance can be described for the full operational range of a wheel by incorporating slip as an additional variable but still using the same dimensional analysis techniques.

---

* P = net pull, M = torque input to the axle, r_a = effective tire radius in the soil, and z = sinkage. Subscript 20 to P , M , and z indicate performance at 20 percent slip.

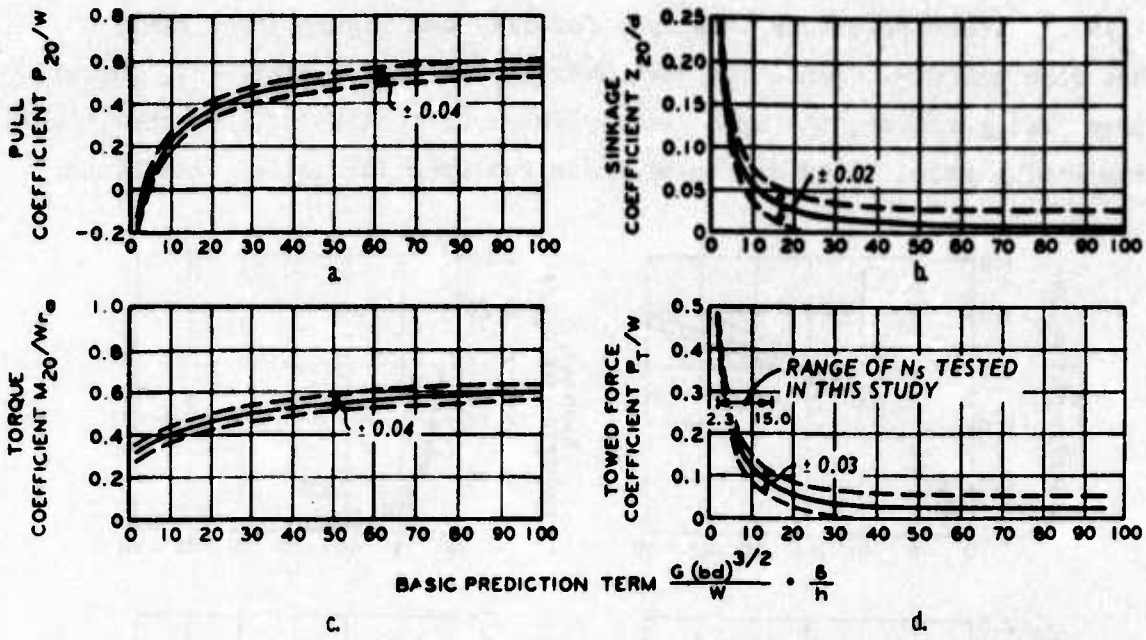

Figure 7. Relation of performance coefficients to sand mobility number for turn angle $\alpha = 0$, v_w (wheel velocity) = 1.5 m/sec for powered condition, and v_a (carriage velocity) = 1.5 m/sec $\approx v_w$ for towed condition[21]

Conclusions Regarding Follow-On Research

20. Based on the results of the studies described in paragraphs 8-19, it was concluded that follow-on research on towed wheels operating in turned mode in soft soils should focus primarily on the following influences on performance: (a) soil type (clay, sand, etc.), (b) soil strength, and (c) tire deflection. Also, additional information on the influences of wheel load and tire geometry seemed to be needed. The WES numeric prediction system, presently available only for predicting performance of wheels operating at turn angles of 0 deg (Figures 6 and 7), should be checked to determine whether it can be used to predict performance of wheels operating at turn angles other than 0 deg. Finally, but beyond the scope of this phase of the study, research must be directed toward the influence of turn angles on the performance of powered wheels.

PART III: TEST PROGRAM

Soils

Description

21. The tests reported herein were conducted basically on two soils that represent the limits of the soil-type spectrum: purely cohesive soil and purely cohesionless soil. Fully saturated, fat clay (Vicksburg clay) was used in the tests on cohesive soil. This material is classified as CH (Figure 8) according to the Unified Classification System and was used in establishing the prediction system for clay described in paragraphs 18 and 19 (Figure 6). For most of the tests in cohesionless soil, an air-dry riverbed sand (mortar sand; SP) was used (Figure 8). This material was chosen to complete the body of data collected in earlier tests* and is not identical with the Yuma sand (SP-SM; Figure 8) used in establishing the prediction system for sand described in paragraphs 18 and 19 (Figure 7). To compare the results obtained in mortar sand with the relations developed in the prediction system, a few tests were conducted on air-dry Yuma sand during this study.

Preparation

22. The soils were prepared in movable soil bins that were 0.8 m deep, 1.6 m wide, and long enough to accommodate test lanes 16 m long. The procedures used to prepare the clay and the sands with the desired consistencies and relative densities, respectively, are described in Reference 25. The uniformity of the soil and its strength were checked by using the WES standard cone penetrometer (base diameter: 2.03 cm, apex angle: 30 deg). Strength was expressed as average cone penetrometer resistance C for the clay, and as average cone penetration resistance gradient G for the sands; in both cases, the depth range for which these values were determined was 0-15 cm. The strength values for the individual tests are listed in Tables 1-3. The major strength

---

* This body of data was collected on mortar sand during the study for the Air Force (paragraph 6 and Reference 19).

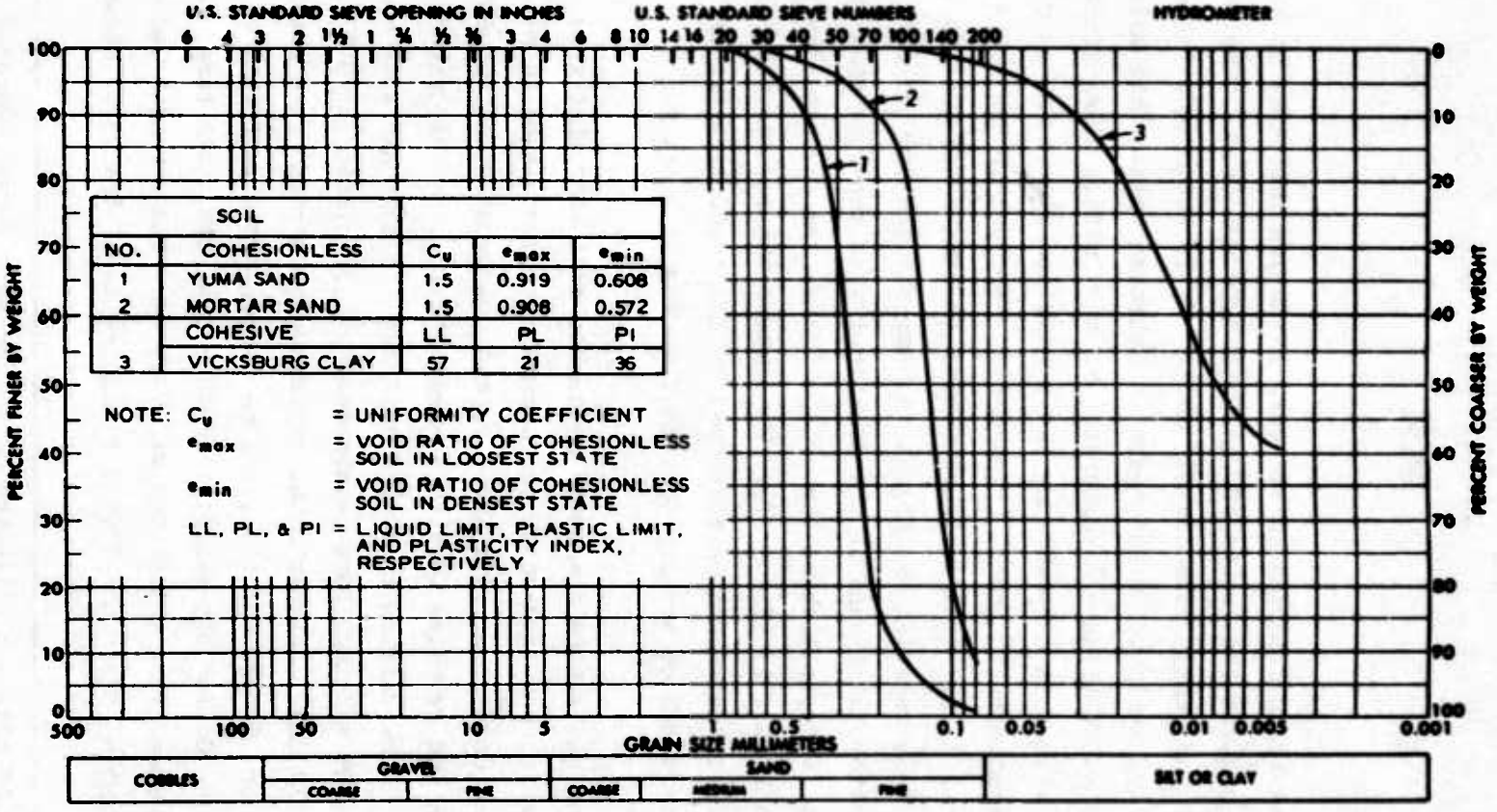

Figure 8. Grain-size distribution and basic properties of test so'ls

values for the soils tested and their corresponding consistencies[26] or relative densities[27] are listed in the following tabulation.

Soil	C , kPa*	Consistency	G , MPa/m*	Relative Density
Vicksburg clay	280	Soft	--	--
	350	Medium-stiff	--	--
	500	Medium-stiff	--	--
Mortar sand	--	--	1.3	Medium-dense
	--	--	2.6	Dense
	--	--	3.0	Dense
	--	--	4.2	Very dense
Yuma sand	--	--	0.8	Medium-dense
	--	--	1.3	Medium-dense
	--	--	1.9	Dense

* Values represent nominal values; actual values differ slightly (Tables 1-3).

Equipment

Tires

23. The following pneumatic tires were tested during this program: an 8.50-10, 8-PR aircraft tire and a 7.00-6, 6-PR aircraft tire, both having longitudinal rib tread design characteristic of aircraft tires, and a 6.00-9, 4-PR trailer tire buffed free of tread. Pertinent tire data are listed in Table 4. The selection of these tires was somewhat dictated by the fact that the aircraft tires had been used in the earlier study for the U. S. Air Force[19] (paragraph 6), and by the dimensions of the dynamometer system, which will be described in the following paragraphs.

Dynamometer system

24. The dynamometer system, or test carriage, used in this study (Figure 9) is part of the basic equipment available at the WES to investigate running gears in single configuration.[25] The carriage is supported by solid rubber-tired rollers on a pair of overhead rails that are, in turn, suspended from cantilevers and crossarms. The carriage is towed by an endless cable that is fastened fore and aft to it and passes

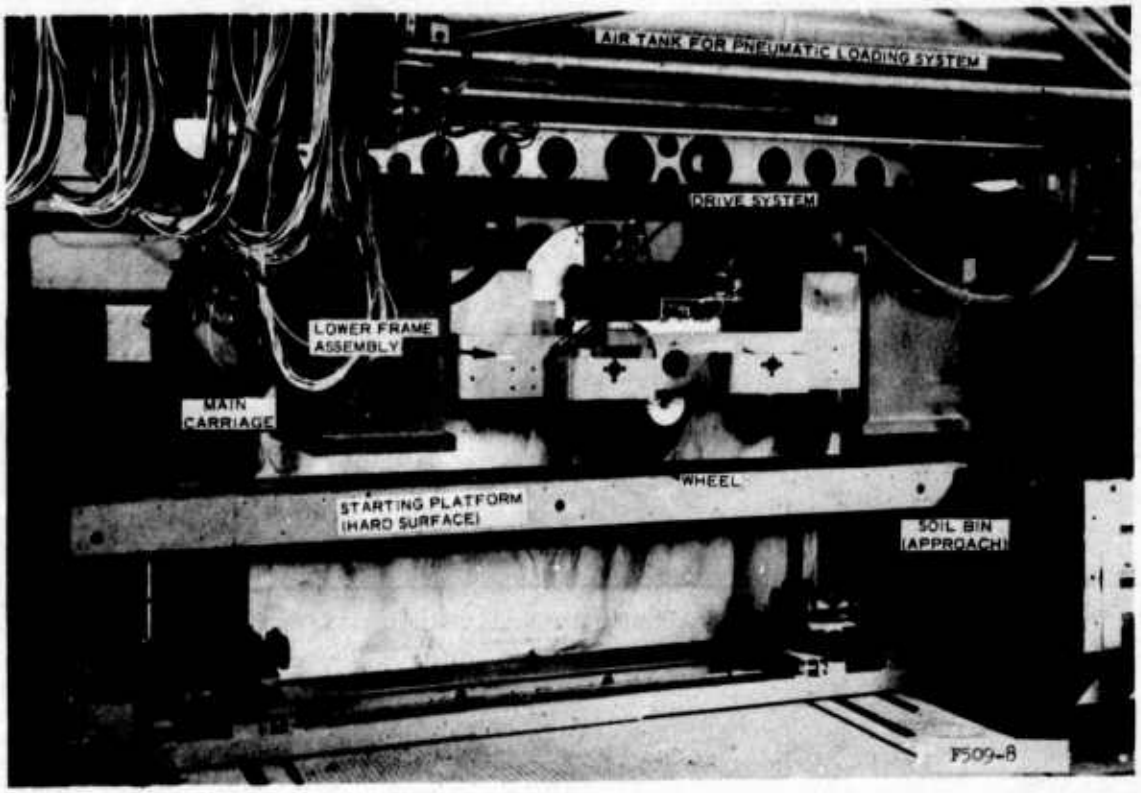

Figure 9. Overall view of dynamometer carriage

over pulleys at the end of the track system, and is driven by sheaves mounted on a platform above the overhead rails. The speed of the towing cable, and thus the velocity of the carriage, can be varied from 0 to about 9 m/sec. The test carriage and the cable can be shifted transversely across the width of the soil bin.

25. The carriage consists of a main structure (Figure 9), which contains the pneumatic load system, and a lower frame assembly to which, under normal circumstances (tests exclusively in straight paths), the test wheel is mounted. However, for the program described in this report, the main carriage system was modified so that the wheels could be tested at various turn angles. The major modification was an additional subframe designed so that a wheel could be bolted to it (Figure 10). The subframe can be bolted to the basic inner frame (Figure 11) of the lower frame assembly at the desired turn angle. Turn angles can be varied from 0 to 20 deg in 5-deg intervals. In this configuration, the

Figure 10. Wheel equipped with 8.50-10, 8-PR tire mounted in subframe

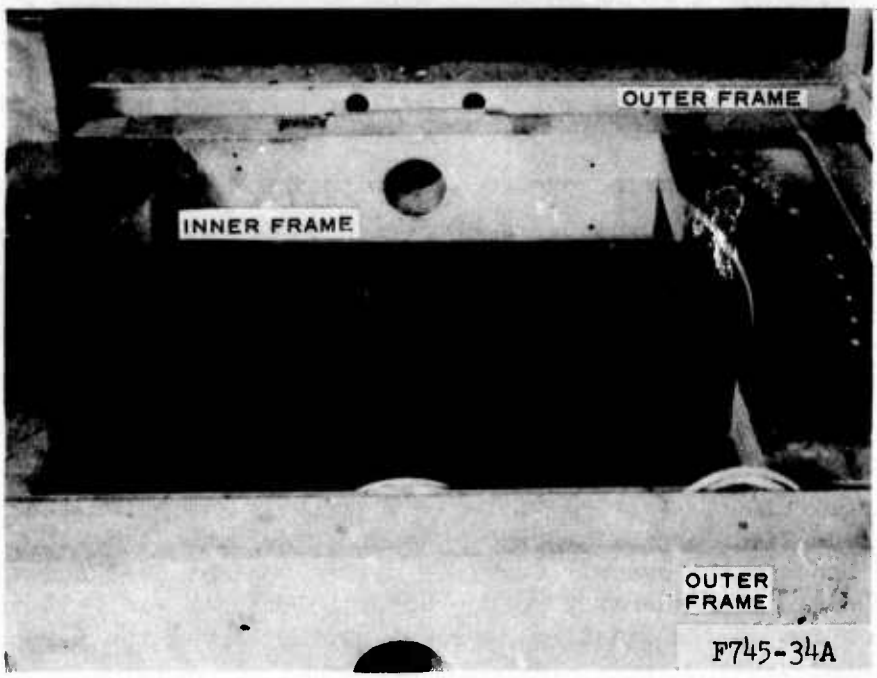

Figure 11. Lower frame assembly of dynamometer system (without subframe and wheel)

carriage can accommodate wheels with diameters up to about 65 cm and with widths up to about 22 cm.* The wheels can be tested either powered or towed. In the latter case, the chains that connect the drive system with the wheel axle (Figure 12) are removed.

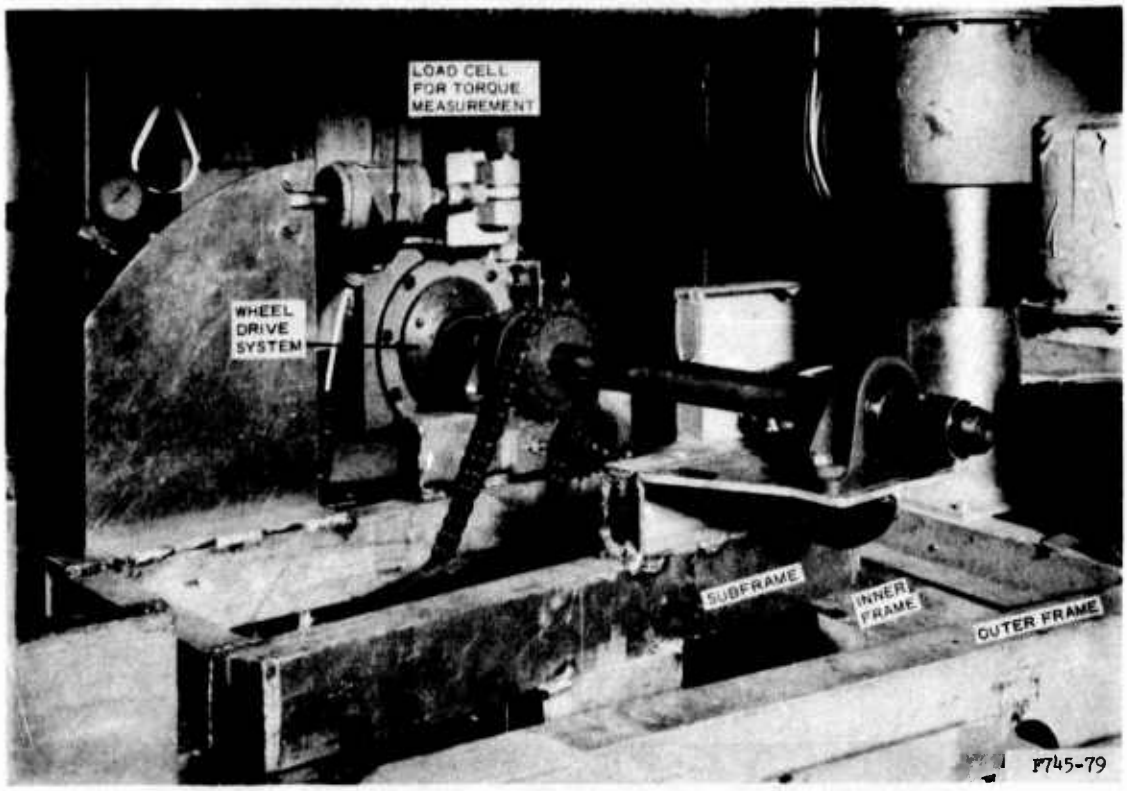

Figure 12. Subframe mounted in place and wheel drive system

26. The dynamometer system is equipped to measure the following quantities continuously during each test: wheel load, pull of a powered wheel or drag force of a towed wheel (Figure 13) in line with the longitudinal axis of carriage travel, lateral forces exerted by the wheel on the inner carriage frame perpendicular to the direction of travel of the carriage, wheel hub movement, carriage velocity, angular velocity of the

* This restraint in wheel diameters is probably the major shortcoming of the modified carriage; however, much larger wheels could not be tested because the overall carriage system was not designed to accommodate excessive lateral forces. Nevertheless, it was felt that this modification of the existing carriage system served the purposes of this pilot study.

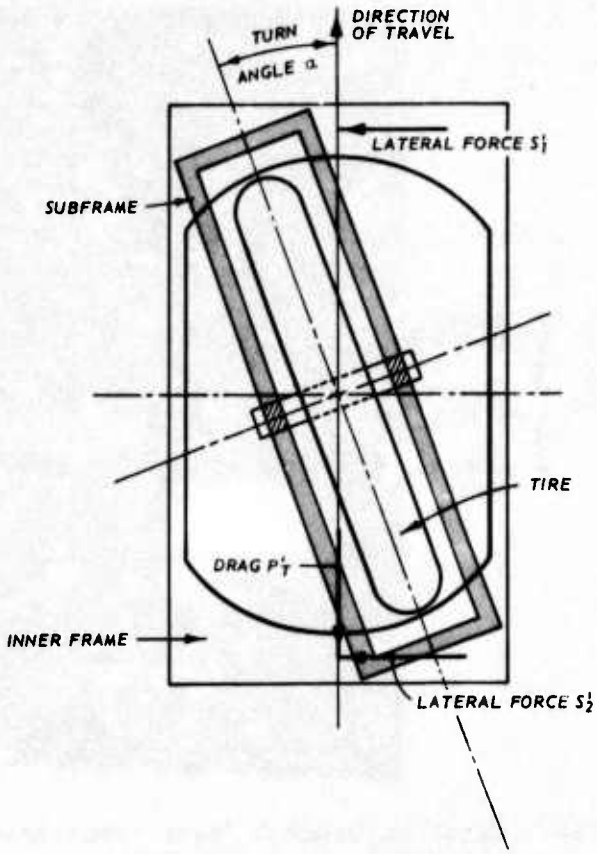

Figure 13. Scheme of forces measured in horizontal plane of inner frame

wheel, and applied torque (powered tests).

27. The lower frame assembly consists basically of the inner frame and the outer frame (Figures 11, 12, and 14). The inner frame is hinged at all four corners to load cells that are connected to the outer frame (Figure 14). This mechanism allows relative movement at the two frames longitudinally while the four load cells measure the vertical load. The relative longitudinal movement is opposed by a load cell mounted horizontally between the two frames so that the reading from this cell is a measure of pull or drag force. In addition, two load cells are installed parallel to the front and rear ends of the inner frame and connected by bars with the outer frame (Figure 14). These load cells monitor the side forces exerted by the wheel on the inner frame. Hub movement is measured by a potentiometer connecting the lower frame assembly with the main carriage body. Carriage velocity is

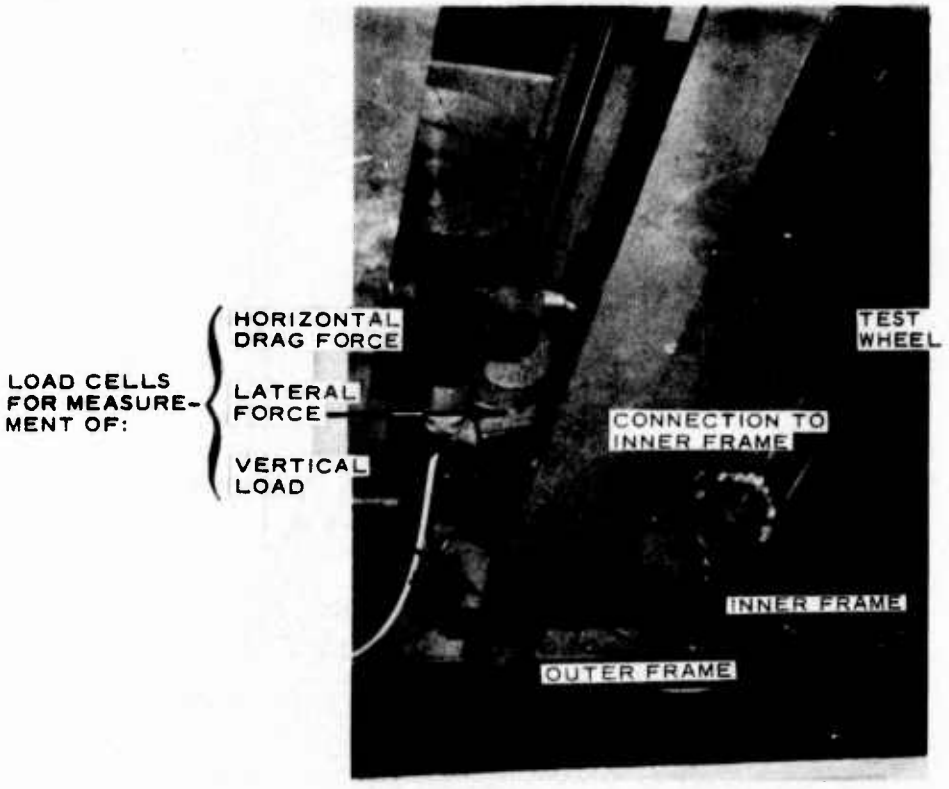

Figure 14. Close-up beneath lower frame assembly, with force-measuring devices

measured by a tachometer; also measured are time and distance traveled. Angular velocity of a wheel is measured by a potentiometer and a tachometer (Figure 10). If a wheel is powered,* the applied torque is recorded by a load cell connecting the subframe with the drive motor, which is mounted to the outer frame. Knowing the recorded force and the length (moment arm) of the connecting member allows the determination of the applied torque.

Data recording and processing systems

28. The various measurements reach the recording station as electrical (analog) signals through a system of cables. The primary recording system is a tape recorder that stores the analog signals in raw form, with no signal conditioning, for further data processing

* Not used in this study.

(digitizing). A secondary recording system is a 36-channel, direct-writing oscillograph, which requires signal conditioning. This latter system affords the test engineer an opportunity to take a quick look at the data as required to assist in planning subsequent tests, and to rapidly determine whether all circuits are functioning properly for a given test. The accuracy of the oscillograph readings depends on the scale used and the expertise of the reader.

29. Only results obtained from the primary recording system were used in the analysis of this test program. The data recorded on magnetic tape were digitized and further processed on a digital computer. As final results of this process, a high-speed printer produced for each test the following parameters that had been computed as average values from the measured parameters (Figures 1 and 13): lateral force $S' = S'_1 + S'_2$, drag P'_T, side force S, towed force P_T, resultant R, angle ε* formed between resultant and direction of the test carriage, eccentricity e of the resultant (pneumatic trail), trail moment M_t, and wheel hub movement. In addition, the averages of wheel load W, carriage velocity v_a, translational velocity v_w of the wheel, and slip s in the plane of the wheel were computed and printed.

Test Procedures

30. A towed-test technique was used in all tests during this study, i.e., the wheel was not connected to the drive system and, therefore, was allowed to roll freely if towed. Before each test, the wheel was loaded to the desired wheel load and tire deflection, both of which were nearly constant during a specific test. The carriage was then towed down the test lane at a programmed velocity, which was held constant during each test while the translational velocity of the wheel developed freely, depending on the test condition. Most of the tests were conducted at a carriage velocity of about 3.0 m/sec, which was the same velocity used in the study for the U. S. Air Force[19] (paragraph 6).

---

* $\tan \varepsilon = S'/P'_T$.

However, a few tests were conducted at a carriage velocity of about 1.5 m/sec to check the results of the tests conducted at 3.0 m/sec for velocity influences before they were compared with the WES numeric prediction system (paragraphs 18 and 19), which had been established from results of tests conducted at 1.5 m/sec.

Tests Conducted

31. The tests conducted in this program are tabulated below according to tires, soil types, and turn angles. Wheel loads were varied between 1000 and 7000 N. Tire deflections were 0.15, 0.25, 0.35, and 0.40. Cone penetration resistances in the clay ranged from 255 to 543 kPa, and cone penetration resistance gradients in the sands ranged from 0.7 to 4.6 MPa/m. Test results are presented in Tables 1-3.

Tire	No. of Tests: Vicksburg Clay	Mortar Sand	Yuma Sand	Turn Angle α, deg
8.50-10; 8-PR	4	2	--	0
	5	7	1	5
	5	4	2	10
	4	5	1	15
	3	2	--	20
7.00-6; 6-PR	2	3	--	0
	2	2	--	5
	4	2	--	10
	3	2	--	15
	3	2	--	20
6.00-9; 4-PR	--	--	--	0
	3	5	1	5
	6	2	1	10
	2	5	2	15
	1	1	--	20
Totals	47	44	8	

PART IV: ANALYSIS OF DATA

Methods of Analysis

32. The analysis is divided into two parts according to the two basic soil types tested, clay and sand. Each part is, in turn, divided into two sections, one describing the influence of certain controllable factors (for example, wheel load) on selected performance parameters, and one describing the development of a dimensionless performance prediction system. The basic considerations on which these two sections are founded and the corresponding means of analysis are described in general terms in the following paragraphs.

Factors influencing performance

33. Performance parameters. Four basic performance parameters, derived by dimensional analysis,[13,17] were used to characterize the towed performance of the wheels, or tires, tested. These dependent variables were (illustration of the forces in Figure 1):

a. Towed force coefficient P_T/W, where P_T is towed force acting in the plane of the wheel and W is wheel load.

b. Side force coefficient S/W, where S is side force acting perpendicular to wheel.

c. Resultant coefficient R/W,* where R is the resultant of side force S and towed force P_T and is also the resultant of lateral force S' and drag P'_T.

d. Ratio of lateral force to drag S'/P'_T,* which represents the tangent of the angle ε by which the resultant R is inclined with reference to the direction of travel.

In addition, the influence of variation in test condition on the trail moment M_t and the eccentricity e of the resultant was investigated to a limited extent.

---

* Actually, R/W and S'/P'_T can be derived from P_T/W and S/W for any given situation, if the two latter coefficients are known. However, R/W and S'/P'_T were included in the analysis to get a better qualitative feeling for their variation when P_T/W and S/W were changing with the corresponding test conditions.

34. Independent variables. The following factors, or independent variables, that were thought to influence the performance of the wheels were investigated.

a. Turn angle α .

b. Soil strength in terms of C or G .

c. Tire deflection δ/h .

d. Wheel load W .

e. Product of tire width and diameter bd .*

The influences of tire width and diameter could not be studied separately because of the physical restrictions of the test setup (paragraph 25) and the restrictions in available tire sizes. It was impossible, for instance, to test two tires having the same diameters, but different widths, or vice versa. In addition to the variables listed above, it was necessary to determine whether the translational velocity of the carriage within the range tested would influence wheel performance (paragraph 30).

35. Method of evaluation. Each of the performance parameters listed in paragraph 33 was plotted versus turn angle α such that, besides α , only one of the other independent parameters listed in paragraph 34 would vary. For example, if the influence of soil strength was to be investigated, only results of tests were used for which C or G , respectively, was changed from test to test, but δ/h , W , and bd were held constant. By this means, the influence of each independent variable on the corresponding performance parameters could be evaluated separately.

Development of prediction system

36. Performance parameters. In addition to the performance parameters listed in paragraph 33, the parameters considered to be important enough to be included were: (a) sinkage coefficient z_T/d ,** and (b) slip s .

---

* bd was chosen instead of b/d because the former appears in both mobility numbers (Equations 1 and 2).

** z_T was determined from the measured hub movement of the wheel using a method previously developed for α [28] .

37. Independent variables. Besides the turn angle α, the clay mobility number N_c and the sand mobility number N_s (Equations 1 and 2) were used as independent variables. As mentioned in paragraphs 18 and 19, the independent variables b-e in paragraph 34 had been combined to develop N_c and N_s, respectively, by means of dimensional analysis when the prediction system for the performance of wheels with pneumatic tires operating at zero turn angle was developed.[17,18] The ranges of the individual variables, such as C, G, etc. (paragraph 31), resulted in the following ranges of the two mobility numbers:

a. Clay mobility number N_c : 2.5-11.5

b. Sand mobility number N_s : 2.3-15.0

These ranges are indicated in Figures 6d and 7d, respectively, and show that for all practical purposes, the ranges of mobility numbers covered in this study are those within which the most drastic changes in performance occur when turn angle is zero.

38. Prediction system. The existing prediction systems for the towed conditions at zero turn angle in clay (Figure 6d) and in sand (Figure 7d) were extended to cover turn angles ranging from 0 to 20 deg by simply plotting the individual performance parameters measured for one given turn angle versus the corresponding N_c or N_s values, respectively, and describing the observed trend by a curve of best visual fit. The result was a family of curves for each performance parameter under consideration, each curve describing the relation between the performance parameter and the mobility number for a given turn angle.

Tests in Clay

Factors influencing performance

39. Velocity. The influence of translational velocity within the range of about 1.5-3.0 m/sec on the performance of a powered wheel at 20 percent slip and zero turn angle was found to be negligible for all practical purposes (Reference 18, Plate 16a). The small differences

that occurred were well within the scatter of the data. In addition, for cohesionless soils, the influence of wheel velocity (within the range mentioned) can be expected to be much smaller for the towed condition than for the 20-percent-slip condition.[20] When these two facts are considered, the influence of wheel velocity would also be expected to be negligible for the towed wheel at zero turn angle in clay. However, whether this would be true if the wheel were operating in turned mode had to be investigated.

40. Results from two tests, in which all variables* except the carriage velocity v_a were kept almost constant, are compared in Figure 15. None of the four performance parameters seem to be influenced by v_a. The same is true for the translational velocity of the wheel and, consequently, for slip (not shown in Figure 15). Therefore, the data from tests conducted at $v_a = 1.5$ m/sec are included without modification in the further analysis of the results of the tests conducted at $v_a = 3.0$ m/sec. Furthermore, and more important, use of the formerly developed prediction system for $v_a = 1.5$ m/sec (paragraphs 18 and 19, Figure 6d) as a valid system for the case of a turn angle of 0 deg (see, for instance, closed symbols in Figure 16) seems to be justified and to be comparable with the data obtained at $v_a = 3.0$ m/sec in this study.

41. Soil strength. The influence of soil strength on the four performance parameters is demonstrated in Figure 16 for the 8.50-10, 8-PR tire and in Figure 17 for the 7.00-6, 6-PR tire. For a given soil strength, the relations between the individual performance parameters and the turn angle α showed more or less the same general trend observed by Schwanghart[13] for sandy loam (Figure 2), including an increase in sinkage and slip with increasing turn angle (not shown at this point). However, two facts must be mentioned. First, the increase of towed

---

* There were, of course, some slight differences in these variables, because it was not possible to keep C and W exactly constant from test to test. See, for instance, tests A-73-037-3 and A-73-039-3 (Table 1, 6.00-9 tire). These small differences contributed to the data scatter shown in Figure 15.

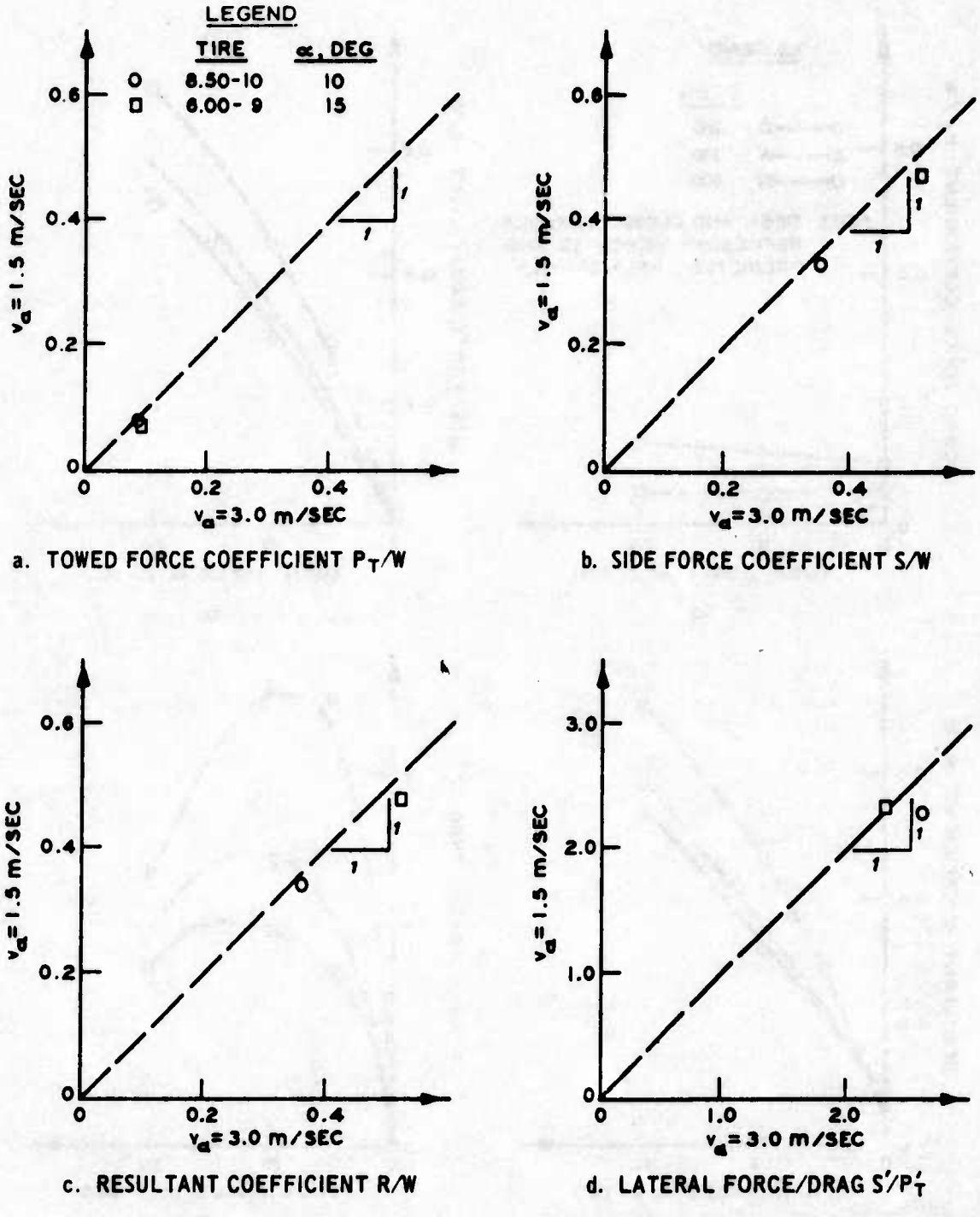

a. TOWED FORCE COEFFICIENT P_T/W

b. SIDE FORCE COEFFICIENT S/W

c. RESULTANT COEFFICIENT R/W

d. LATERAL FORCE/DRAG S'/P'_T

Figure 15. Comparison of performance parameters of the 8.50-10, 8-PR and 6.00-9, 4-PR tires operating under similar conditions at carriage velocities (v_a) of 3.0 and 1.5 m/sec on clay

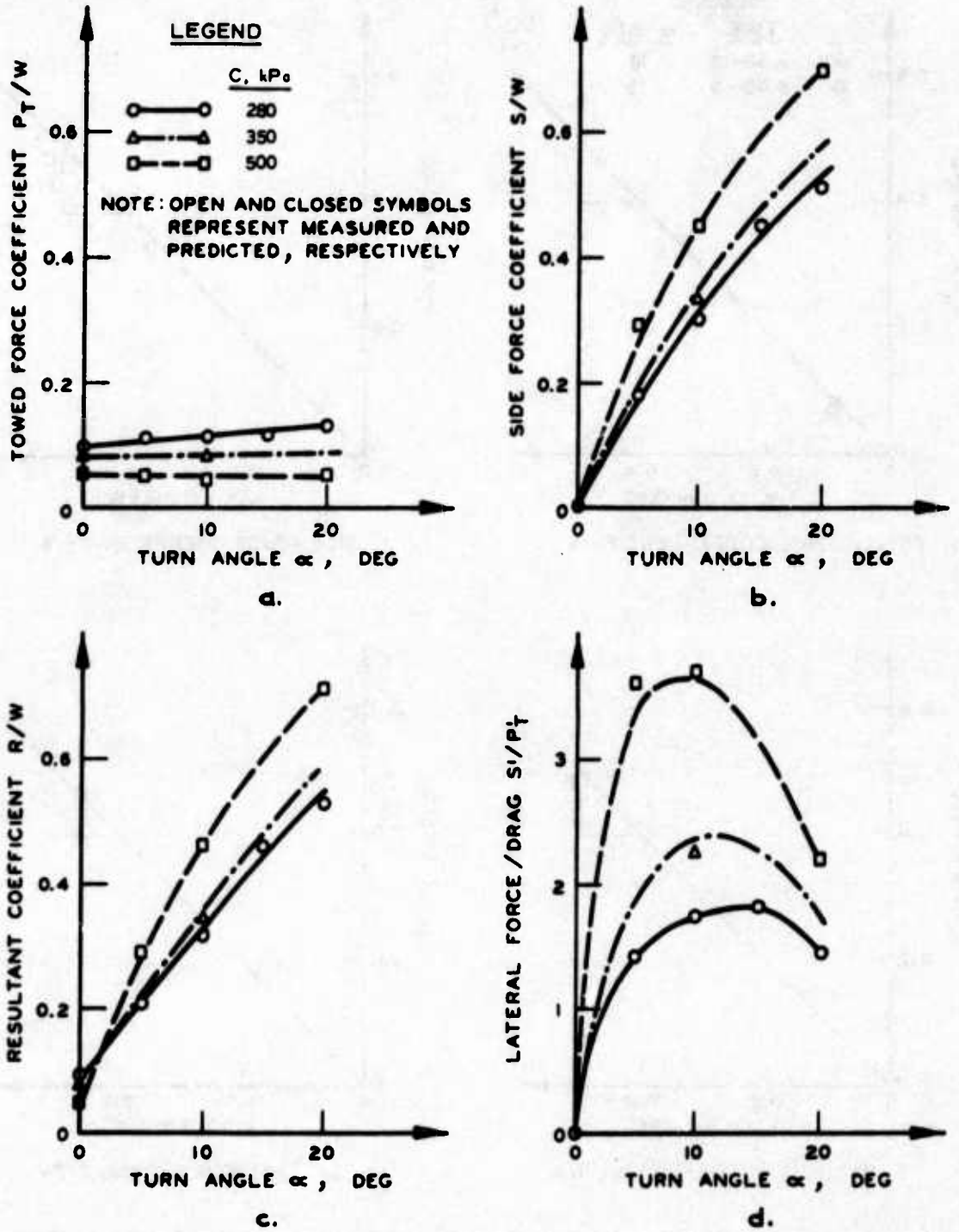

Figure 16. Influence of turn angle and soil strength on performance parameters for 8.50-10, 8-PR tire on clay with tire deflection $\delta/h = 0.35$ and design wheel load $W' = 5800$ N

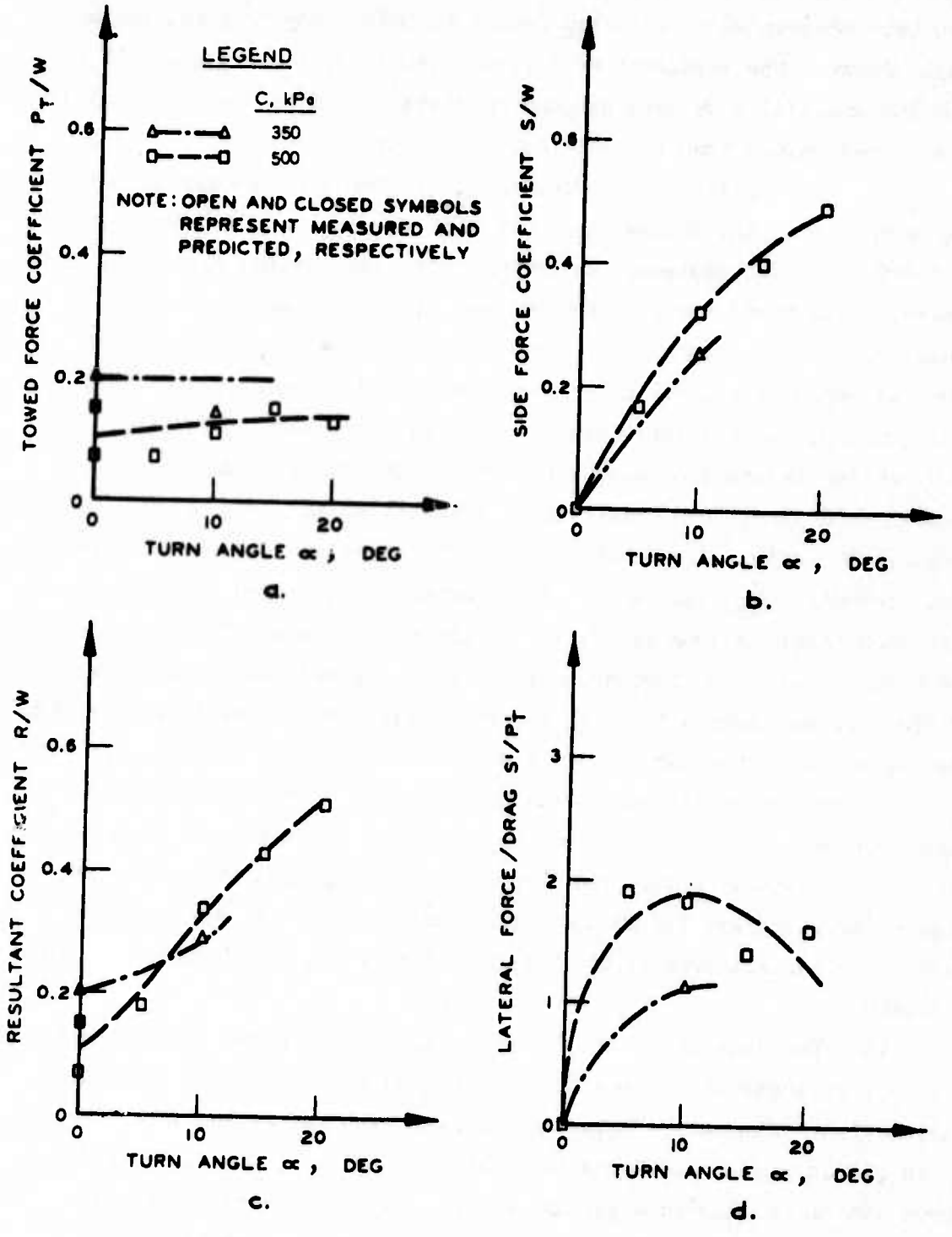

Figure 17. Influence of turn angle and soil strength on performance parameters for 7.00-6, 6-PR tire on clay with tire deflection $\delta/h = 0.35$ and design wheel load $W' = 5800$ N

force coefficient that was not very drastic in sandy loam (Figure 2a) is even less pronounced in the clay tested in this study (Figures 16a and 17a). Second, the relations of lateral force/drag to turn angle (Figures 16d and 17d) show more pronounced peaks in clay and also generally higher peak values than the same relations for sandy loam.

42. For a given turn angle, the performance parameters vary with soil strength in the following manner (Figures 16 and 17). Towed force coefficient P_T/W decreases as average cone penetration resistance increases; this trend was expected because it is the same that P_T/W showed at $\alpha = 0$ (Figure 6d). However, side force coefficient S/W shows an opposite trend: S/W increases with increasing soil strength. Consequently, lateral force/drag S'/P'_T and resultant coefficient R/W show similar trends (see also the trends observed by Schwanghart[13] on concrete and sandy loam, Figure 2). However, in the case of R/W (Figures 16c and 17c) a "crossover" of the relations for the different soil strengths occurred because the trends of P_T/W and S/W contradict each other as long as P_T/W is larger than S/W (for instance at $\alpha = 0$ deg), and R/W decreases with increasing soil strength. However, if S/W becomes dominant, R/W decreases with decreasing soil strength. The magnitude of the turn angle at which the relations between R/W and α cross each other depends on the tire size if tire deflection and wheel load are constant (Figures 16c and 17c), which results in a dependency on contact area. The larger the contact area (8.50-10 tire, Figure 16c), the smaller is the influence of P_T/W or R/W ; with decreasing contact area (7.00-6 tire, Figure 17c), P_T/W becomes more dominant.

43. The fact that side force coefficient increases with increasing soil strength at a given turn angle deserves at least a qualitative explanation. Sinkage is known to increase with decreasing soil strength, which should cause side force to react similarly. However, the side force can be considered a passive earth pressure created as the tire moves sideways against the soil. With simplifying assumptions (horizontal soil surface, vertical sidewall of the tire, no friction between sidewall and soil, purely cohesive soil), the side force per length of

tire contact area S_c can be expressed as[29]

$$S_c = c\lambda_p z \tag{3}$$

where

c = cohesion

λ_p = passive earth pressure coefficient = 2

z = sinkage

44. For a numeric example, results were chosen from two tests that were conducted with the 8.50-10, 8-PR tire at a turn angle of 20 deg (Figure 16 and Table 1). Cohesion was estimated from cone penetration resistances C measured in previous investigations with Vicksburg clay.[30] The necessary soil properties and parameters and the calculated side forces S_c are listed below

Test No.	C , kPa	c , N/cm^2	z_T , cm	S_c , N/cm^2
A-73-012-3	271	2.26	4.3	19.4
A-73-025-3	543	4.34	3.8	33.0

Although the absolute magnitudes of S_c are too small to arrive at the actual measured side forces S (Figure 16b),* it appears that S_c increases with increasing soil strength, i.e., cohesion has a larger influence on performance than does sinkage. In addition, it is also possible that in a stiff soil, the sidewall of the tire remains more vertical than in a softer soil that would allow the sidewall to tilt over more toward the direction of travel. In the latter case, this would result in an increase in tire width and contact area, the load being the same. Because of this effect, the sinkage in the soft soil would not be as large as would be expected for the nominal contact area. Thus, for the two different soil strengths, the increase in cohesion has a greater influence on side forces than does the decrease in sinkage.

---

* Although the absolute values of S_c and S did not compare, at least the comparison of the percentage of increase supported this qualitative explanation; S_c increased by a factor of 1.7 and S increased by a factor of about 1.4.

45. The influence of soil strength on trail moment and eccentricity (Figure 1) is demonstrated (Figure 18) with some specific results

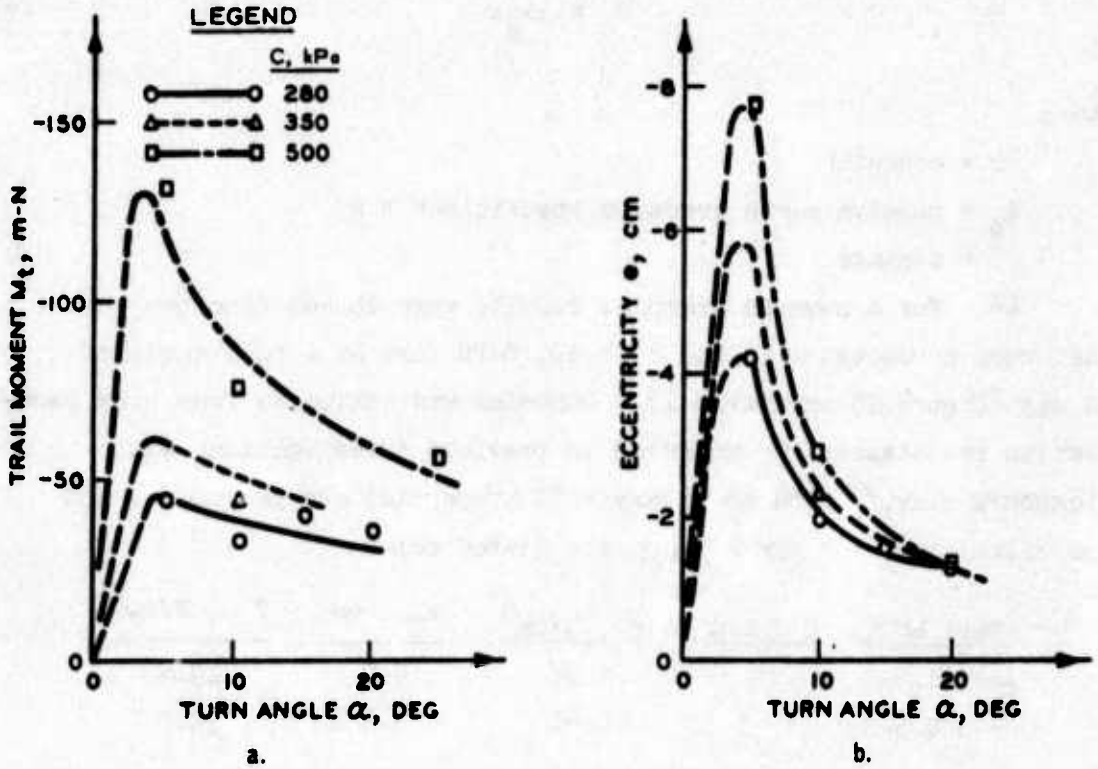

Figure 18. Influence of turn angle and soil strength on trail moment and eccentricity for 8.50-10, 8-PR tire on clay with tire deflection $\delta/h = 0.35$ and design wheel load $W' = 5800$ N

from tests with the 8.50-10, 8-PR tire. Both parameters increase from zero with increasing turn angle until they reach a maximum at an angle of about 4-5 deg. Thereafter, they decrease gradually with increasing turn angle. The influence of soil strength shows more or less the same trend as observed for side forces: For a given turn angle, trail moment and eccentricity increase with increasing strength. Both parameters are negative, indicating that the resultant R (Figure 1) acts on the tire behind the center of the wheel (projected to the ground plane).

46. Tire deflection. The influence of tire deflection on wheel performance is shown in Figure 19 for tests with the 8.50-10, 8-PR tire and in Figure 20 for tests with the 6.00-9, 4-PR tire. For a given turn angle, the towed force coefficient increases with decreasing deflection

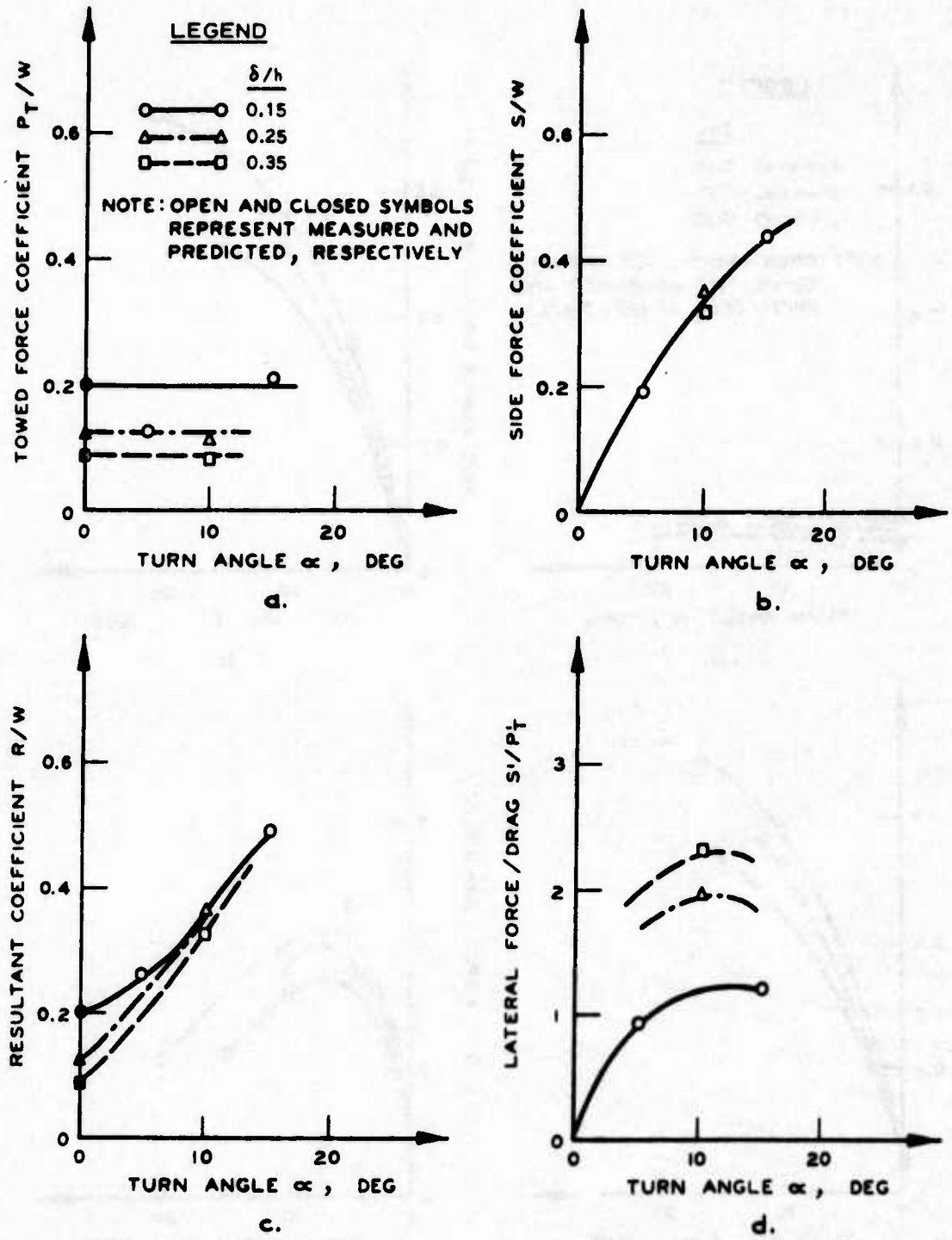

Figure 19. Influence of turn angle and tire deflection on performance parameters for 8.50-10, 8-PR tire on clay with average cone penetration resistance C = 350 kPa and design wheel load W' = 5800 N

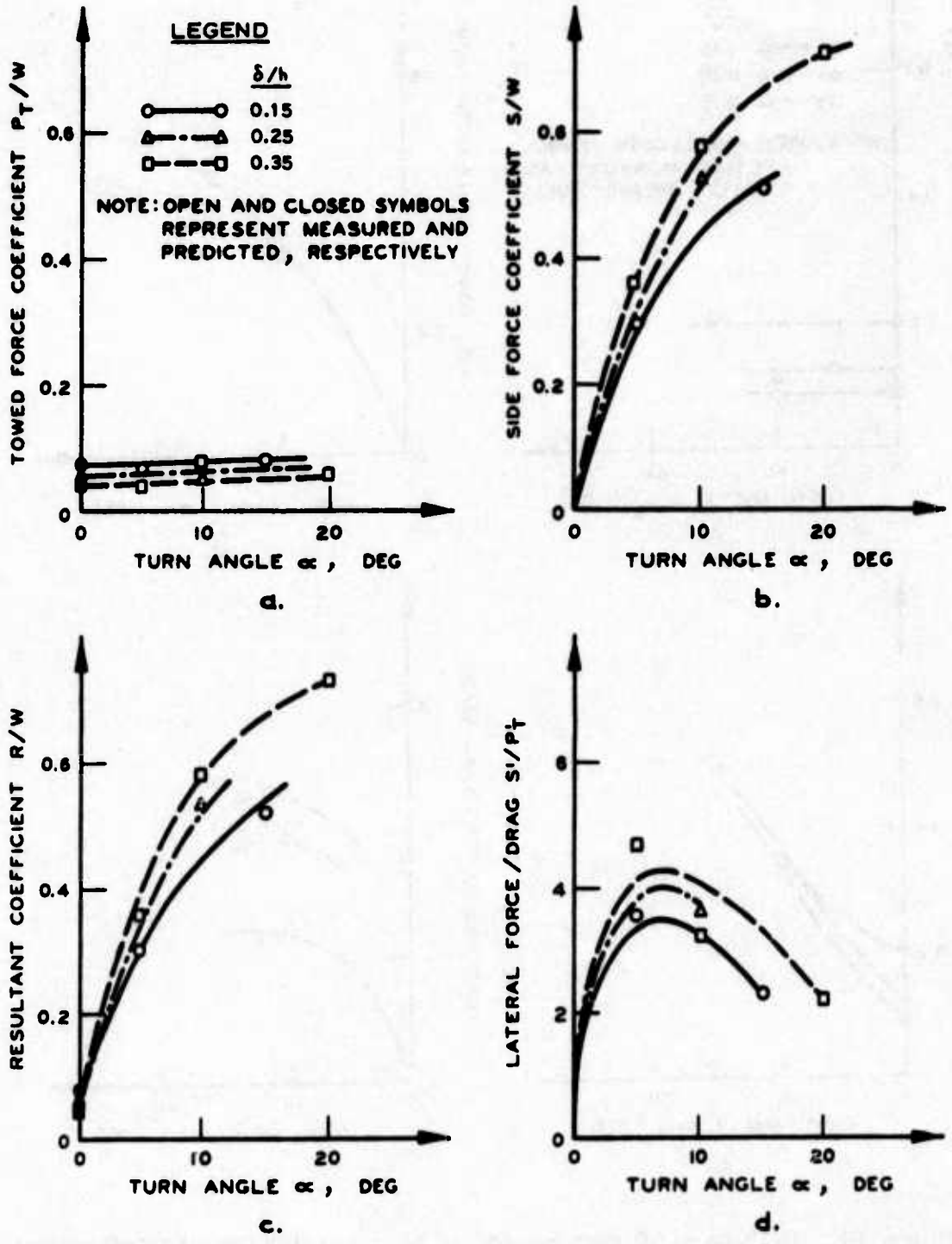

Figure 20. Influence of turn angle and tire deflection on performance parameters for 6.00-9, 4-PR tire on clay with average cone penetration resistance C = 350 kPa and design wheel load W' = 2000 N

(Figures 19a and 20a) as one would expect from the towed force behavior observed for zero turn angle (Figure 6d). In the results from the few tests with the 8.50-10, 8-PR tire, practically no separation by deflection was observed in the relation between side force coefficient and turn angle (Figure 19b). The relation of resultant coefficient to turn angle (Figure 19c) follows the trend as determined for towed force coefficient since the latter is dominant in its magnitude over side force coefficient, that is, for turn angles smaller than about 10 deg. The influence of deflection on lateral force/drag for a given turn angle (Figure 19d) shows a similar trend to that previously discussed and for the reasons given in paragraph 42.

47. For the 6.00-9, 4-PR tire (Figure 20b), side force coefficient increases with increasing deflection. This can be explained by the fact that with increasing deflection the length of the contact area (Figure 1) increases. This length, together with the sinkage, determines the side force for a given soil strength and load. At the relatively small towed force coefficient indicated (Figure 20a), sinkages are not large for this test condition; thus, the contact length dependent on deflection is dominant, resulting in the family of curves shown in Figure 20b. The relations for the resultant coefficient (Figure 20c) and for lateral force/drag (Figure 20d) follow the same trend and for the same reasons as given in paragraph 42.

48. The trends for trail moment and eccentricity from the results of the tests with the 8.50-10, 8-PR tire are shown in Figure 21. For a given turn angle, the trail moment and eccentricity are positive for low deflections and negative for high deflections, indicating that the resultant moves from the forward position of the tire in contact with the soil (M_t and e are positive; Figure 1) to the rearward position as deflection increases. This also indicates that trail moment and eccentricity are not necessarily zero only at zero turn angle, but that there exist certain combinations of turn angle and deflection for which trail moment and eccentricity are also zero (e.g., $\alpha = 8.5$ deg and $\delta/h = 0.25$, Figure 21).

49. Wheel load. The influence of wheel load on the four

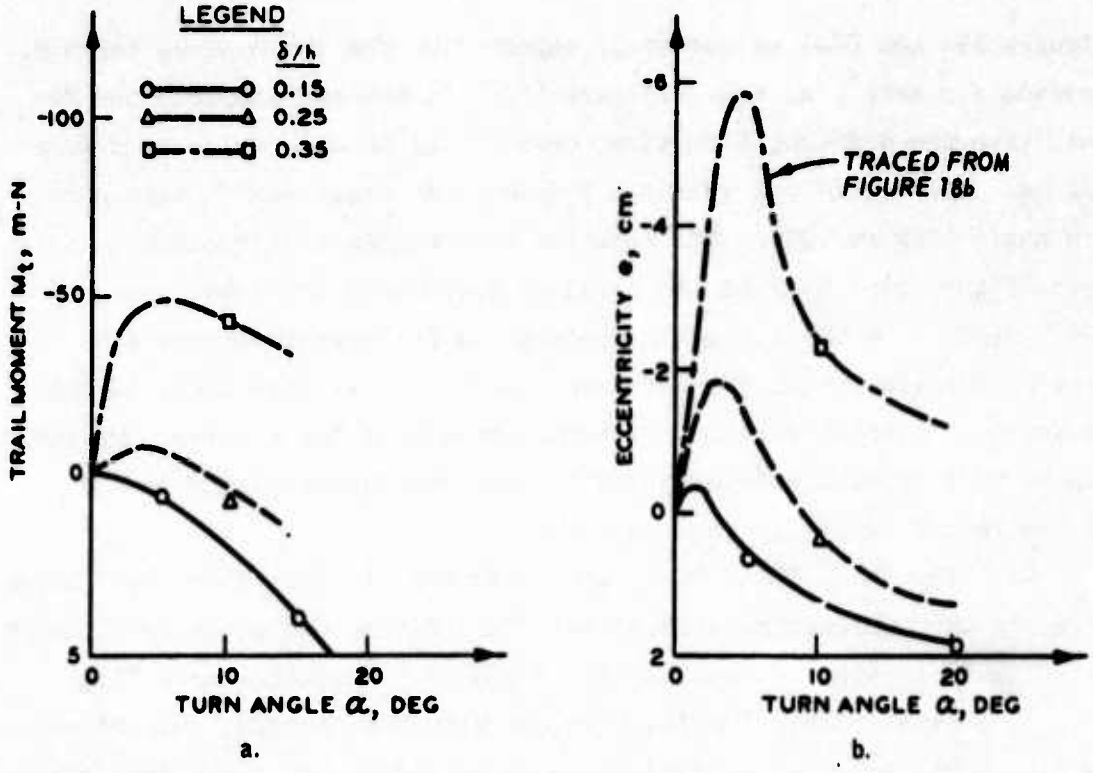

Figure 21. Influence of turn angle and tire deflection on trail moment and eccentricity for 8.50-10, 8-PR tire on clay with average cone penetration resistance C = 350 kPa and design wheel load W' = 5800 N

performance parameters is depicted for various test conditions in Figures 22-25. In all instances towed force coefficient increases at a given turn angle with increasing load (Figures 22a-25a), as expected (Figure 6d). However, side force coefficient shows the reverse trend (Figures 22b-25b), i.e., at a given turn angle the side force coefficient decreases with increasing load. Although this trend also occurred to a small extent in Schwanghart's data (Figure 4b), and therefore does not seem to be too unusual, at least a qualitative explanation for it is deemed necessary.

50. The first step was to find out how side force depends on wheel load for a given test condition. The data collected with the 6.00-9, 4-PR tire operating at a turn angle of 10 deg, at the same tire deflection, and on the same soil strength, but under four different wheel loads (Figure 24b), were plotted as side force versus

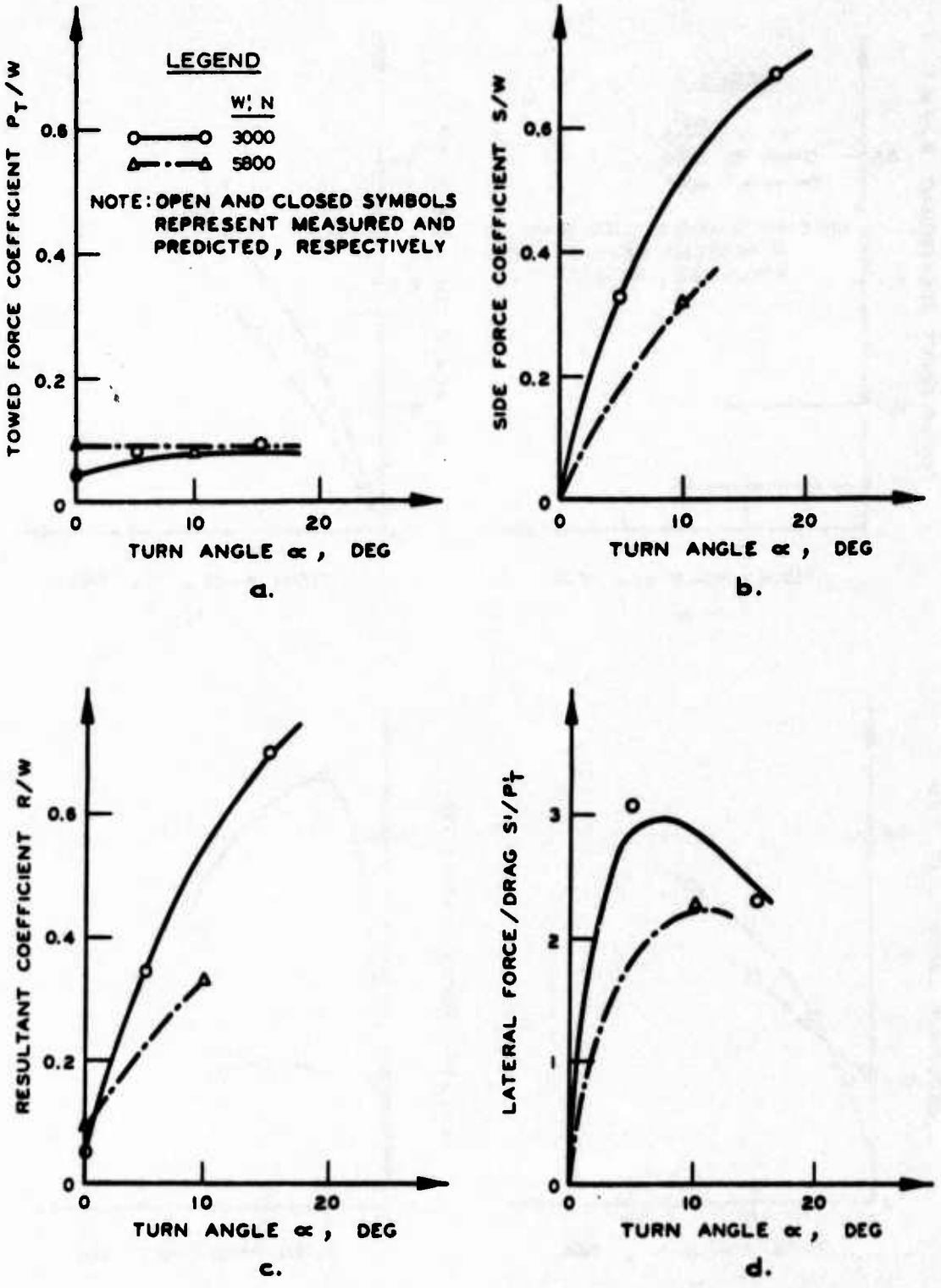

Figure 22. Influence of turn angle and wheel load on performance parameters for 8.50-10, 8-PR tire on clay with tire deflection $\delta/h = 0.35$ and average cone penetration resistance $C = 350$ kPa

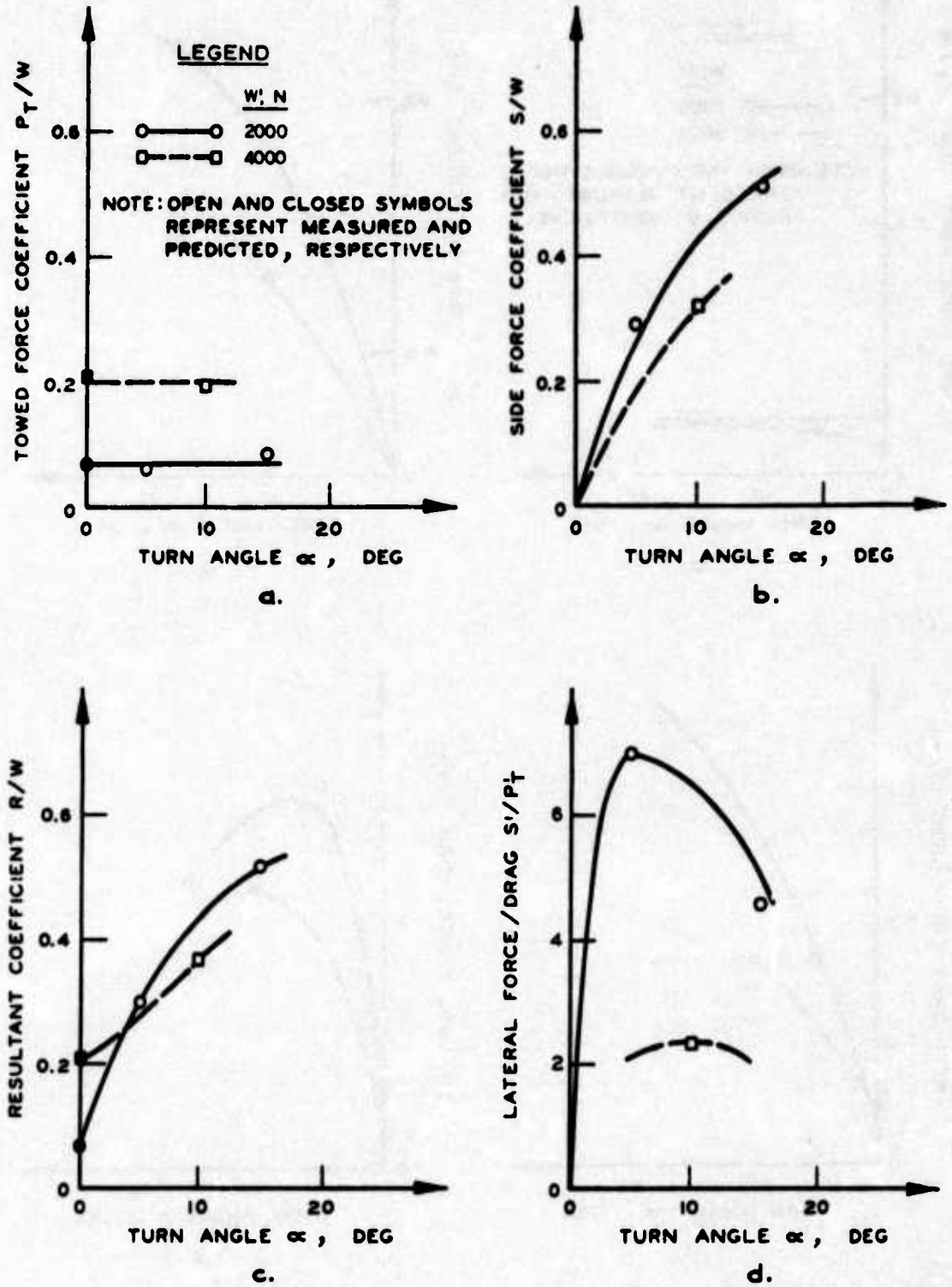

Figure 23. Influence of turn angle and wheel load on performance parameters for 6.00-9, 4-PR tire on clay with tire deflection $\delta/h = 0.15$ and average cone penetration resistance $C = 350$ kPa

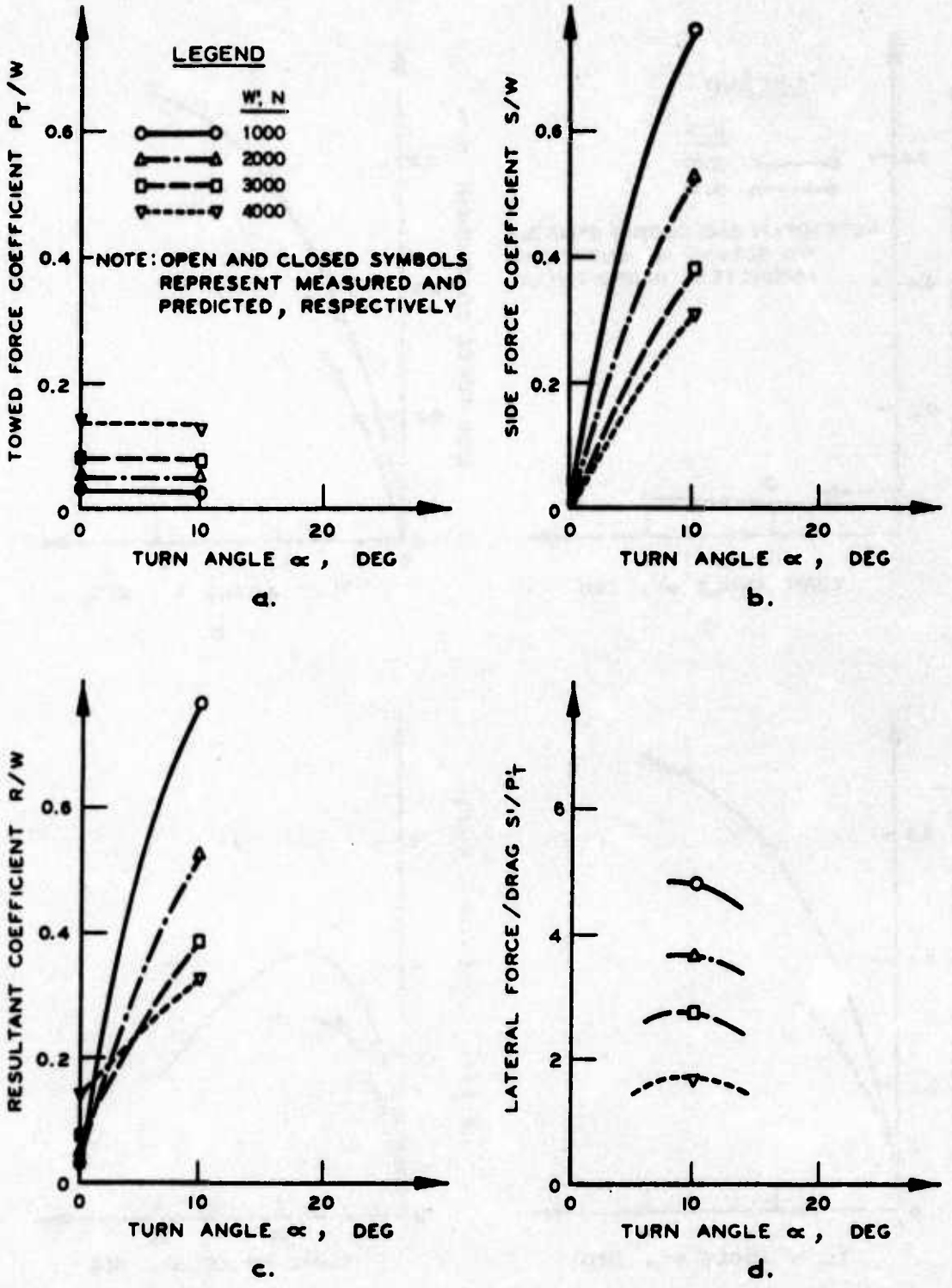

Figure 24. Influence of turn angle and wheel load on performance parameters for 6.00-9, 4-PR tire on clay with tire deflection $\delta/h = 0.25$ and average cone penetration resistance $C = 350$ kPa

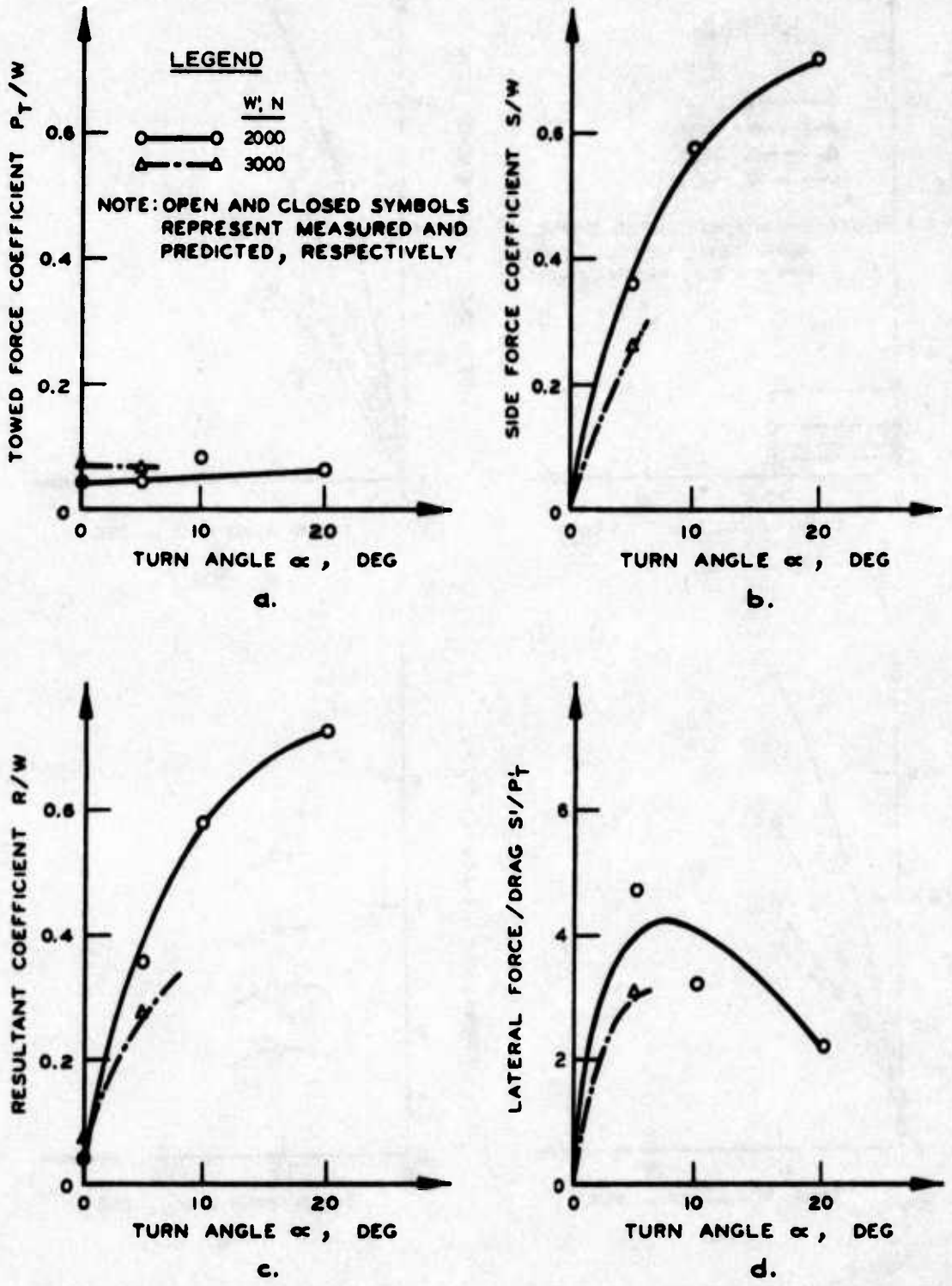

Figure 25. Influence of turn angle and wheel load on performance parameters for 6.00-9, 4-PR tire on clay with tire deflection $\delta/h = 0.35$ and average cone penetration resistance $C = 350$ kPa

load (Figure 26). As expected, side force increases with load; however,

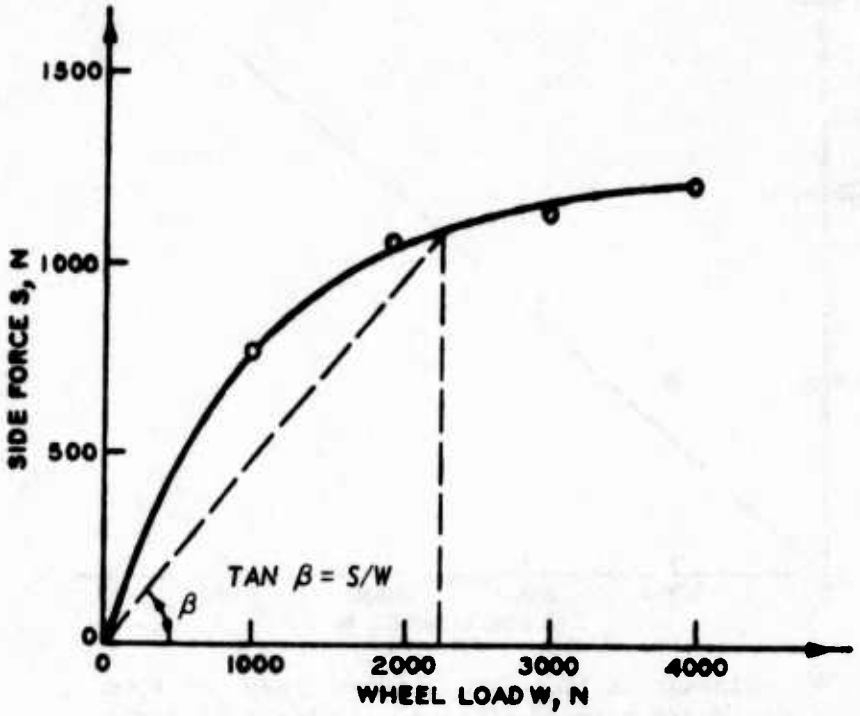

Figure 26. Side force as function of wheel load for 6.00-9, 4-PR tire at 10-deg turn angle on clay with tire deflection $\delta/h = 0.25$ and average cone penetration resistance C = 350 kPa

the rate of increase of side force decreases with increasing load, as was observed originally in Figure 24b.

51. The reason for the above-mentioned trend was sought in the relation between sinkage and wheel load, because only sinkage influences the side force directly if deflection and soil strength are kept constant (Equation 3). Therefore the sinkages in the corresponding tests were plotted versus load (Figure 27). Sinkage increases with load at an approximately linear rate for the specific loads and test conditions of this program. Obviously, there is a load for those test conditions at which the wheel will sink up to the hub, i.e., the bearing capacity of the soil is exceeded and failure by plastic flow of the soil occurs. However, for these test conditions, the sidewall of the tire operating in turned mode deformed by tilting forward toward the direction of travel, resulting in an increase in contact area compared with the

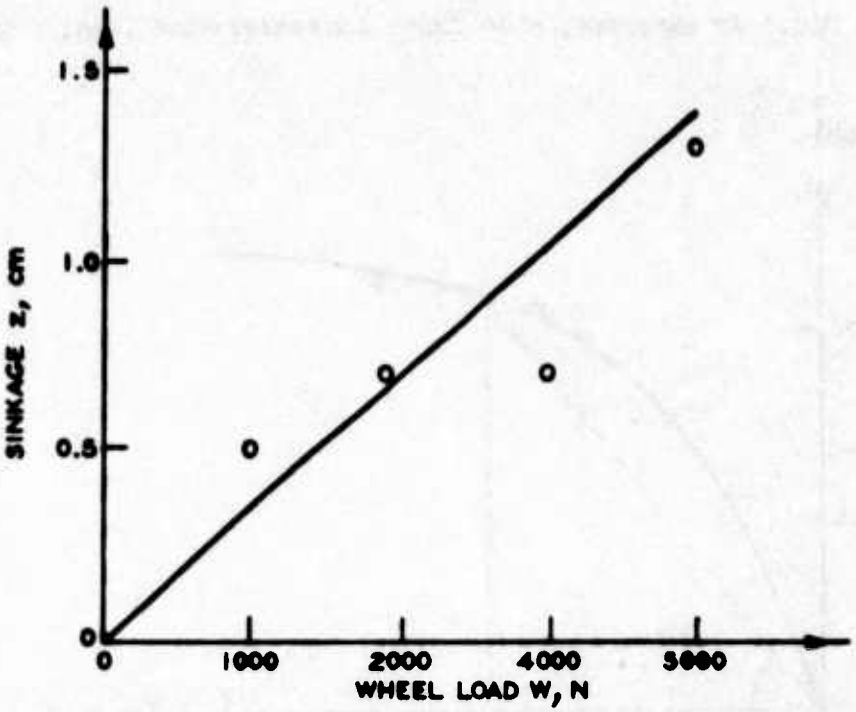

Figure 27. Sinkage as function of wheel load for 6.00-9, 4-PR tire at 10-deg turn angle on clay with tire deflection $\delta/h = 0.25$ and average cone penetration resistance C = 350 kPa

nominal contact area under a static loading condition. As the load is increased from test to test, the tire sidewall deforms more and more, again increasing the contact area. With constant deflection, the nominal contact area is practically constant and independent of wheel load; thus, the increase in actual contact area with increasing load can be assumed to provide so much more supporting area for the wheel load on this cohesive soil that the sinkage increases with load (for the range of wheel loads tested) as shown in Figure 27. Naturally, the influence of wheel load on the side force coefficient is reflected in the relations for resultant coefficient (Figures 22c-25c) and for lateral force/drag (Figures 22d-25d) because of the dominance of side force over towed force.

52. No noticeable separation of the trail moment and eccentricity data by wheel load was observed for the 8.50-10, 8-PR tire (Figure 28), nor for the other two tires. However, the general trend of the relations in Figure 28 is similar to that presented in Figures 18 and 21.

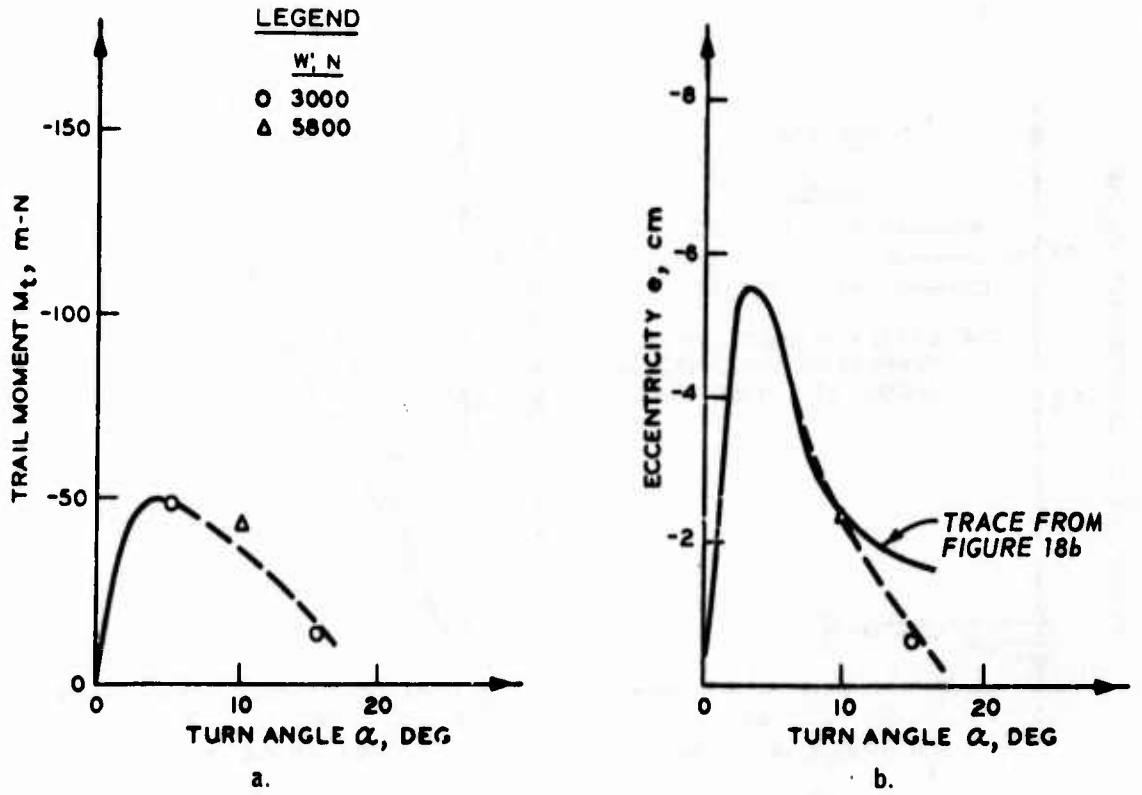

Figure 28. Influence of turn angle and wheel load on trail moment and eccentricity for 8.50-10, 8-PR tire on clay with average cone penetration resistance C = 350 kPa and tire deflection $\delta/h = 0.35$

53. Tire width × diameter. The influence of tire width × diameter (bd) on the relations between each of the four basic performance parameters and the turn angle is demonstrated in Figure 29. Basically, towed force coefficient increases, as expected, with decreasing bd for a given turn angle, although there is considerable data scatter at high values of turn angle (Figure 29a). Contrary to this trend, side force coefficient (Figure 29b) increases with increasing bd for a given turn angle. However, in examining these data it must be noted that for constant deflection, wheel load, and soil strength, and at a given turn angle, the width of the tire influences the development of side forces less than does the length of the contact area (paragraph 12). Also, Schwanghart[13] did not find much influence of tire width on the side force coefficient (paragraph 14, Figure 3b). Thus, the influence of diameter (63 cm for 8.50-10, 8-PR tire; 45 cm for 7.00-6, 6-PR tire;

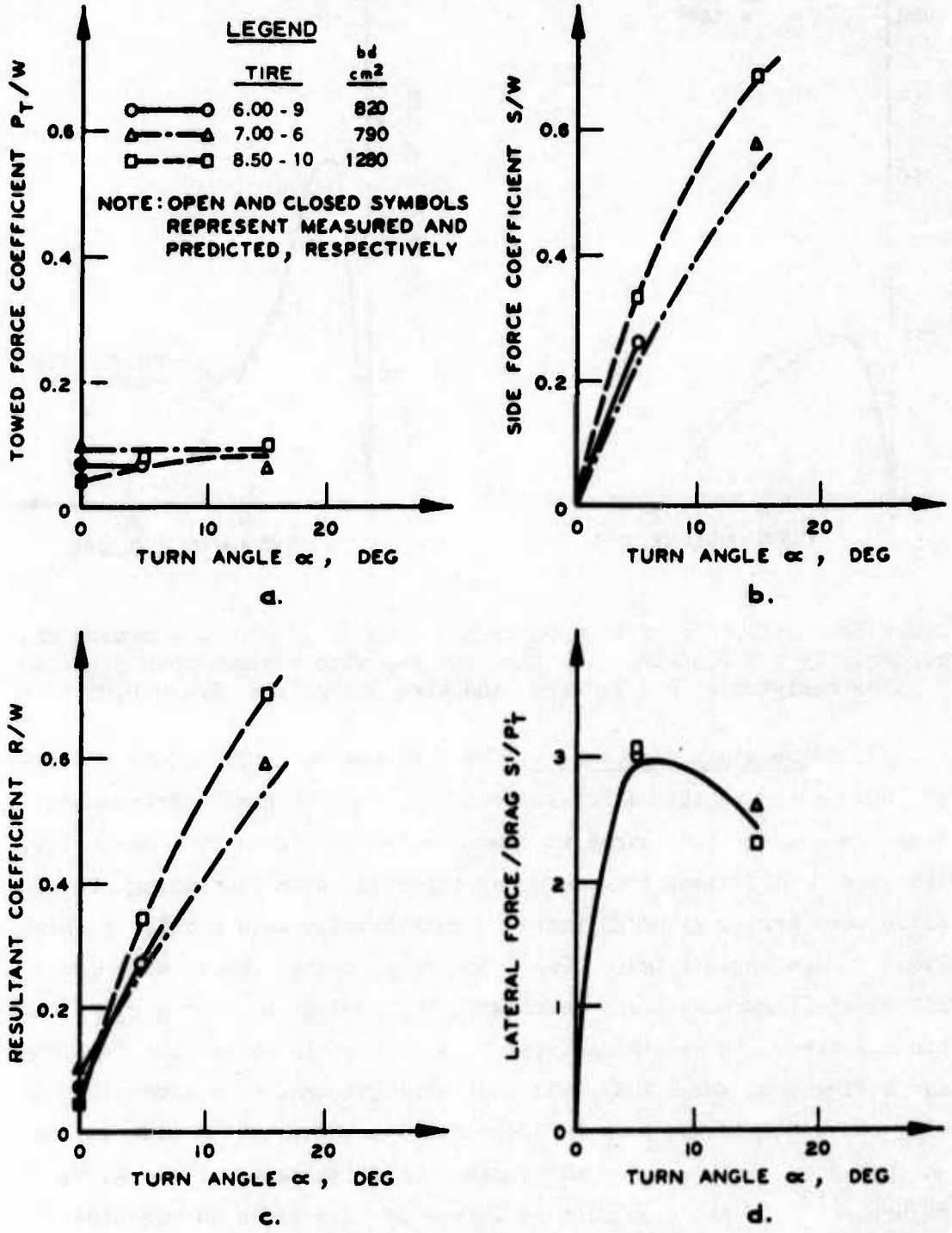

Figure 29. Influence of turn angle and tire width × diameter (bd) on performance parameters for three tires on clay. Tire deflection $\delta/h = 0.35$, average cone penetration resistance $C = 350$ kPa, design wheel load $W = 3000$ N

and 52 cm for 6.00-9, 4-PR tire) is noted primarily in Figure 29b. This, of course, is reasonable, because the diameter is directly related to the length of the contact area, i.e., the latter increases as the diameter increases, all other variables being constant. Thus, for a given turn angle, side force coefficient increases with increasing contact length, i.e., with increasing diameter of the tire.

54. The relations between resultant coefficients and turn angles (Figure 29c) show qualitatively the same trend as in Figure 29b because the side force coefficients are larger than the towed force coefficients, causing the relations for the side force coefficient to be dominant. However, no noticeable separation by bd is observed in the relation between lateral force/drag and turn angle (Figure 29d), which may be attributed at least partially to the data scatter.

55. Data scatter also occurred in the relations of trail moment and eccentricity as functions of turn angle (not shown here for this reason). However, there is a slight indication that trail moment and eccentricity increase with increasing bd for a given turn angle. Generally, the investigation of the influence of tire width and diameter, or even of the product bd, suffers from the fact that only certain restricted sizes of tires could be tested (paragraph 25).

Development of prediction system

56. Justification. The trends of the relations among the four basic performance parameters and the turn angle developed under the various influences of soil strength, tire deflection, wheel load, and the product of tire width and diameter, as discussed in the foregoing paragraphs, seem to justify at least an attempt to establish new relations between performance parameters and the clay mobility number (Equation 1), using the turn angle as an additional independent variable as outlined in paragraphs 36-38. However, this procedure can be justified only within the framework of this pilot study because of the limited range of the individual variables tested.

57. Before the basic prediction system was extended to include turn angle, a last attempt was made to check the feasibility of this approach. Four series of tests that had been conducted with the 8.50-10,

8-PR and 7.00-6, 6-PR tires under two loads, at two deflections, and on two different soil strengths (Figure 30) were investigated. The combinations of the independent variables calculated for each test resulted in clay mobility numbers N_c (Equation 1) that ranged from 2.6 to 3.3 (because the individual independent variables could not be kept exactly constant from test to test), with an average N_c of 3.1.* With N_c almost constant, it should have been possible to describe the results of the four test series using only one relation between each individual performance parameter and turn angle (e.g. between towed force coefficient and turn angle). The results of this attempt are shown in Figure 30. The figure also shows that this approach is reasonably successful, considering that part of the data scatter occurred because N_c was not constant. It was thus concluded that, within the framework of this pilot study, development of the prediction system as described in paragraph 56 is justified.

58. Towed force coefficient. The relation between towed force coefficient (P_T/W) and N_c is shown in Figure 31a. There is no clear separation by turn angle. The solid line represents the same relation as found for $\alpha = 0$ deg (Figure 6d), and the dashed lines indicate the boundaries given by one standard deviation as evaluated for the original data ($\alpha = 0$ deg).[21] Although the data points of this study seem to lie on the lower side between $N_c = 2.5$ and $N_c = 3.5$, it still seems justifiable to use only one relation between P_T/W and N_c, because about 70 percent of the data points fall into the band formed by one standard deviation. The fact that, in most cases, P_T/W is more or less independent of α was observed earlier (e.g. Figure 16a).

59. Side force coefficient. The relation between side force coefficient (S/W) and N_c shows the expected dependency on α (Figure 31b). For a given N_c, S/W increases with increasing α; for a given α, S/W increases with increasing N_c (because of increasing soil strength C, Figure 16b).

---

* If compared with the relation between P_T/W and N_c for $\alpha = 0$ deg (Figure 6d), this magnitude of N_c can be considered as characterizing a rather critical condition.

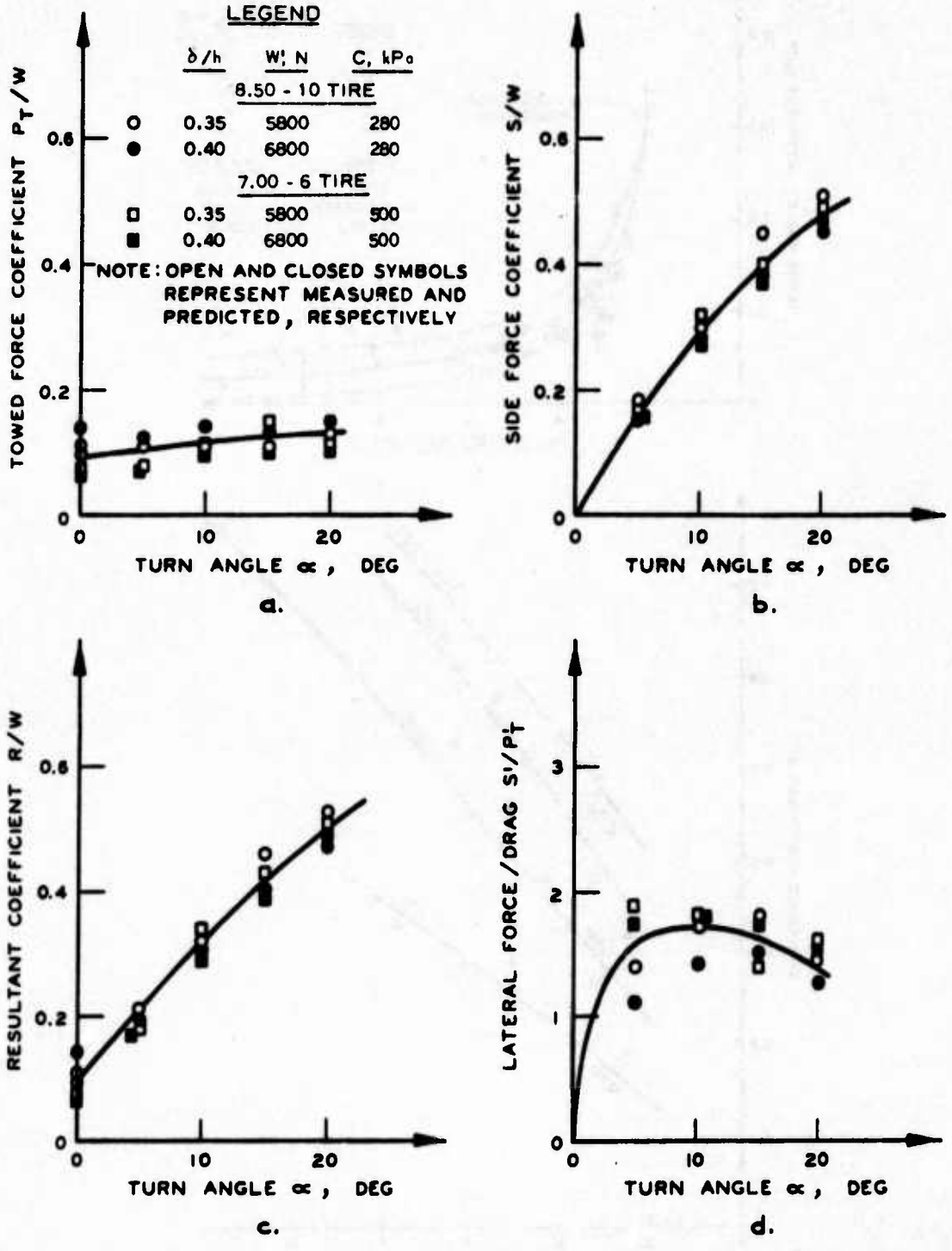

Figure 30. Relations between turn angle and performance parameters for two tires tested at various conditions resulting in an average clay mobility number (N_c) of 3.1

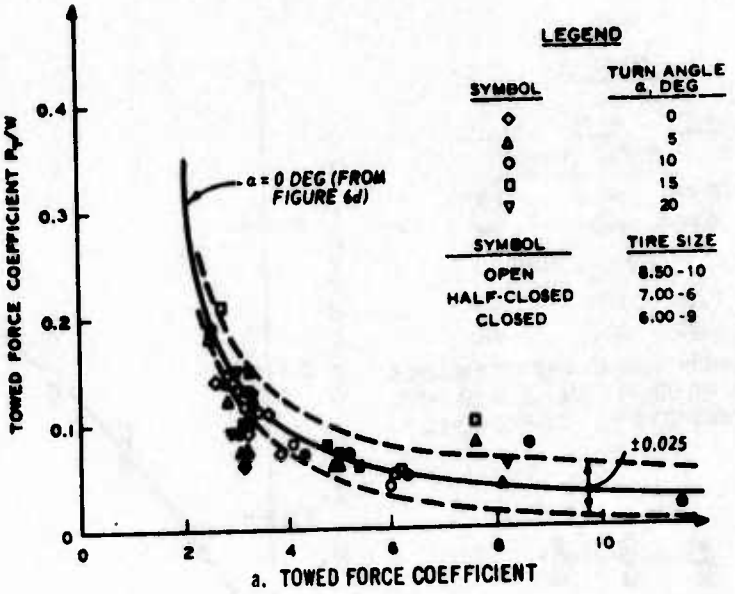

a. TOWED FORCE COEFFICIENT

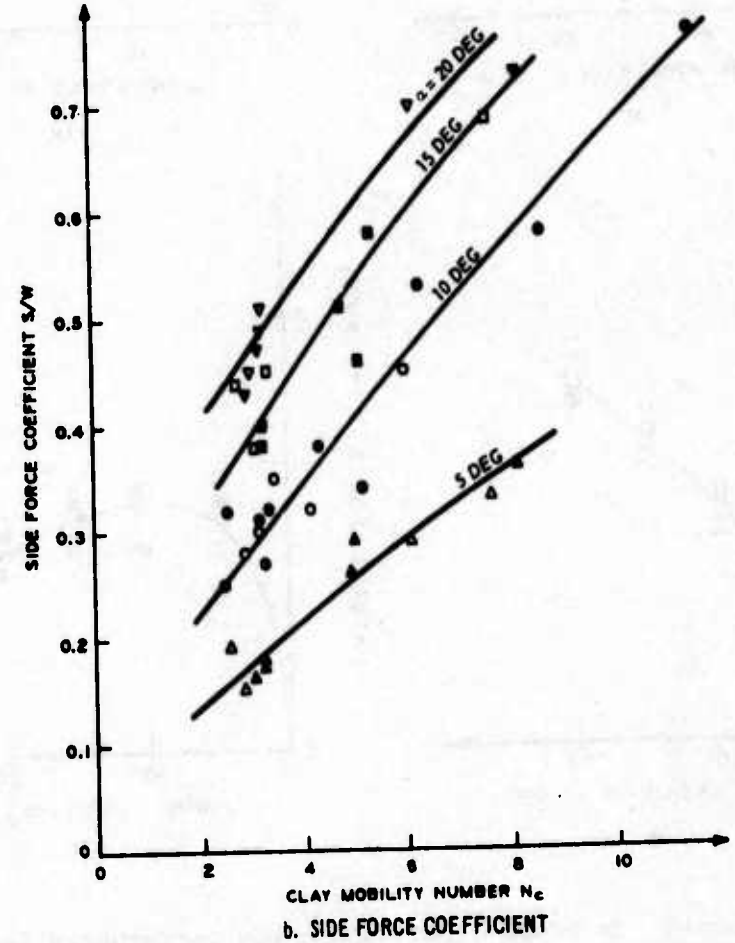

b. SIDE FORCE COEFFICIENT

Figure 31. Performance parameters as functions of clay mobility number and turn angle, three tires (sheet 1 of 3)

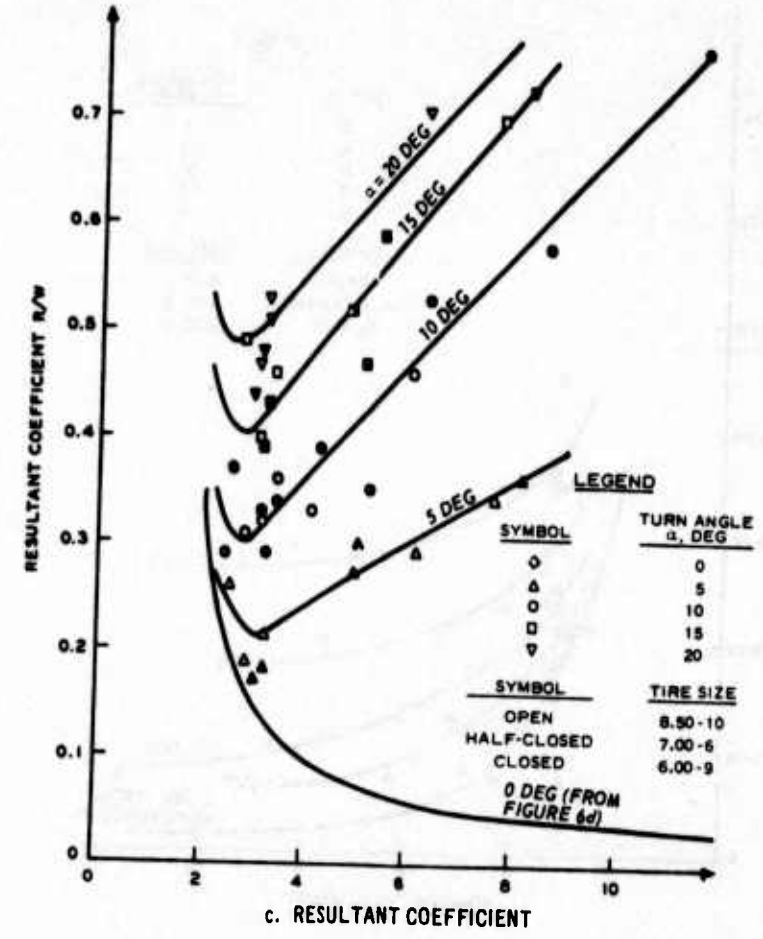

c. RESULTANT COEFFICIENT

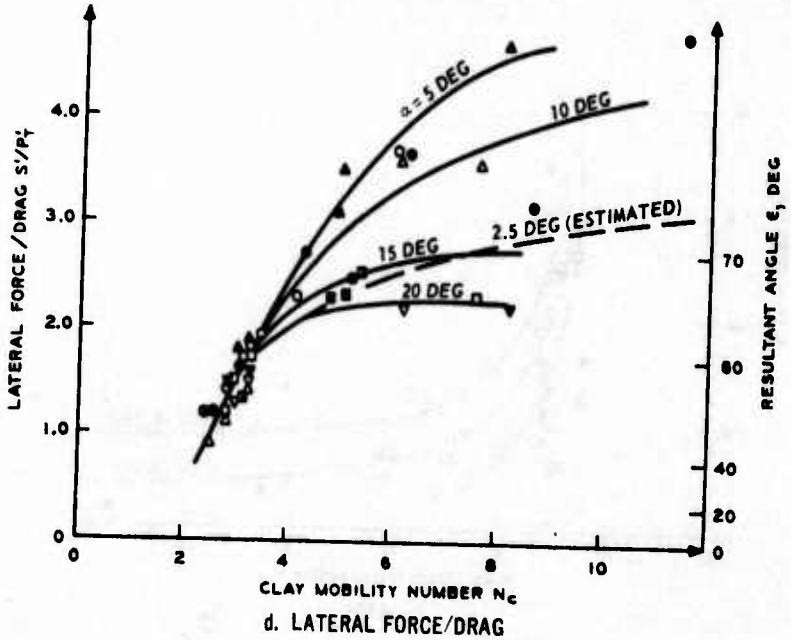

d. LATERAL FORCE/DRAG

Figure 31 (sheet 2 of 3)

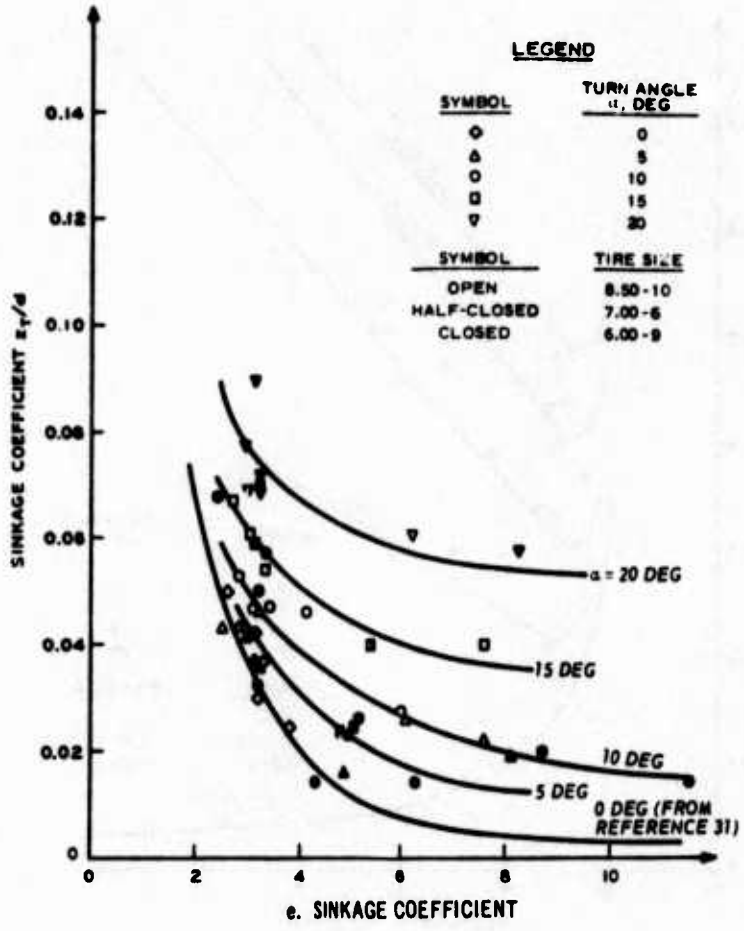

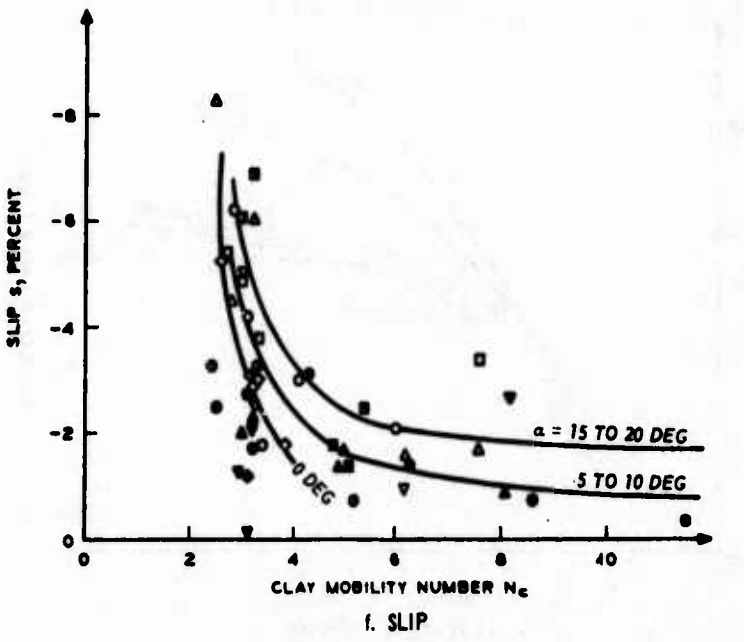

Figure 31 (sheet 3 of 3)

60. Resultant coefficient. Resultant coefficient (R/W) as a function of N_c and α is shown in Figure 31c. This family of curves reflects the combinations of trends observed in Figures 31a and 31b. For example, for α = 5 deg, the influence of P_T/W is dominant for N_c smaller than about 3.0, and R/W decreases with increasing N_c (because of increasing soil strength; paragraph 22 and Figures 16c and 17c). For larger values of N_c, the influence of S/W becomes dominant, and R/W increases with increasing N_c. Where S/W is no longer dominant, the value of N_c decreases slightly with increasing α (e.g. N_c = 3.0 for α = 5 deg, and N_c = 2.6 for α = 20 deg). Furthermore, for any given N_c, R/W increases with increasing α.

61. Lateral force/drag. As in the relation for resultant coefficient, the relations among lateral force/drag (S'/P'_T) (and resultant angle ϵ), N_c, and α could be separated into two zones below and above N_c = 3.5 (Figure 31d). For N_c smaller than about 3.0, the influence of P_T/W is dominant; for all practical purposes, S'/P'_T increases with increasing N_c and is independent of the turn angle. For larger N_c values, the influence of S/W becomes dominant; within this zone, S'/P'_T increases with decreasing α, for a given N_c, down to turn angles of about 5 deg. For smaller turn angles, S'/P'_T decreases again, reflecting the bell-shaped relation between S'/P'_T and α observed earlier (Figure 16d). Note, however, the relatively large scatter in the data for N_c larger than about 3.0, which is partially caused by the occurrence of the maximum for S'/P'_T versus α relations at different α, dependent on soil strength (Figure 16d), deflection (Figure 19d), or wheel load (Figure 22d). Nevertheless, Figure 31d serves for demonstration purposes at this point. In an actual prediction, S'/P'_T would be calculated from the relations established for the prediction of P_T/W and S/W (Figures 31a and 31b; paragraphs 33 and 34) to avoid any errors that might have been built into Figure 31d by using a cross-plotting technique.*

* To plot S'/P'_T versus α for given values of N_c would not have helped to reduce the scatter, because various values of N_c would have had to be interpolated.

62. Sinkage coefficient. Sinkage coefficient (z_T/d) as a function of N_c and α is depicted in Figure 31e. For a given turn angle, z_T/d decreases with increasing N_c (because of increasing soil strength). For a given clay mobility number, z_T/d increases with increasing α. However, there seems to be some unexpected scatter in the data, probably because a method was used to calculate sinkage from the measured movement of the wheel hub, which originally was developed for the condition of $\alpha = 0$ deg (paragraph 36). Nevertheless, sinkage values calculated from hub movements are considered more realistic than actual values of hub movement, which, at least for $\alpha = 0$ deg, were found to be an unsuitable representation of sinkage.[28]

63. Slip. The relations among slip, clay mobility number, and turn angle are not very well defined by the available data. However, the data can be grouped according to ranges of α (Figure 31f). This makes possible an estimate of slip for turn angles of 0, 5-10, and 15-20 deg. For a given α, slip decreases with increasing N_c (because of increasing soil strength), as expected. Furthermore, for a given N_c, slip increases with increasing α.

64. Summary. For the range of conditions tested in this study, relations were established for the four performance parameters under consideration as functions of clay mobility number and turn angle. The relations for determination of towed force and side force coefficients (Figures 31a and 31b) appear to be reasonably accurate. Therefore, they should also be used to calculate the resultant coefficient and the lateral force/drag, if this becomes necessary. However, for estimation purposes, the relations established for the latter two parameters (Figures 31c and 31d) can also be used. Also, relations were established for estimating sinkage coefficient (Figure 31e) and slip (Figure 31f).

Tests in Sand

Factors influencing performance

65. Velocity. Based on the considerations of the influence of

the translational velocities of the carriage or wheel discussed in the interpretation of the clay data (paragraphs 39-40) and on results previously found for cohesionless soils (Reference 18, Plate 6; Reference 20), it can be assumed that the influence of the translational velocity of the carriage and, therefore, the corresponding velocity of the wheel, would not affect the four basic performance parameters, at least for the range of velocity from 1.5 to 3.0 m/sec. Results from the few tests conducted with the 8.50-10, 8-PR and 6.00-9, 4-PR tires under comparable test conditions, but at carriage velocities of 1.5 and 3.0 m/sec, are presented in Figure 32. Comparison of these relations does not show any noticeable influence of carriage velocity on the four basic performance parameters. Therefore, in further analysis, the data from the tests conducted at 1.5 m/sec are treated, without modification, like the data from tests conducted at 3.0 m/sec. Furthermore, it seemed justifiable to use the prediction system developed for carriage speed of 1.5 m/sec (paragraphs 18-19, Figure 7d) without major modifications* as a valid system for zero turn angles (see for instance closed symbols in Figure 33a).

66. Soil strength. The influence of soil strength on the four basic performance parameters is depicted in Figure 33 for tests conducted with the 8.50-10, 8-PR tire and in Figure 34 for tests with the 6.00-9, 4-PR tire. Towed force, side force, and consequently, resultant force coefficients (P_T/W , S/W , and R/W , respectively) increase with increasing turn angle for a given soil strength (Figures 33a-33c and 34a-34c), whereas the relation of lateral force/drag (S'/P'_T) to turn angle α shows the characteristic bell-shaped trend (Figures 33d and 34d), as was observed for clay (Figure 16d). The rate of increase with α is smallest for P_T/W and largest for S/W .

67. For a given turn angle, P_T/W decreases with increasing soil strength (Figures 33a and 34a), as expected, based on the trend of the original prediction curve developed for zero turn angle (Figure 7d). However, as for clay (Figure 16b), S/W increases with increasing soil

* The only modification that had to be made consisted of an adjustment of the strength gradient G to take care of some differences in mortar and Yuma sands. This modification is described in paragraph 79.

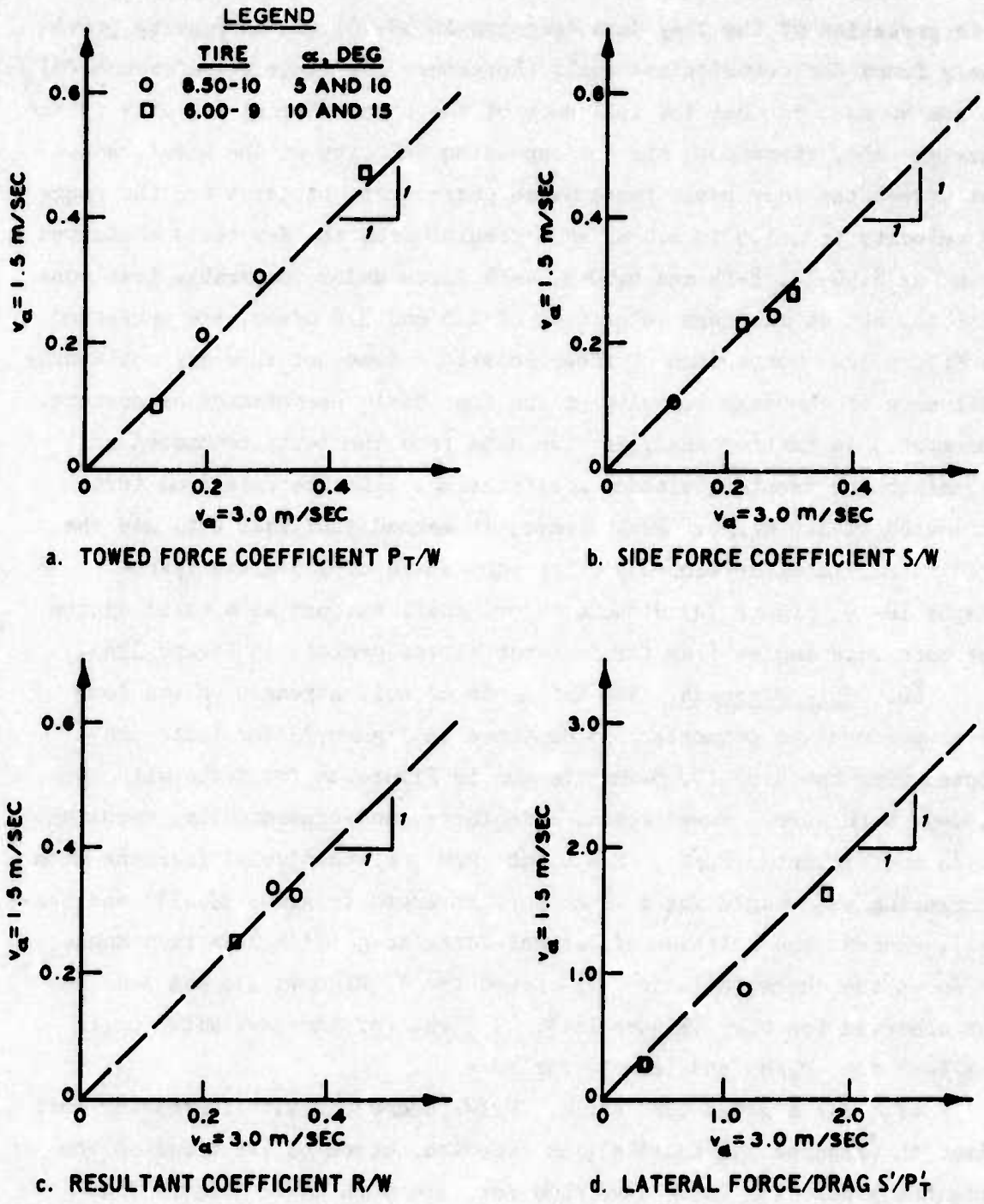

Figure 32. Comparison of performance parameters of 8.50-10, 8-PR and 6.00-9, 4-PR tires operating under similar conditions at carriage speeds (v_a) of 3.0 m/sec and 1.5 m/sec on mortar sand

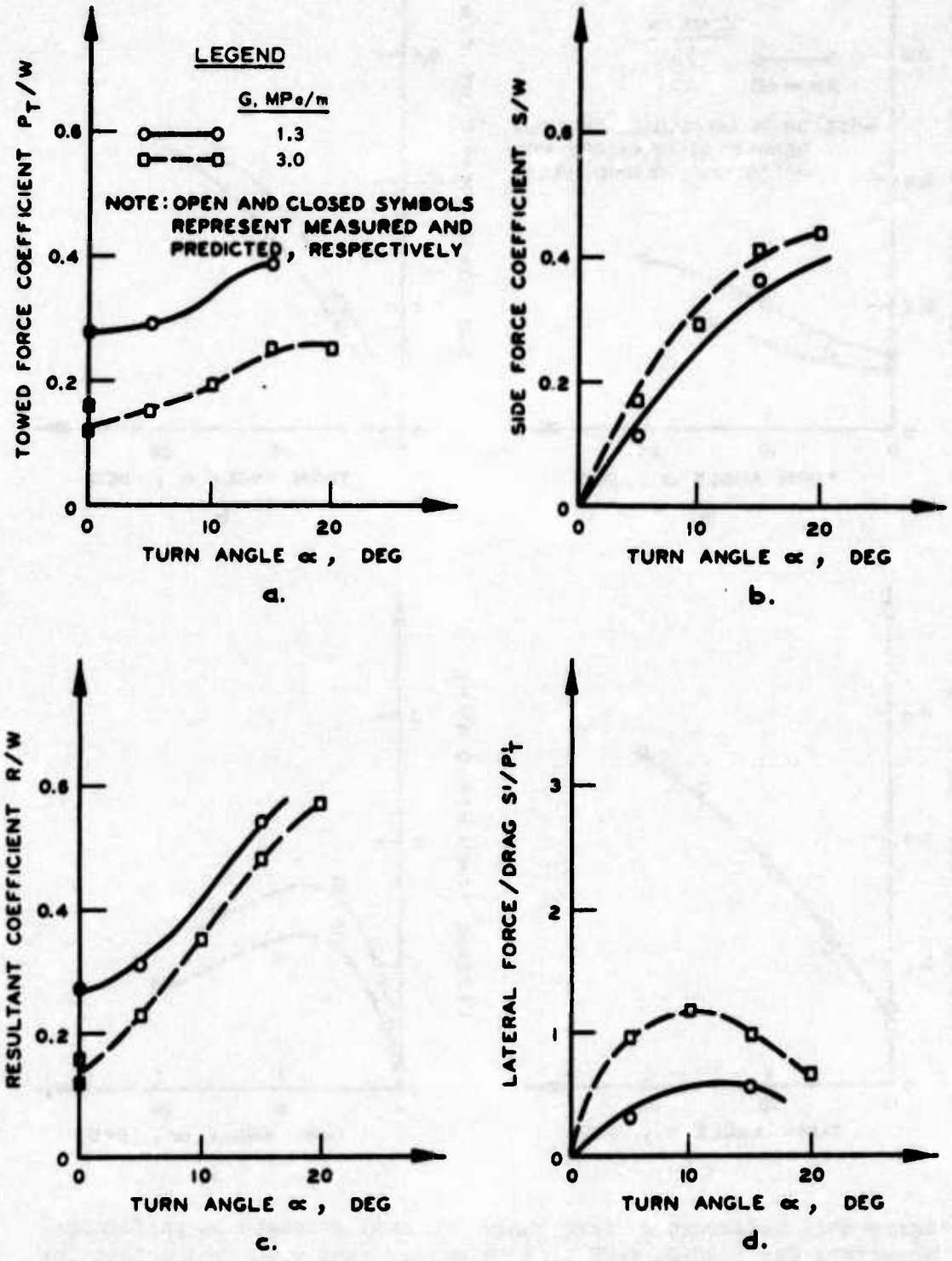

Figure 33. Influence of turn angle and soil strength on performance parameters for 8.50-10, 8-PR tire on mortar sand with tire deflection $\delta/h = 0.35$ and design wheel load $W' = 4000$ N

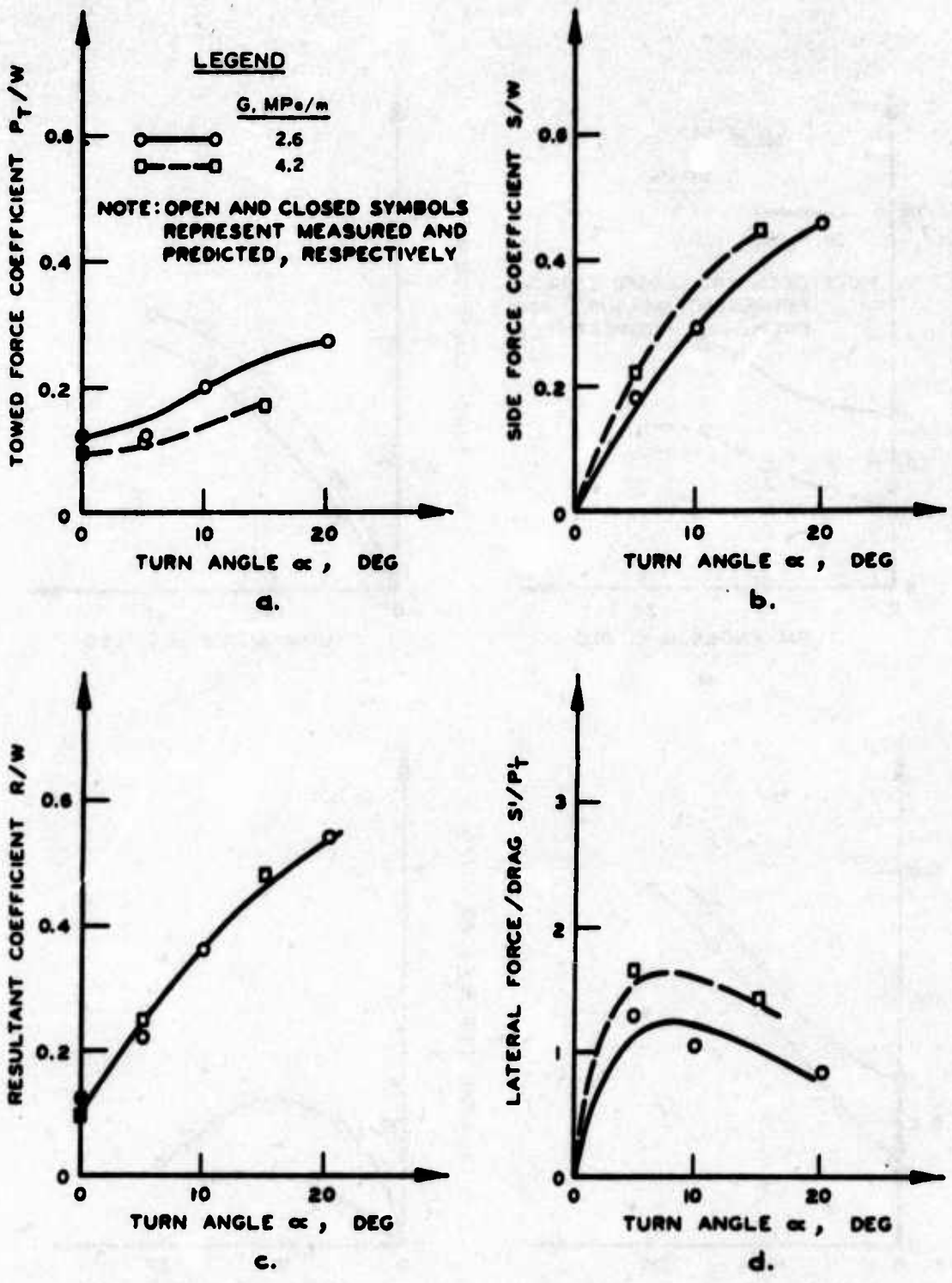

Figure 34. Influence of turn angle and soil strength on performance parameters for 6.00-9, 4-PR tire on mortar sand with tire deflection $\delta/h = 0.35$ and design wheel load $W' = 2000$ N

strength (Figures 33b and 34b). This can be explained by reasoning similar to that used for clay (paragraph 43); that is, the stronger soil offers a greater resistance to lateral movement of the tire than the softer soil, although the sinkage may be more in the latter soil.

68. Also, for a given turn angle, the influence of P_T/W on the resultant coefficient (R/W) is larger (large sinkages) than the influence of S/W . In the case of the 8.50-10, 8-PR tire, P_T/W is dominant with the result that, for a given turn angle, R/W increases with decreasing soil strength (Figure 33c). In the case of the 6.00-9, 4-PR tire, the influence of P_T/W is at least strong enough to compensate for the opposing effect of S/W , so that the relation between R/W and α is independent of soil strength (Figure 34c). The relations between S'/P'_T and α , however, maintain the trend of the side force coefficient: For a given α , S'/P'_T increases with increasing soil strength (Figures 33d and 34d), as was observed for clay (Figure 16d).

69. The influence of soil strength on trail moment and eccentricity is demonstrated (Figure 35) with the results from the same tests

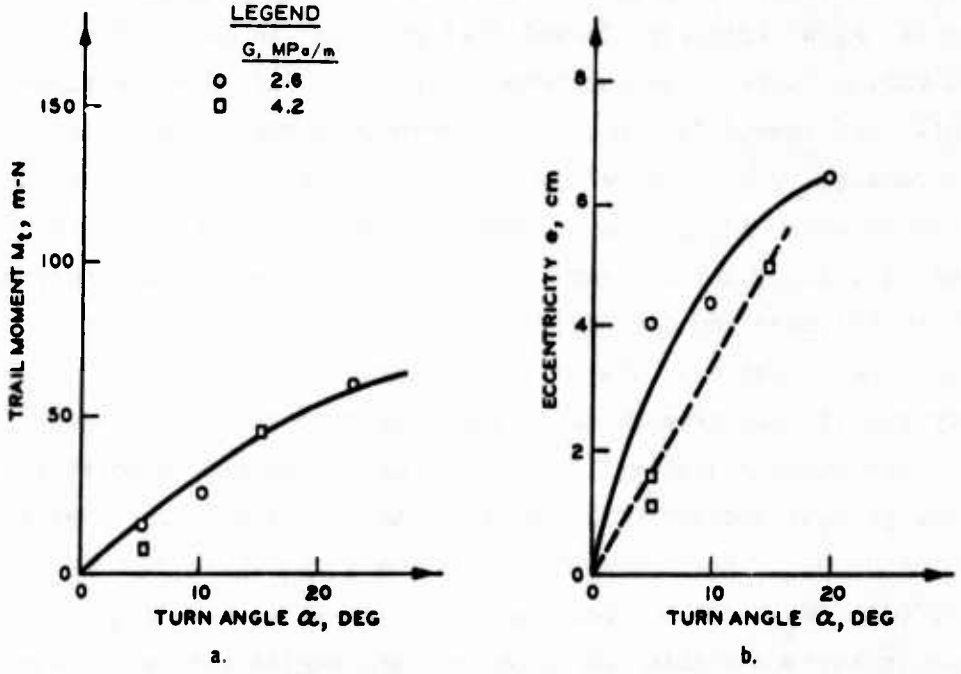

Figure 35. Influence of turn angle and soil strength on trail moment and eccentricity for 6.00-9, 4-PR tire on mortar sand with tire deflection $\delta/h = 0.35$ and design wheel load $W' = 2000$ N

with the 6.00-9, 4-PR tire as those in the foregoing paragraphs. Although there is a slight trend for separation by soil strength, it is not distinct enough to draw any definite conclusions. It must be mentioned, however, that in contrast to the results in clay (Figure 18), M_t and e increase continuously with increasing α without reaching a maximum, within the range of turn angles tested. Furthermore, both M_t and e remain positive, indicating that the resultant R (Figure 1) acts on the tire in front of the center of the wheel.

70. Tire deflection. The influence of tire deflection (δ/h) on the performance parameters is shown in Figure 36 for tests with the 8.50-10, 8-PR tire, and in Figure 37 for tests with the 6.00-9, 4-PR tire. In both cases, P_T/W increases with decreasing δ/h for a given turn angle (Figures 36a and 37a), and the reverse trend is observed in the relations between S/W and α. The reasons for the latter are the same as given during the discussion of the clay data (paragraph 46): With increasing deflection, the length of the tire contact area increases and contributes to the increase of the side force.

71. As in the influence of soil strength (paragraph 68), the influence of P_T/W (Figures 36a and 37a) on R/W is larger for the range of turn angles tested than the reverse influence of S/W (Figures 36b and 37b). The result is that, for a given turn angle, R/W increases with decreasing δ/h (Figures 36c and 37c). On the other hand, the relations between S'/P'_T and α show the same trend as those between S/W and α, i.e., for a given α, S'/P'_T increases with increasing deflection (Figures 36d and 37d).

72. The relations between trail moment and turn angle did not show any significant separation of the data by deflection (Figure 38a). On the other hand, a distinct separation by deflection is noted in the relations between eccentricity and turn angle (Figure 38b). Again, as in the influence of soil strength on M_t and e (paragraph 69, Figure 35), both M_t and e increase with increasing turn angle but do not reach a maximum within the range of turn angles tested. Presumably they reach a maximum at still higher angles since both should turn to zero when the turn angle reaches 90 deg.

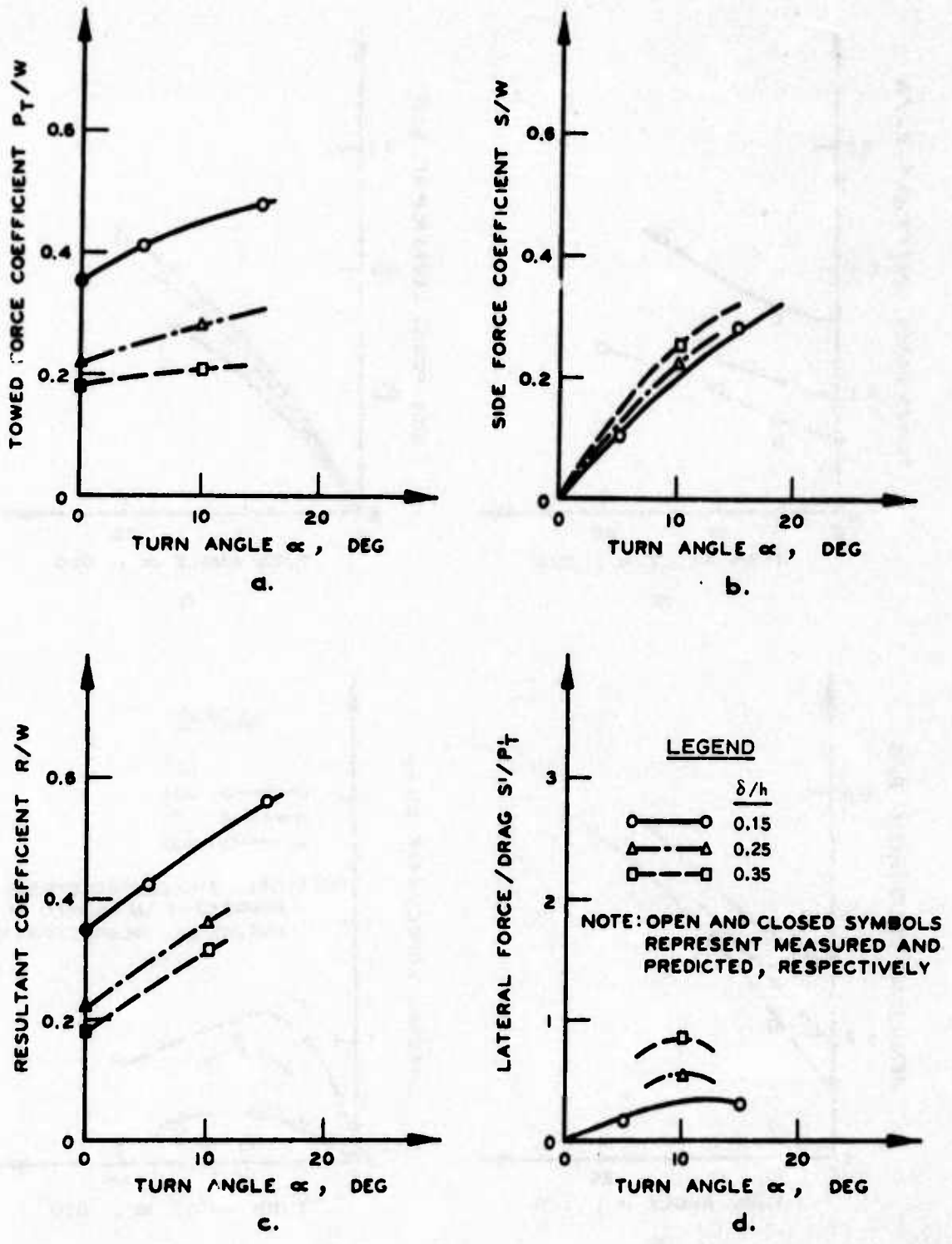

Figure 36. Influence of turn angle and deflection on performance parameters for 8.50-10, 8-PR tire on mortar sand with average penetration resistance gradient G = 2.6 MPa/m and design wheel load W' = 4000 N

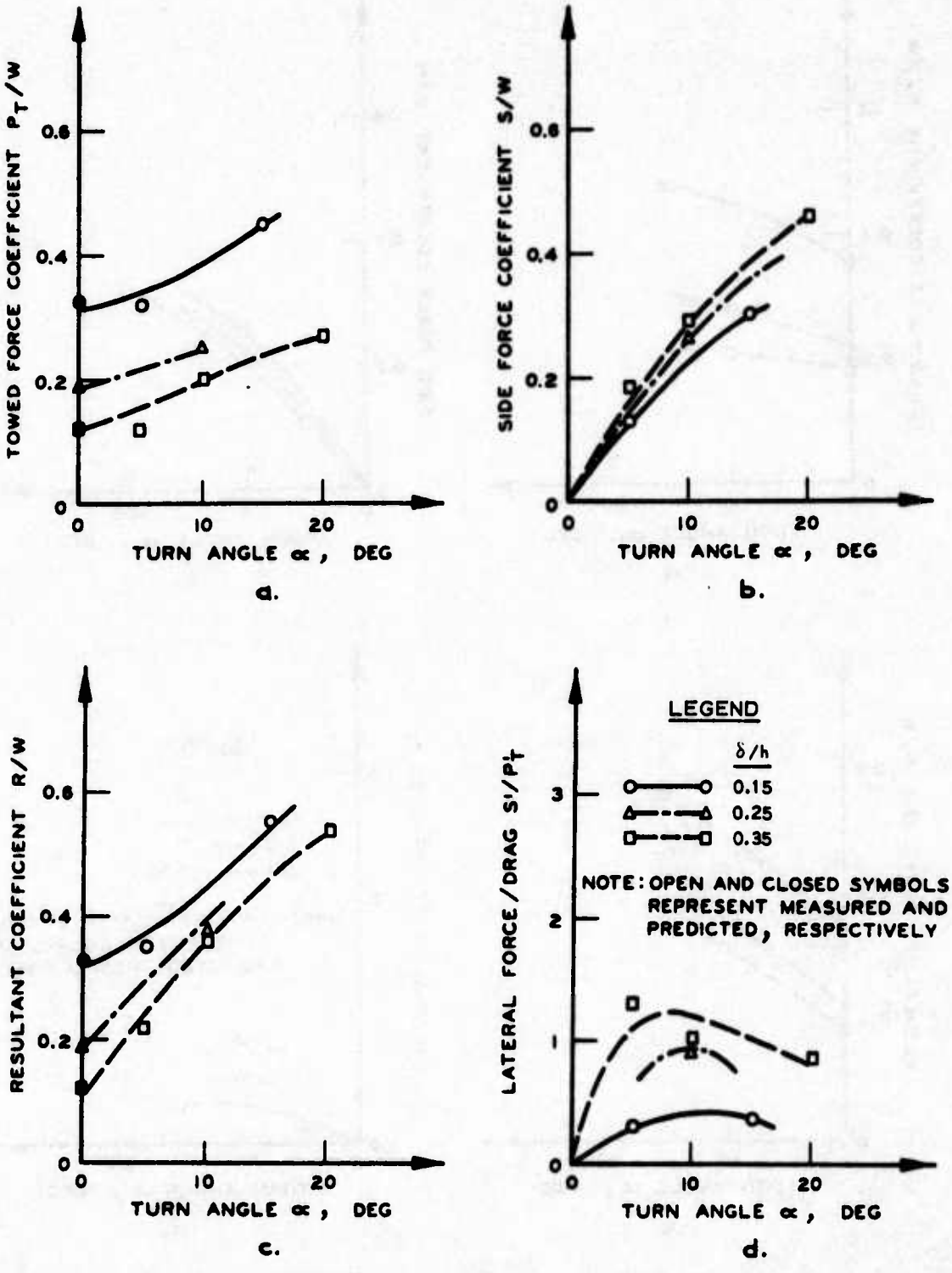

Figure 37. Influence of turn angle and deflection on performance parameters for 6.00-9, 4-PR tire on mortar sand with average penetration resistance gradient G = 2.6 MPa/m and design wheel load W' = 2000 N

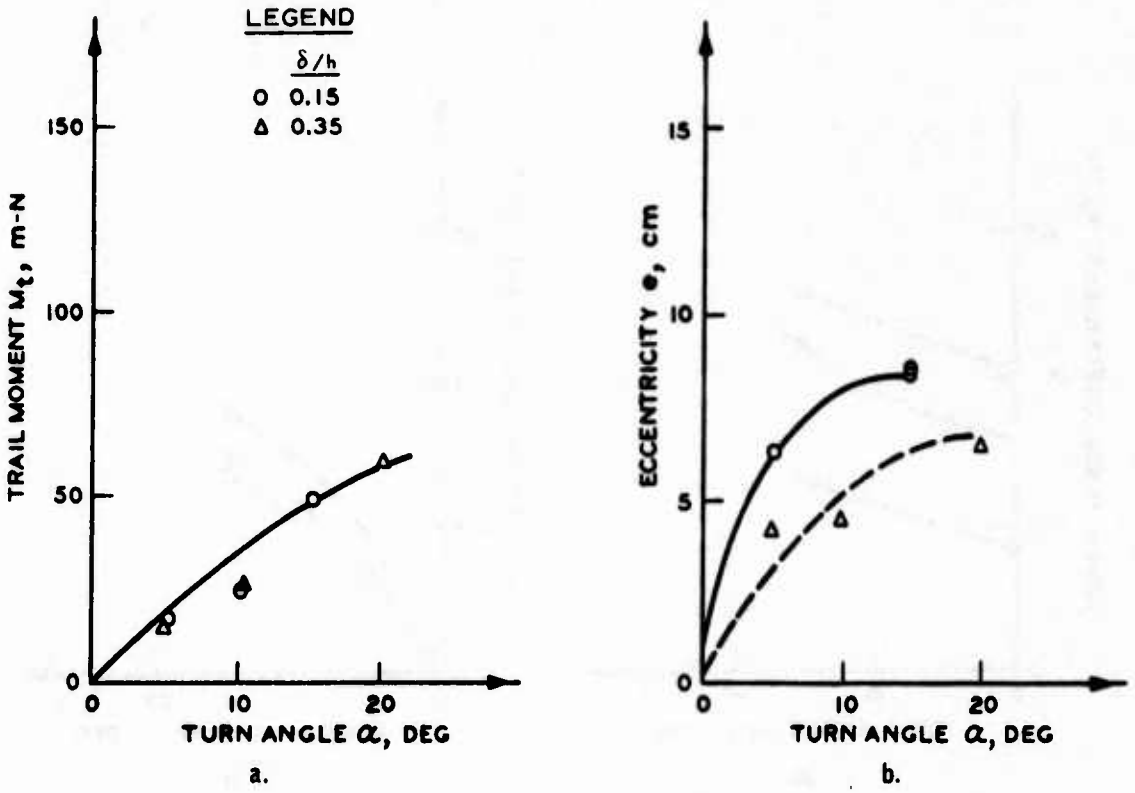

Figure 38. Influence of turn angle and deflection on trail moment and eccentricity for 6.00-9, 4-PR tire on mortar sand with average penetration resistance gradient G = 2.6 MPa/m and design wheel load W' = 2000 N

73. Wheel load. The influence of wheel load on the four basic performance parameters is demonstrated with results of a few tests with the 6.00-9, 4-PR tire (Figure 39). For a given turn angle, P_T/W increases with increasing wheel load (Figure 39a), as expected from the trend of the relation between P_T/W and N_s for $\alpha = 0$ deg (Figure 7d). Also, for a given load, P_T/W increases with increasing turn angle. However, the rate of increase is less than for the relations between S/W and α (Figure 39b). In the latter case, S/W increases for a given turn angle as the wheel load decreases.

74. Although the increase of S/W with decreasing load for a given turn angle is much smaller (Figure 39b) than it is for corresponding relations in clay, where S/W is dominant over P_T/W (Figures 22-25), the same reasoning can be used to explain this trend qualitatively (paragraphs 50-51). Figure 40 shows the relation between side force (S)

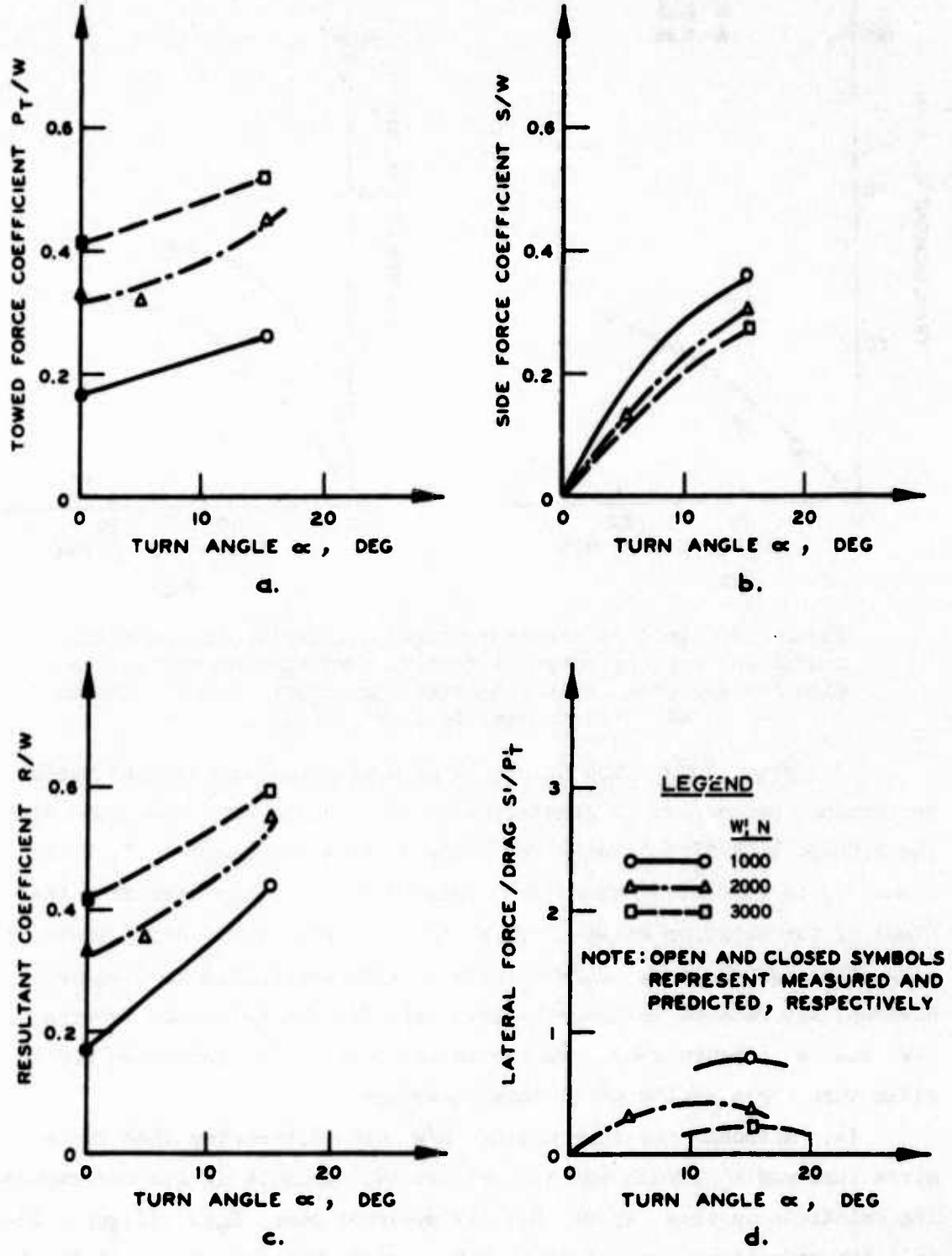

Figure 39. Influence of turn angle and wheel load on performance parameters for 6.00-9, 4-PR tire on mortar sand with average penetration resistance gradient G = 2.6 MPa/m and tire deflection $\delta/h = 0.15$

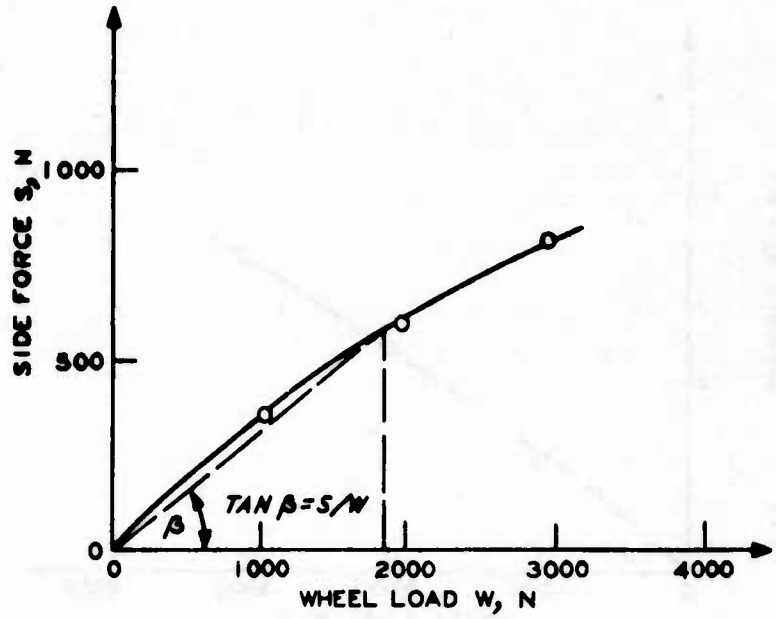

Figure 40. Side force as function of wheel load for 6.00-9, 4-PR tire at 15-deg turn angle on mortar sand with tire deflection $\delta/h = 0.15$ and average penetration resistance gradient $G = 2.6$ MPa/m

and wheel load (W) for the tests conducted at 15-deg turn angle (Figure 39). This relation demonstrates the rate of increase in S with increasing W , or the decrease in S/W with increasing W . This trend was, of course, predetermined by the trend developed between sinkage and wheel load (Figure 41; see also paragraph 51 for same effect in clay).

75. Trail moment (M_t) and eccentricity (e) as functions of turn angle (α) show a distinct separation by wheel load (Figure 42). For a given turn angle, M_t and e increase with increasing load. For a given wheel load, M_t and e increase with increasing turn angle, as was observed during the discussion of the influences of soil strength (paragraph 69) and deflection (paragraph 72). This, and the fact that in most of the tests the resultant acted on the tire in front of the wheel center (positive M_t and e ; Figure 1), seems to be characteristic of tire performance in sand, at least for the conditions tested.

76. Tire width × diameter. Unfortunately, the influence of this parameter (bd) on the performance parameters could not be investigated

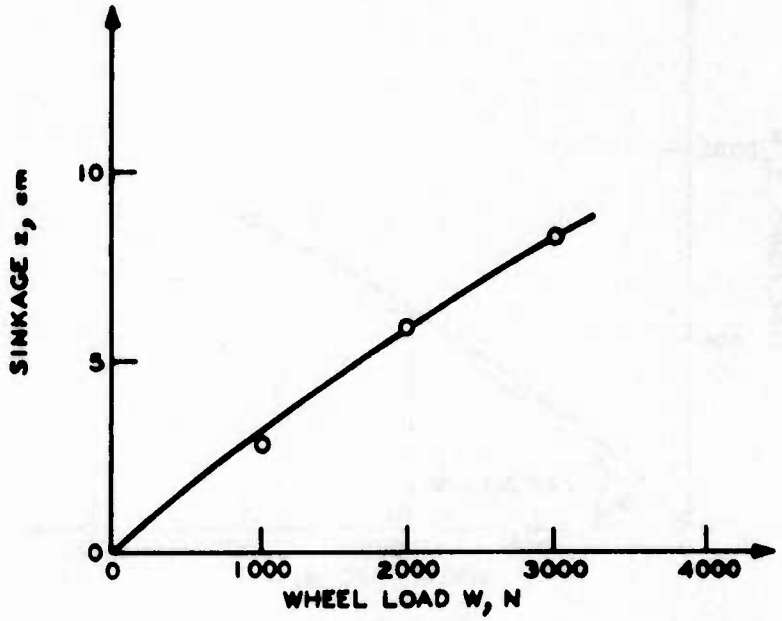

Figure 41. Sinkage as function of wheel load for 6.00-9, 4-PR tire at 15-deg turn angle on mortar sand with tire deflection $\delta/h = 0.15$ and average penetration resistance gradient $G = 2.6$ MPa/m

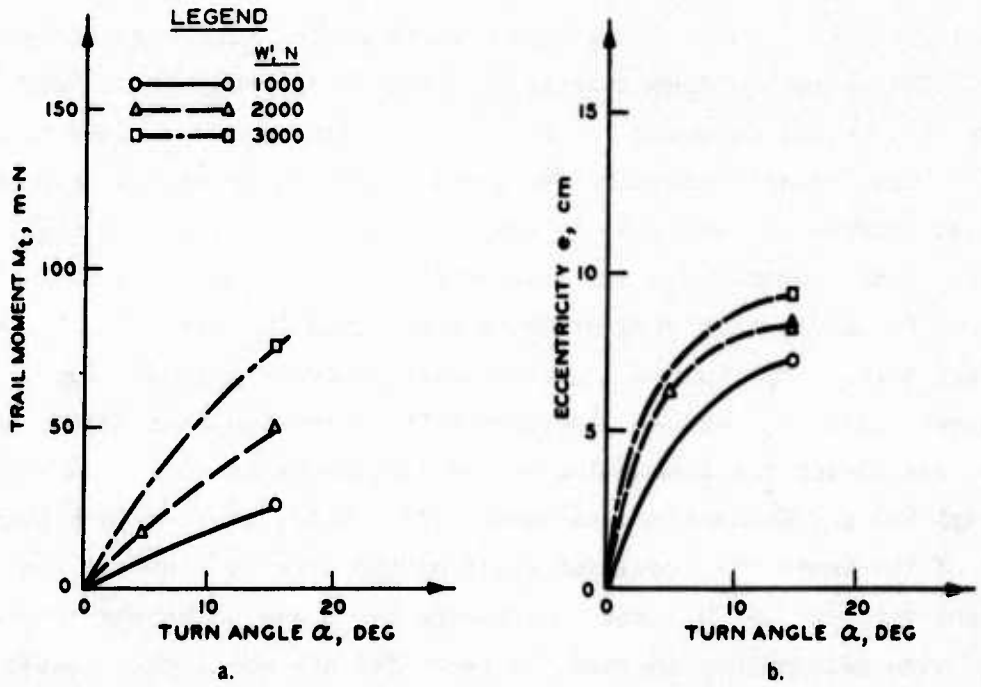

Figure 42. Influence of turn angle and wheel load on trail moment and eccentricity for 6.00-9, 4-PR tire on mortar sand with average penetration resistance gradient $G = 2.6$ MPa/m and tire deflection $\delta/h = 0.15$

to the extent that it was for the tests in clay (paragraphs 53-55) because only limited data were available for this purpose. However, based on that limited information, the same trend can be assumed as was found for clay, but it is not as pronounced, i.e., for a given turn angle, P_T/W would decrease, and S/W and R/W would increase with increasing values of bd, whereas no definite influence would be noticed on the relation between S'/P'_T and α.

Development of prediction system

77. Justification. As in the development of the prediction system for clay (paragraph 56), the trends of the various influences, such as soil strength, deflection, wheel load, and product of tire width and diameter, on the four basic performance parameters seem to justify an attempt to establish relations between performance parameters and the sand mobility number (Equation 2), with turn angle as an additional independent variable (paragraphs 36-38). However, the prediction system to be developed herein will be valid only for the relatively limited range of variables investigated in this pilot study.

78. Before the prediction system itself was extended to include the turn angle, the feasibility of this approach was checked out once more. As in the clay analysis (paragraph 57), four series of tests that had been conducted with the 8.50-10, 8-PR and 7.00-6, 6-PR tires under four loads and two deflections, but on almost the same soil strength (average $G = 3.1$ and 3.0 MPa/m), were investigated. The combinations of the independent variables calculated for each test resulted in sand mobility numbers ranging from 8.7 to 13.1,* with an average of 10.4. The relations among the four basic performance parameters and turn angles, as obtained from the results of these four test series, are shown in Figure 43. Each of four relations in Figure 43 could be described by a single curve, indicating that the sand mobility number (Equation 2) can be used with some justification to represent the independent variables (soil strength, deflection, etc.).

---

* The range resulted from the fact that the individual independent variables could not be kept exactly constant from test to test.

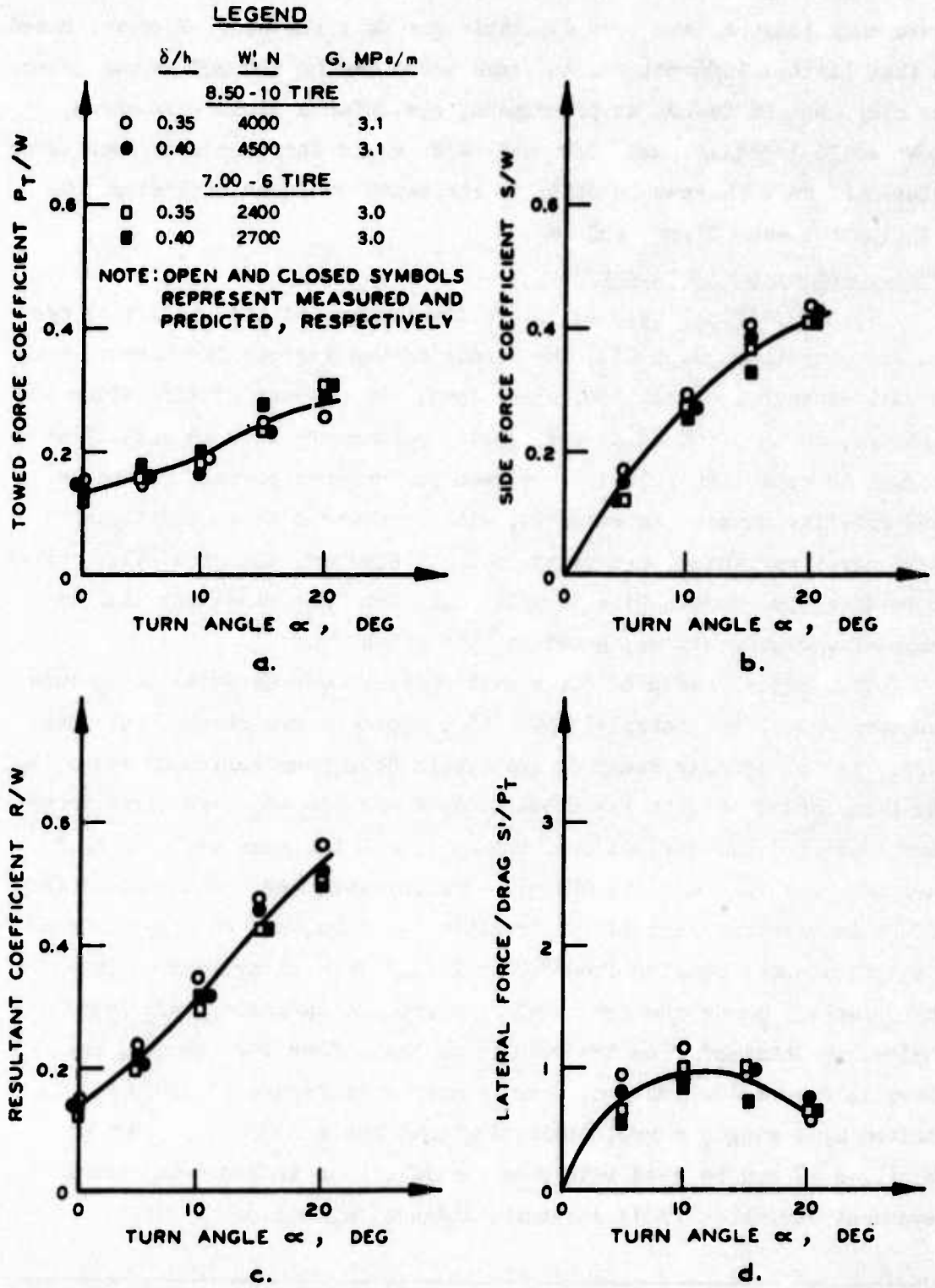

Figure 43. Relations between turn angle and performance parameters for two tires tested at various conditions resulting in average sand mobility number (N_s') of 10.4

79. Modification of soil strength measurements. The original prediction system for zero turn angle was established with results of tests conducted in Yuma sand exclusively (paragraph 18 and Figure 7). Early attempts to use the same system for predicting performance (in terms of P_{20}/W, Figure 7a) of single wheels operating in mortar sand were not successful. The agreement between measured and predicted performance may be acceptable for practical purposes; however, it is not acceptable for research purposes. In an attempt to arrive at a common denominator, at least for the two sands under consideration, relations developed[27,32] between cone penetration resistance gradient G and relative density D_r of the two sands were examined (Figure 44).

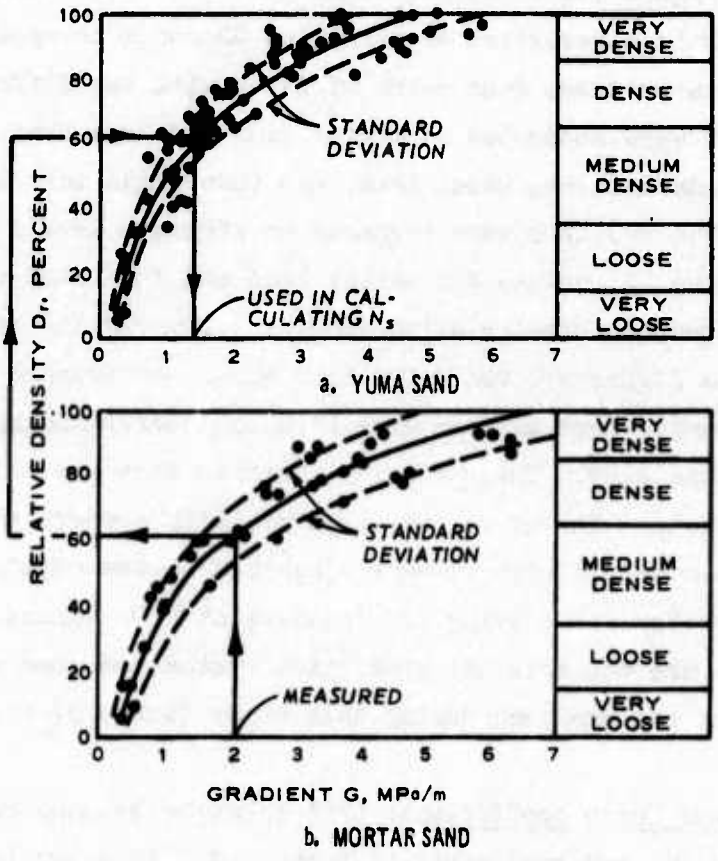

Figure 44. Relation between relative density and penetration resistance gradient[27]

80. To test a hypothesis that the two sands would exhibit similar performance if their relative densities were the same, the G values

for various tests conducted in mortar sand were converted into "equivalent" G values of Yuma sand at the same relative density. For example, in mortar sand a value of G = 2.0 MPa/m corresponds to D_r = 62 percent (Figure 44b); the same relative density in Yuma sand corresponds to G = 1.4 MPa/m (Figure 44a). Thus, G = 2.0 in mortar sand is equivalent to G = 1.4 in Yuma sand. Using these "equivalent" G values in calculating sand mobility numbers to predict performance in mortar sand by means of the Yuma-sand prediction system (Figure 7a) led to satisfactory results.[18,32]

81. Because it appeared to be desirable to maintain the original prediction system developed from towed tests conducted at zero turn angle on Yuma sand (Figure 7), a determination had to be made as to whether or not the technique described in paragraph 80 could be applied in this study. For this purpose, four pairs of tests with two different tires and turn angles were conducted on mortar sand and Yuma sand. For each pair of tests, deflection, wheel load, and turn angle were kept constant; however, the test sections were prepared to strength levels such that the corresponding G values for mortar sand and Yuma sand were different but indicated the same relative density. The results of these tests are depicted in Figure 45, where the four basic performance parameters obtained for mortar sand are compared with the corresponding parameters obtained for Yuma sand. These results indicate that the outlined approach is feasible. Therefore, the sand mobility numbers N_s' calculated for mortar sand (Table 2) were converted to the common mobility number N_s for Yuma sand using the "equivalent" G values. This made it possible to use the original prediction system and some additional tests conducted on Yuma sand during this study (Table 3) for further analysis.

82. Towed force coefficient. The relation between towed force coefficient (P_T/W) and sand mobility number (N_s) is shown in Figure 46a. In contrast to the same situation for clay (Figure 31a), P_T/W is dependent on the turn angle for $\alpha > 10$ deg at a given N_s. For turn angles between 0 and 10 deg, however, use of the relation between P_T/W and N_s that had been developed for $\alpha = 0$ deg (Figure 7d) is

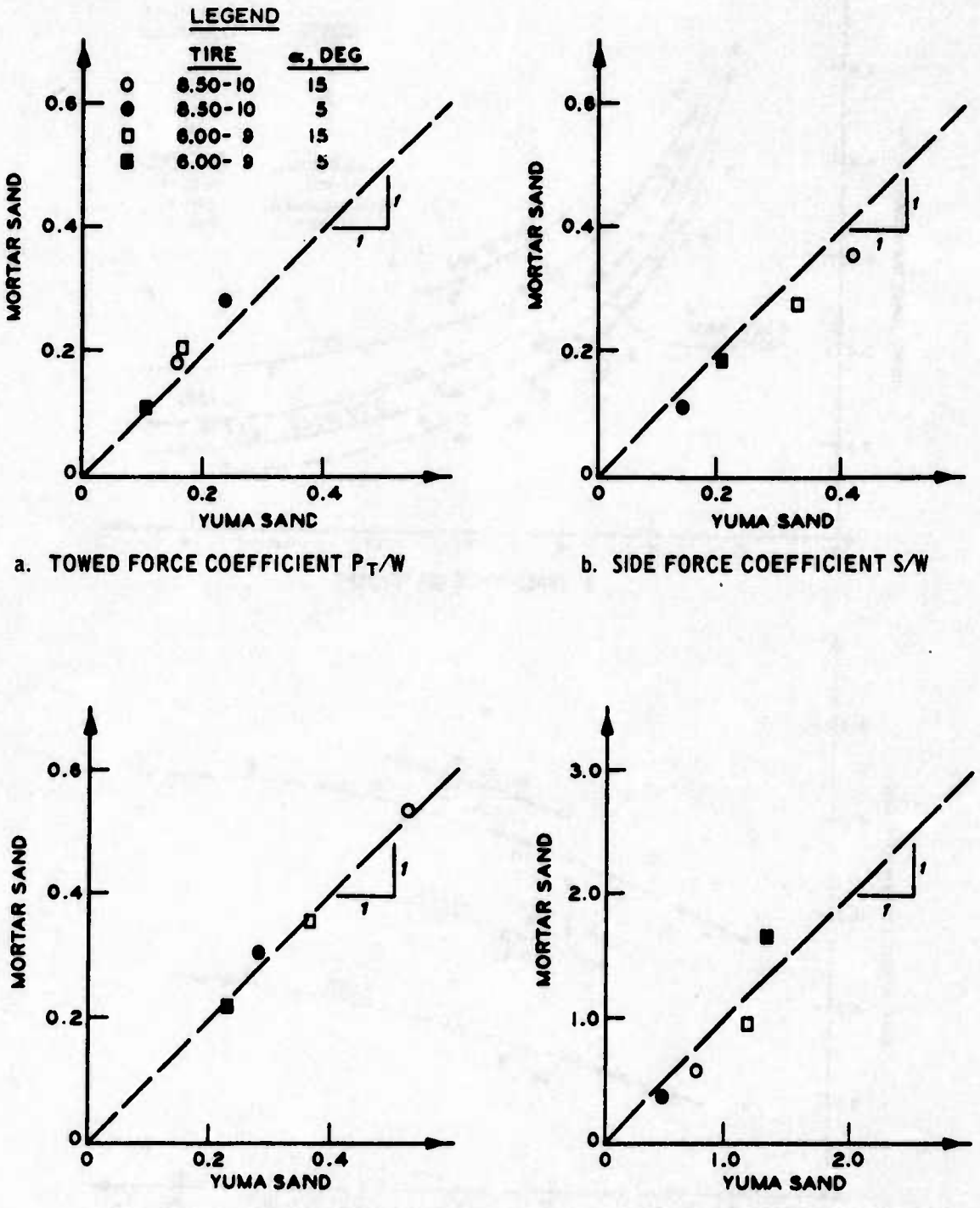

Figure 45. Comparison of performance parameters of 8.50-10, 8-PR and 6.00-9, 6-PR tires operating under similar conditions on Yuma and mortar sands

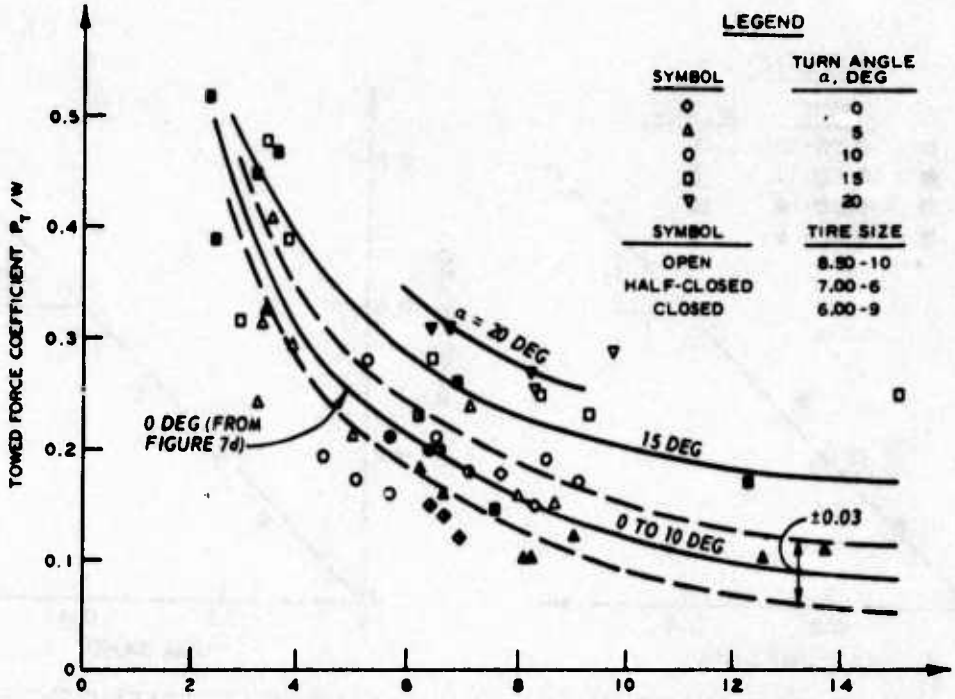

a. TOWED FORCE COEFFICIENT

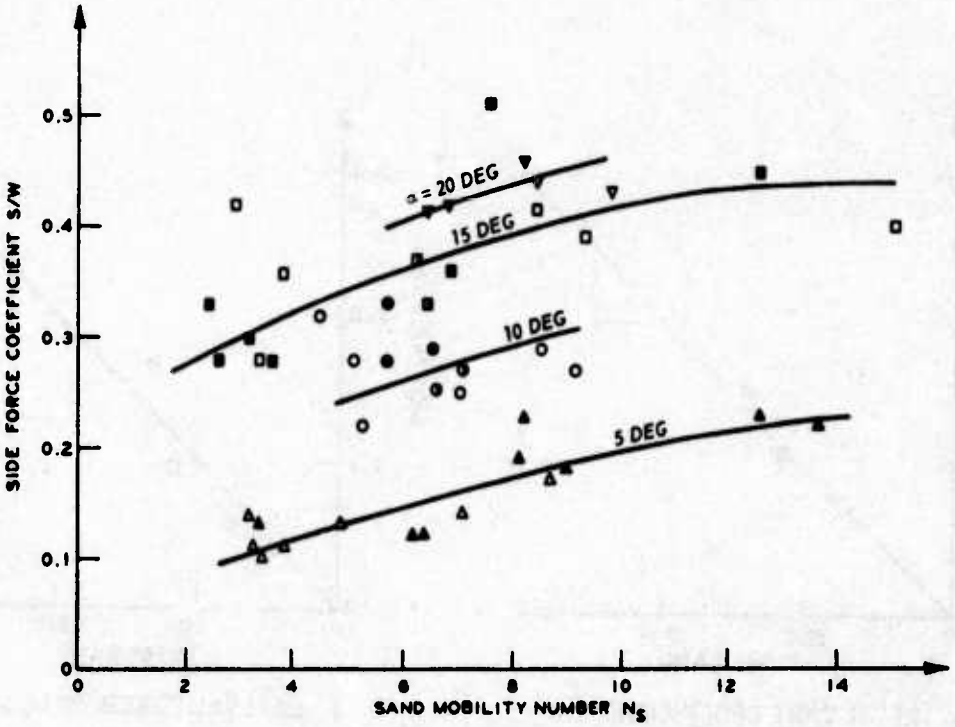

b. SIDE FORCE COEFFICIENT

Figure 46. Performance parameters as functions of sand mobility number and turn angle; three tires (sheet 1 of 3)

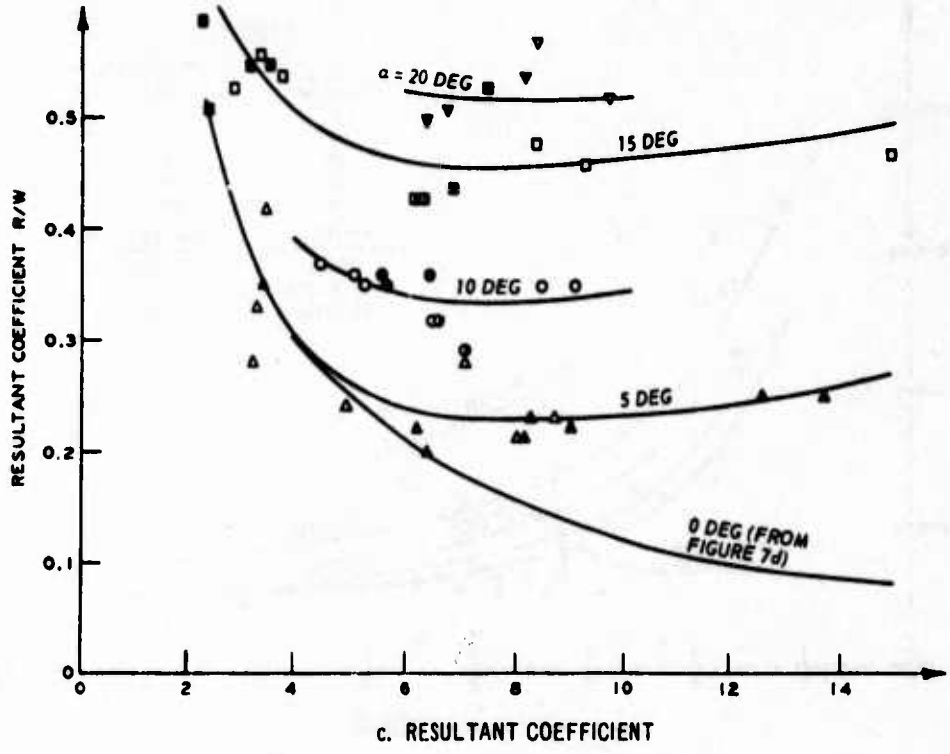

c. RESULTANT COEFFICIENT

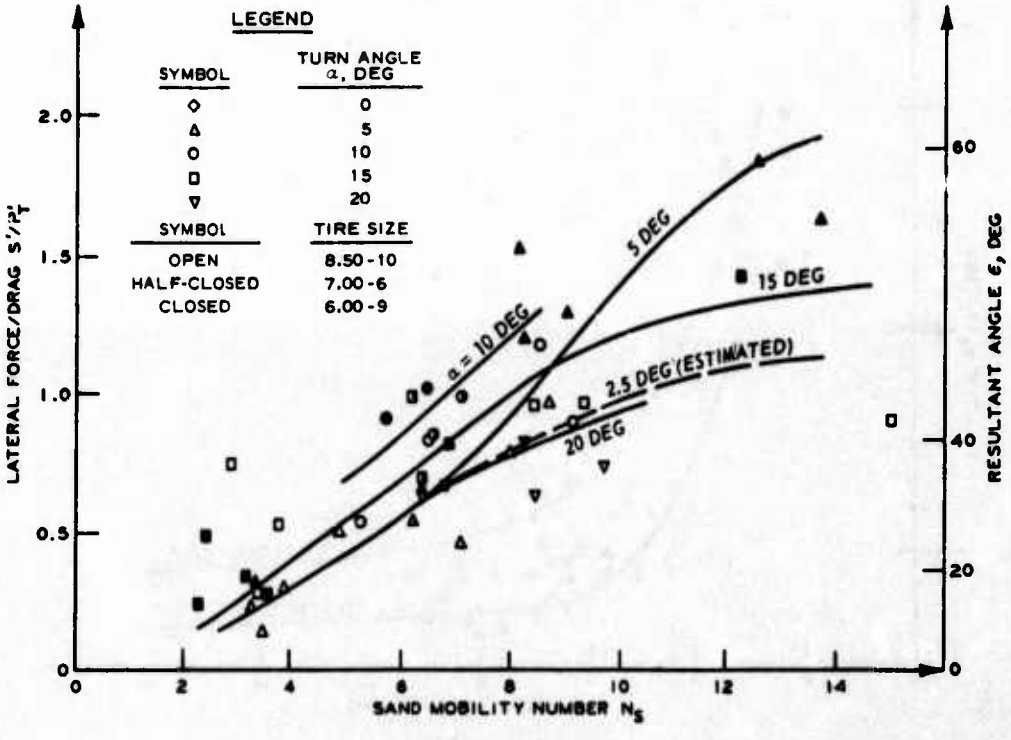

d. LATERAL FORCE/DRAG

Figure 46 (sheet 2 of 3)

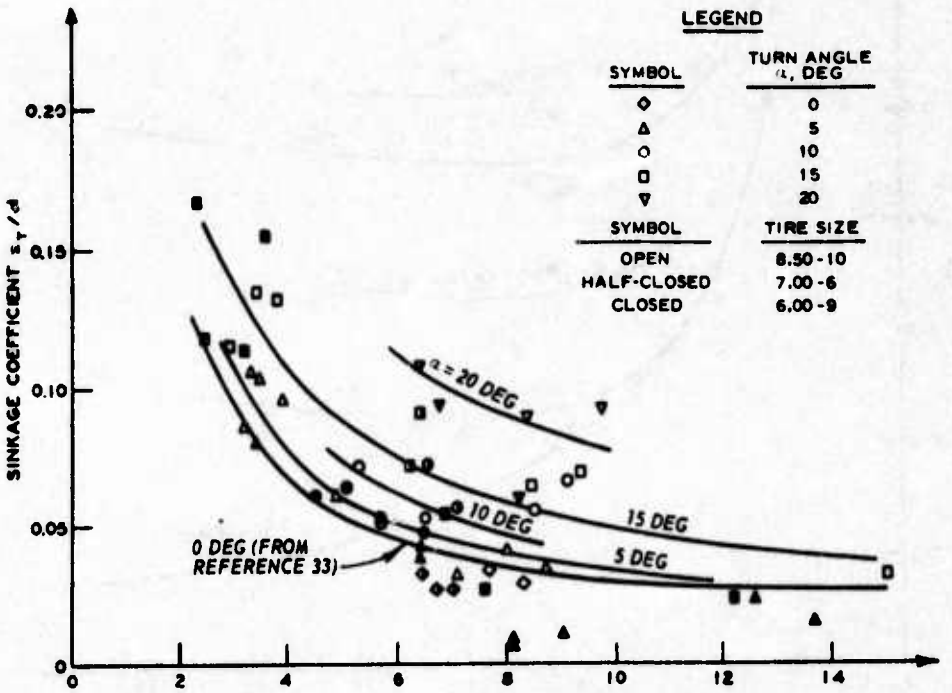

e. SINKAGE COEFFICIENT

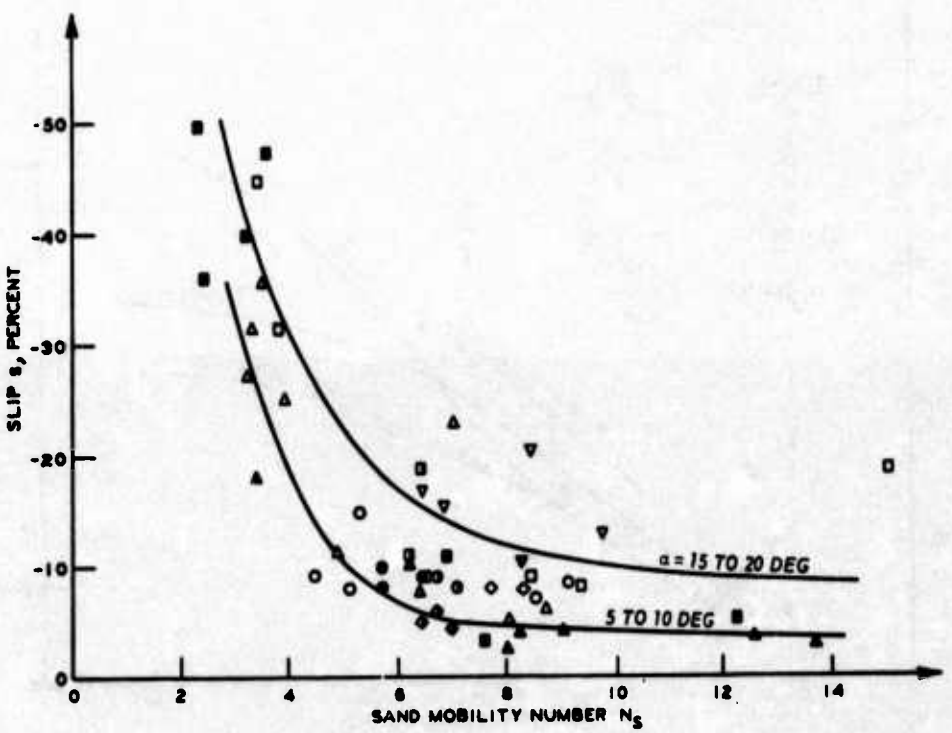

f. SLIP

Figure 46 (sheet 3 of 3)

reasonable, although only about 55 percent of the data points of this study fall within the band of the original data formed by one standard deviation (Figure 46a). Generally, the data scatter is greater in the relations for sand than in corresponding relations for clay, not only in the relation of P_T/W and N_s, but also in the relations discussed in the following paragraphs.

83. Side force coefficient. The relation between side force coefficient (S/W) and N_s shows the expected trend (Figure 46b). For a given N_s, S/W increases with increasing turn angle. For a given turn angle, S/W increases with increasing N_s (because of increasing soil strength). However, in comparison with the same relation obtained for clay (Figure 31b), this increase with N_s is not as pronounced.

84. Resultant coefficient. Resultant coefficient (R/W) as a function of N_s and α is depicted in Figure 46c. This family of curves reflects the individual trends for P_T/W in Figure 46a and for S/W in Figure 46b. For a given α larger than zero, R/W decreases with increasing N_s for N_s values smaller than about 7-8, i.e., in this area P_T/W is the dominant factor, contributing to the magnitude of the resultant coefficient. For larger values of N_s, R/W increases with increasing N_s, reflecting a slightly dominant influence of S/W on R/W. Further, for a given N_s, R/W increases with increasing α.

85. Lateral force/drag. Lateral force/drag (S'/P'_T) and resultant angle (ε), respectively, as functions of N_s and α are shown in Figure 46d. For a given turn angle, S'/P'_T increases with increasing N_s. For a given N_s, S'/P'_T first increases until a maximum is reached and then decreases, reflecting the bell-shaped relation between S'/P'_T and α observed earlier (for example, Figure 34d). However, there seems to exist two zones similar to those found in the relation between R/W and N_s (Figure 46c). That is, for N_s smaller than about 8, the maximum value of S'/P'_T is reached at about $\alpha = 10$ deg, whereas for N_s larger than about 8, this maximum seems to be reached at about $\alpha = 5$ deg. In other words, in the relation between S'/P'_T and α (Figures 33d and 34d), the maximum shifts to the left (with decreasing α) when N_s increases. As in clay (paragraph 61), however, Figure 46d

serves only for demonstration purposes. For an actual prediction, S'/P'_T would be calculated from the relations established for P_T/W and S/W (Figures 46a and 46b; paragraph 33).

86. Sinkage coefficient. Sinkage coefficient (z_T/d) as a function of N_s and α is shown in Figure 46e. As expected, z_T/d decreases for a given turn angle with increasing N_s, and for a given N_s, increases with increasing turn angle. As in the relations for clay (Figure 31e), there is some data scatter, probably for the same reasons as outlined in paragraph 62.

87. Slip. The relation between slip and N_s as a function of α is shown in Figure 46f. Although the data scatter does not allow the establishment of a complete family of curves in 5-deg intervals of the turn angle, the data can at least be grouped into two ranges: α = 5-10 deg, and α = 15-20 deg. Not unexpectedly, slip decreases with increasing N_s (because of increasing soil strength) within a given range of α; for a given N_s, slip increases with increasing α.

88. Summary. Relations were established for the four performance parameters under consideration as functions of the sand mobility number and turn angle. The most important relations are those to determine towed force and side force coefficients (Figures 46a and 46b). They are reasonably accurate and should also be used to calculate the resultant coefficient and lateral force/drag, if necessary. However, if the two latter parameters are to be estimated only, their corresponding relations (Figures 46c and 46d) can be used. Also, relations were developed for estimating sinkage coefficient and slip (Figures 46e and 46f).

Comparison of Side Forces Developed in Clay and in Sand

89. At the present, the performance of single tires operating in clay and in sand cannot be compared directly, for example, on the basis of equal mobility numbers, because of the different ways the various independent variables influence the performance in the two soils. This fact is reflected in the way the variables were arranged (Equations 1 and 2) when the mobility numbers were developed. However, to get at least

a qualitative idea about the difference in the side force coefficients for the two soils, S/W was compared on the following basis. For each soil there exists certain combinations of tire geometry, deflection, wheel load, and soil strength that would create the same towed force coefficients in sand and in clay; for example, at $\alpha = 5$ deg, $N_c = 2.0$ and $N_s = 4.1$ at the same towed force coefficient of 0.3 for clay and sand (Figures 31a and 46a, respectively). With these values for N_c and N_s, the corresponding side force coefficients could be determined from Figures 31b and 46b (S/W = 0.13 for clay; S/W = 0.12 for sand). This means that the side force coefficients are compared on the basis of the tire developing the same towed force coefficient in clay and in sand.

90. The results of this analysis are shown in Figure 47. For

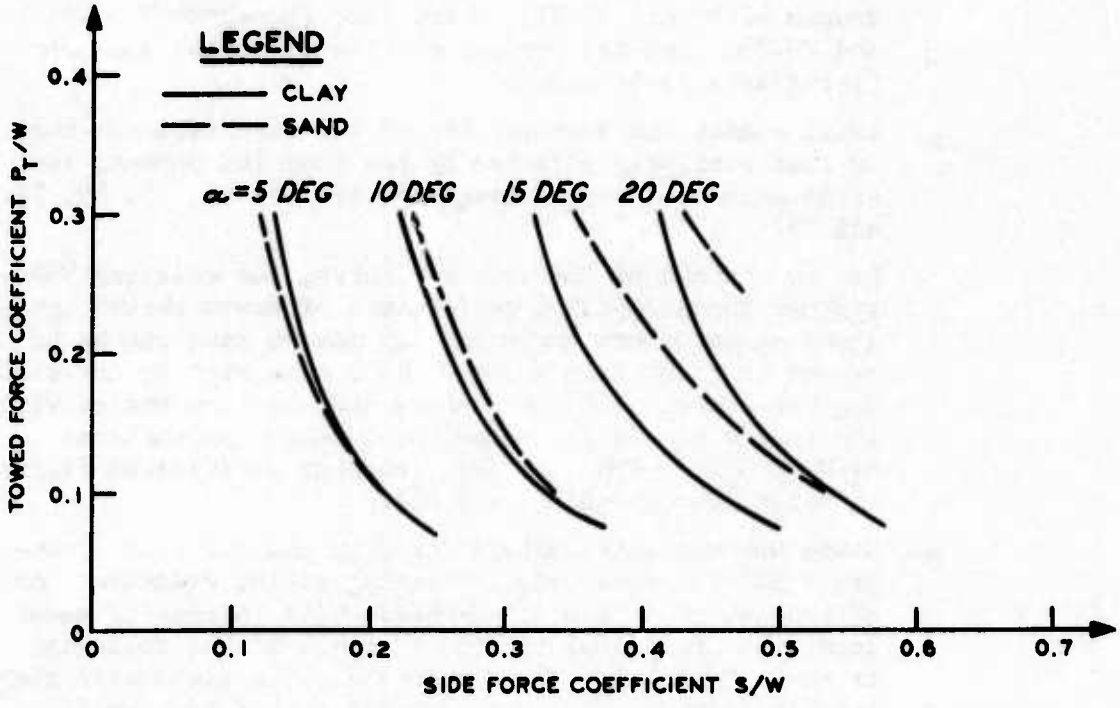

Figure 47. Comparison of side force coefficients in sand and clay for given towed force coefficients and turn angles

turn angles up to about 10 deg, S/W is almost the same in clay and in sand at a given towed force coefficient. For larger turn angles, S/W is smaller in clay than in sand.

PART V: CONCLUSIONS AND RECOMMENDATIONS

Conclusions

91. Based on the analysis of the data obtained during this pilot study, the following conclusions can be drawn with regard to the performance of single towed wheels equipped with pneumatic tires and operating in turned mode:

a. Performance expressed in terms of towed coefficient (P_T/W), side force coefficient (S/W), resultant coefficient (R/W), and lateral force/drag (S'/P_T') is influenced both in clay and in sand by the following independent variables: turn angle (α), soil strength (paragraphs 41-44 and 66-68), tire deflection (paragraphs 46-47 and 70-71), wheel load (paragraphs 49-51 and 73-74), and the product of tire width and diameter (paragraphs 53-54 and 76).

b. Trail moment and eccentricity of the resultant are more or less similarly affected by the same independent variables mentioned in a (paragraphs 45, 48, 52, 55, 69, 72, and 75).

c. For the ranges of the test variables, the existing WES systems for predicting performance of towed wheels operating at zero turn angle on clay and on sand can be extended to treat turn angles larger than zero by correlating the common mobility numbers and the turn angles with the following six individual performance parameters: P_T/W, S/W, R/W, S'/P_T', sinkage coefficient (z_T/d), and slip (paragraphs 64 and 88).

d. Since the mobility numbers for clay and for sand (paragraph 18) increase with increasing width, diameter, and deflection of a tire and decrease with increasing wheel load, the individual relations developed the following trends. For clay, P_T/W decreases with increasing clay mobility number (N_c), but does not show a very well-defined dependency on α (paragraph 58). In sand, P_T/W decreases with increasing sand mobility number N_s, but the influence of α is noticeable, i.e., for a given N_s, P_T/W increases with increasing α (paragraph 82). S/W for clay and sand, however, increases with increasing mobility number for a given α, and also increases with α if the mobility number is kept constant (paragraphs 59 and 83). R/W and S'/P_T' follow either the trend of P_T/W or S/W, depending on which of the two latter parameters has the dominant influence

(paragraphs 60-61 and 84-85). z_T/d and slip follow the same trend for clay and sand as that observed for P_T/W in sand (paragraphs 62-63 and 86-87).

e. For a tire developing the same towed force coefficient in clay as in sand, the side force coefficients are the same for both soil types as long as turn angles are not larger than about 10 deg. For larger turn angles, side force coefficients at a given towed force coefficient are smaller in clay than in sand (paragraphs 89-90).

f. The study fulfilled its major purpose, i.e. to serve as a pilot program. The results are better than expected and leave only few recommendations with regard to further studies with towed wheels operating in turned mode.

Recommendations

92. It is recommended that:

a. A few multipass tests be conducted with the present dynamometer system to cover ranges of variables (in the mobility numbers) not tested in this study (Figures 6 and 7), and to study, at least qualitatively, the influence of multiple passes on wheel performance.

b. The influence of tire width and diameter be investigated to a larger extent than was possible during this study. This, of course, would require the design of a dynamometer system that could accommodate tires of larger dimensions.

c. The pilot study plan to investigate the corresponding performance of powered wheels be implemented.

d. Possibilities be studied for combining the existing prediction systems for purely cohesive and cohesionless soils in such a way that the predictions can be compared and eventually that the combined system can be used for semicohesive c-ϕ soils.

REFERENCES

1. U. S. Army Engineer Waterways Experiment Station, CE, and U. S. Army Tank-Automotive Command, "The AMC '71 Mobility Model," Technical Report No. 11789 (LL 143), Jul 1973, U. S. Army Tank-Automotive Command, Warren, Mich.

2. Close, W. and Murrey, C. L., "A Device for Measuring Mechanical Characteristics of Tyre on the Road," Proceedings, Automobile Division Institute of Mechanical Engineers, 1956-57, p 47.

3. Gough, V. E. and Roberts, G. B., "Dunlop Cornering Force Machine," Transactions of the Institute of Rubber Industry, Vol 33, No. 5, 1957.

4. Edwards, S. G., "Dynamic Measurements of Vehicle Grout Wheel Loads Using a Special Purpose Transducer," General Motors Engineering Journal, Vol 11, No. 4, 1964.

5. Homan, R., Steinheiber, H., and Wittmann, H. J., "Fahrzeugprufstande," ATZ, Vol 70, No. 2, 1968, p 52.

6. American Society for Testing and Materials, "Proposed Standard Model of Test for Traction of Tires in Cornering Without Driving Torque Application Using Highway Vehicles; Draft," 1972 Annual Report of Subcommittee F-9.20 on Dynamic Response, ASTM Committee F-9 on Tires.

7. Grimm, J. L. et al. "The B. F. Goodrich Tire Dynamics Machine," Paper No. 940B presented at the meeting of the Society of Automotive Engineers, 1960.

8. Krempel, G., "Untersuchungen am Kraftfahrzeugreifen," ATZ, Vol 69, No. 1, 1967, p 1.

9. Freman, C. A., "Experimental Determination of the Effect of Traction on Cornering Force," Paper No. 186B presented at the meeting of the Society of Automotive Engineers, 1960.

10. Bekker, M. G., Introduction to Terrain-Vehicle Systems, University of Michigan Press, Ann Arbor, 1969.

11. Kremer, H. and Sohne, W., "Die Seitenfuhrungskrafte starrer richt angetriebener Rader," Grundlagen der Landtechnik, Vol 9, 1957, p 101.

12. Taylor, P. A. and Birthwistle, R., "Experimental Studies of Force Systems on Steered Agricultural Tyres," Proceedings, Institute of Mechanical Engineers, London, Vol 181, Part 2A, 1966-67.

13. Schwanghart, H., "Lateral Forces on Steered Tyres in Loose Soil," Journal of Terramechanics, Vol 5, No. 1, 1968, p 9.

14. Grecenko, A., "Slip and Draft of the Wheel with Tyre on Soft Ground," Proceedings, Third International Conference of the International Society for Terrain-Vehicle Systems, Essen, Vol 2, 1969, p 76.

15. Green, A. J., "Effect of Yaw Angle on Steering Forces for the Lunar Roving Vehicle Wheel," Technical Report M-71-7, Oct 1971, U. S. Army Engineer Waterways Experiment Station, CE, Vicksburg, Miss.

16. Krick, G., "Behavior of Tyres Driven in Soft Ground with Side Slip," Journal of Terramechanics, Vol 9, No. 4, 1973, p 9.

17. Freitag, D. R., "A Dimensional Analysis of the Performance of Pneumatic Tires on Soft Soils," Technical Report No. 3-688, Aug 1965, U. S. Army Engineer Waterways Experiment Station, CE, Vicksburg, Miss.

18. Turnage, G. W., "Performance of Soils Under Tire Loads; Application of Test Results of Tire Selection for Off-Road Vehicles," Technical Report No. 3-666, Report 8, Sep 1972, U. S. Army Engineer Waterways Experiment Station, CE, Vicksburg, Miss.

19. Air Force Flight Dynamics Laboratory, "Turned Tire Tests," Military Interdepartmental Purchase Request No. FY 1456-73-00006, 30 Apr 73, Wright-Patterson Air Force Base, Ohio.

20. Melzer, K.-J., "Performance of the Boeing LRV Wheels in a Lunar Soil Simulant; Effects of Speed, Wheel Load, and Soil," Technical Report M-71-10, Report 2, Dec 1971, U. S. Army Engineer Waterways Experiment Station, CE, Vicksburg, Miss.

21. Turnage, G. W., "Tire Selection and Performance Prediction for Off-Road Wheeled-Vehicle Operations," Fourth International Conference of the International Society for Terrain-Vehicle Systems, Stockholm, Apr 1972, Vol 1, p 61.

22. Smith, M. E., "Performance of Soils Under Tire Loads; An Extended System for Predicting Tire Performance in Fine-Grained Soils," Technical Report No. 3-666, Report 9 (in preparation), U. S. Army Engineer Waterways Experiment Station, CE, Vicksburg, Miss.

23. Melzer, K.-J., "Power Requirements for Wheels Operating in Fine-Grained Soils," Miscellaneous Paper M-73-2, Apr 1973, U. S. Army Engineer Waterways Experiment Station, CE, Vicksburg, Miss.

24. _____, "Power Requirements for Wheels Operating in Sand," Proceedings, International Conference on Prospectives of Agricultural Tractor Development, Warsaw, Sep 1973, Vol I, p 197.

25. McRae, J. L., Powell, C. J., and Wismer, R. D., "Performance of Soils Under Tire Loads; Test Facilities and Techniques," Technical Report No. 3-666, Report 1, Jan 1963, U. S. Army Engineer Waterways Experiment Station, CE, Vicksburg, Miss.

26. Melzer, K.-J., "Use of the WES Cone Penetrometer in Cohesive Soils," paper presented at the European Symposium on Penetration Testing, Stockholm, Jun 1974.

27. _____, "Measuring Soil Properties in Vehicle Mobility Research: Relative Density and Cone Penetration Resistance," Technical Report No. 3-652, Report 4, Jul 1971, U. S. Army Engineer Waterways Experiment Station, CE, Vicksburg, Miss.

28. Smith, M. E., "Performance of Soils Under Tire Loads: Analysis of Tests in Yuma Sand Through August 1962," Technical Report No. 3-666, Report 2, Appendix A, Aug 1965, U. S. Army Engineer Waterways Experiment Station, CE, Vicksburg, Miss.

29. Schultze, E., "Erdstatische Berechnungen," Mitteilungen a.d. Institut f. Verkehrswasserbau, Grundbau und Bodenmechanik, Aachen, No. 40, 1967, p 188.

30. Smith, J. L., "Strength-Moisture-Density Relations of Fine-Grained Soils in Vehicle Mobility Research," Technical Report No. 3-639, Jan 1964, U. S. Army Engineer Waterways Experiment Station, CE, Vicksburg, Miss.

31. Turnage, G. W. and Brown, D. N., "Prediction of Aircraft Ground Performance by Evaluating Ground Vehicle Rut Depths," Miscellaneous Paper M-73-16, Dec 1973, U. S. Army Engineer Waterways Experiment Station, CE, Vicksburg, Miss.

32. Melzer, K.-J., "Relative Density--Three Examples of Its Use in Research and Practice," Proceedings of the Symposium on Evaluation of Relative Density and Its Role in Geotechnical Projects Involving Cohesionless Soils, Los Angeles, Calif., Jun 1972, ASTM Special Technical Publication No. 523, p 463.

33. Turnage, G. W. and Green, A. J., "Performance of Soils Under Tire Loads; Analysis of Tests in Sand from September 1962 Through November 1963," Technical Report No. 3-666, Report 4, Feb 1966, U. S. Army Engineer Waterways Experiment Station, CE, Vicksburg, Miss.

Table 1

Results of Tire Tests on Vicksburg Clay

Test No.	Penetration Resistance C kPa	Carriage Velocity v_a m/sec	Turn Angle α deg	Deflection δ/h	Load W N	Forces Acting on Carriage: Drag P'_T N	Forces Acting on Carriage: Lateral Force S', N	Forces Acting on Wheel: Towed Force P_T, N	Forces Acting on Wheel: Side Force S, N	Forces Acting on Wheel: Resultant, R N	Resultant Angle ε, deg	Eccentricity e, cm	Trail Moment M_t, m-N	Slip s %	Sinkage at Towed Point z_T, cm	Towed Force Coefficient P_T/W	Side Force Coefficient S/W	Resultant Coefficient R/W	Lateral Force/Drag S'/P'_T = tan ε	Sinkage Coefficient at Towed Point z_T/d	Clay Mobility No. N_c
8.50-10, 8-PR Tire																					
A-73																					
-001-3	328	3.1	0	0.35	5888	422	≈0	422	≈0	422	≈0.0	--	≈0	-1.8	1.5	0.07	0.00	0.07	0.00	0.024	3.8
002-3	283	3.0	0	0.35	5828	625	≈0	625	≈0	625	≈0.0	--	≈0	-3.0	2.3	0.11	0.00	0.11	0.00	0.037	3.3
003-3	255	3.0	0	0.40	7034	956	≈0	956	≈0	956	≈0.0	--	≈0	-5.3	3.1	0.14	0.00	0.14	0.00	0.050	2.6
004-3	267	3.0	5	0.40	6806	881	978	793	1044	1314	47.6	-4.8	-51	-4.5	2.7	0.12	0.15	0.19	1.11	0.043	2.8
005-3	262	3.2	10	0.40	6741	1240	1705	942	1870	2079	53.8	-2.9	-54	-6.2	3.4	0.14	0.28	0.31	1.38	0.053	2.8
006-3	287	3.1	15	0.40	6820	1549	2300	899	2606	2758	55.8	-2.3	-60	-4.9	3.8	0.13	0.38	0.40	1.49	0.061	3.0
007-3	286	3.1	20	0.40	6816	1993	2535	1000	3046	3207	51.0	-1.0	-30	-5.0	4.3	0.15	0.45	0.47	1.27	0.069	3.0
008-3	275	3.0	5	0.35	5831	727	1006	635	1063	1240	53.4	-4.2	-45	-6.1	2.9	0.11	0.18	0.21	1.39	0.046	3.2
009-3	269	3.0	10	0.35	5812	934	1612	636	1748	1860	59.9	-1.0	-33	-4.2	2.9	0.11	0.30	0.32	1.73	0 046	3.1
010-3	276	3.1	0	0.35	6861	521	≈0	521	≈0	521	≈0.0	--	≈0	-1.9	1.9	0.09	0.00	0.09	0.00	0.030	3.2
011-3	283	3.2	15	0.35	5856	1304	2359	647	2624	2704	61.0	-1.5	-40	-3.8	3.4	0.11	0.45	0.46	1.81	0.054	3.3
012-3	271	3.0	20	0.35	5815	1750	2523	782	2970	3072	55.2	-1.2	-36	-2.5	4.3	0.13	0.51	0.53	1.44	0.069	3.2
024-3	525	3.0	10	0.35	5866	694	2577	236	2659	2669	74.9	-2.9	-76	-2.1	1.7	0.04	0.45	0.46	3.72	0.027	6.0
025-3	543	2.9	20	0.35	5906	1712	3793	314	4147	4159	65.7	-1.3	-55	-1.0	3.8	0.05	0.70	0.71	2.21	0.061	6.2
026-3	526	2.9	5	0.35	5858	452	1940	307	1682	1710	74.7	-7.8	-132	-1.6	1.6	0.05	0.29	0.29	3.63	0.026	6.1
027-3	361	1.5	10	0.35	5934	779	1764	459	1885	1940	66.3	-2.3	-43	-3.0	2.9	0.08	0.32	0.33	2.27	0.046	4.1
028-3	342	3.1	5	0.35	3006	319	977	233	1004	1030	72.0	-4.8	-48	-1.7	1.4	0.08	0.33	0.34	3.06	0.022	7.6
029-3	345	3.1	15	0.35	3062	854	1963	317	2116	2140	66.5	-0.6	-14	-3.4	2.5	0.10	0.69	0.70	2.30	0.040	7.6
030-3	326	2.5	5	0.15	5823	1144	1032	1050	1122	1537	41.5	+0.5	+6	-8.3	2.7	0.18	0.19	0.26	0.90	0.043	2.5
031-2	356	3.2	15	0.15	5843	1849	2197	1219	2598	2869	49.9	+1.5	+39	-5.4	4.2	0.21	0.44	0.49	1.19	0.067	3.7
032-3	343	3.1	10	0.25	5874	974	1903	629	2044	2138	62.9	+0.3	+7	-1.7	2.9	0.11	0.35	0.36	1.96	0.047	3.4
7.00-6, 6-PR Tire																					
A-73																					
-013-3	487	3.1	0	0.35	5895	421	≈0	421	≈0	421	≈0.0	--	≈0	-2.0	1.7	0.07	0.00	0.07	0.00	0.037	3.2
014-3	487	3.1	5	0.35	5941	513	969	428	1009	1096	62.1	-6.1	-62	-2.3	1.7	0.07	0.17	0.18	1.89	0.037	3.2
015-3	507	3.2	10	0.35	5941	975	1739	657	1886	1997	60.7	-2.8	-52	-3.3	2.6	0.11	0.32	0.34	1.79	0.057	3.3
016-3	488	3.2	15	0.35	5959	1489	2098	893	2405	2566	54.5	-0.5	-11	-6.9	3.2	0.15	0.40	0.43	1.41	0.070	3.2
017-3	487	3.1	20	0.35	5953	1581	2512	770	2916	3017	55.1	-1.8	-53	-2.1	3.2	0.13	0.49	0.51	1.59	0.070	3.2
018-3	498	3.2	20	0.35	6861	1710	2470	633	2915	2983	57.7	-1.7	-49	-1.3	3.5	0.09	0.43	0.44	1.44	0.077	2.9
019-2	506	3.1	0	0.40	6742	418	≈0	418	≈0	418	≈0.0	--	≈0	-1.2	1.9	0.06	0.00	0.06	0.00	0.042	3.1
020-3	481	3.0	5	0.40	6785	563	1004	476	1051	1154	60.5	-9.3	-98	-2.0	1.9	0.07	0.16	0.17	1.78	0.042	3.0
021-3	505	3.1	10	0.40	6710	917	1694	613	1825	1926	61.3	-5.6	-102	-1.7	2.3	0.09	0.27	0.29	1.85	0.050	3.2
022-3	505	3.2	15	0.40	6734	1282	2324	641	2571	2651	60.9	-4.0	-104	-6.1	2.7	0.10	0.38	0.39	1.81	0.059	3.1
023-3	500	3.1	20	0.40	6758	1737	2741	700	3163	3240	57.5	-2.8	-89	0.0	4.1	0.10	0.47	0.48	1.57	0.090	3.1
045-3	339	3.0	15	0.35	2393	511	1311	155	1396	1405	68.7	0.0	0	-2.4	1.8	0.06	0.58	0.59	2.57	0.040	5.4
046-3	352	2.9	10	0.35	5749	1070	1267	832	1442	1665	50.0	-0.6	-8	-3.3	3.1	0.14	0.25	0.29	1.18	0.058	2.4
047-3	394	2.8	10	0.15	2389	312	771	173	821	836	68.1	+2.3	+19	-0.7	1.2	0.07	0.34	0.35	2.47	0.026	5.2
6.00-9, 4-PR Tire																					
A-73																					
-033-3	387	3.0	5	0.35	2027	153	718	90	731	737	78.0	-1.4	-10	-0.9	1.0	0.04	0.36	0.36	4.69	0.019	8.1
034-3	414	2.9	10	0.35	2036	358	1133	156	1178	1189	72.5	0.0	0	-0.7	1.1	0.08	0.58	0.58	3.17	0.020	8.6
035-3	392	3.0	20	0.35	2026	619	1355	119	1483	1488	65.4	+0.9	+13	-3.7	3.0	0.06	0.73	0.73	2.19	0.058	8.2
036-3	360	3.0	5	0.15	2018	163	573	113	584	595	74.1	+0.7	+4	-1.7	1.2	0.06	0.29	0.30	3.51	0.023	5.0
037-3	348	2.9	15	0.15	2015	416	956	154	1030	1042	66.5	+1.7	+18	-1.8	1.2	0.08	0.51	0.52	2.30	0.023	4.8
038-3	349	3.0	10	0.25	1992	283	1025	101	1057	1061	74.6	+1.0	+10	-1.4	0.7	0.05	0.53	0.53	3.63	0.014	6.3
039-3	368	1.5	15	0.15	2004	368	861	132	927	937	66.9	+1.6	+15	-1.4	1.3	0.07	0.46	0.47	2.34	0.025	5.1
040-3	354	3.0	10	0.25	2975	397	1074	204	1129	1147	69.8	+0.8	+9	-3.1	0.7	0.07	0.38	0.39	2.71	0.014	4.3
041-3	351	2.9	5	0.35	3072	253	778	184	796	817	72.0	-3.9	-31	-1.4	0.8	0.06	0.26	0.27	3.08	0.016	4.9
042-3	342	3.0	10	0.25	3974	680	1112	476	1213	1303	58.6	+1.4	+17	-2.8	1.3	0.12	0.31	0.33	1.64	0.030	3.1
043-3	353	2.9	10	0.15	3957	948	1104	741	1256	1458	49.5	+2.3	+29	-2.5	3.3	0.19	0.32	0.37	1.17	0.064	2.5
044-3	321	3.0	10	0.25	1000	157	756	23	773	774	78.3	+2.7	+21	-0.3	0.5	0.02	0.77	0.77	4.81	0.010	11.5

Table 2

Results of Tire Tests on Mortar Sand

Test No.	Penetration Resistance Gradient G, MPa/m	Carriage Velocity V_a m/sec	Turn Angle α deg	Deflection δ/h	Load W N	Forces Acting on Carriage: Drag P'_T N	Forces Acting on Carriage: Lateral Force S', N	Forces Acting on Wheel: Towed Force P_T, N	Forces Acting on Wheel: Side Force S, N	Forces Acting on Wheel: Resultant, R N	Resultant Angle ε, deg	Eccentricity e, cm	Trail Moment M_t m-N	Slip s %	Sinkage at Towed Point z_T, cm	Towed Force Coefficient P_T/W	Side Force Coefficient S/W	Resultant Coefficient R/W	Lateral Force/Drag S'/P'_T = tan ε	Sinkage Coefficient at Towed Point z_T/d	Tested Sand Mobility No. N'_s	Basic Sand Mobility No. N_s
8.50-10, 8-PR Tire																						
A-73																						
-001-2	2.65	3.1	0	0.35	4065	634	≈0	634	≈0	634	≈0.0	--	≈0	-8.2	2.1	0.16	0.00	0.16	0.00	0.034	10.3	7.7
002-2	2.94	3.1	15	0.35	4025	1387	1316	1023	1630	1912	43.9	+6.1	+100	-9.3	3.9	0.25	0.41	0.48	0.96	0.063	11.5	8.4
003-2	2.96	3.1	20	0.35	4078	1983	1209	1464	1808	2315	32.0	+8.6	+156	-20.1	5.6	0.25	0.44	0.57	0.63	0.090	11.4	8.4
004-2	3.08	3.1	5	0.35	4073	650	638	595	699	935	44.2	+1.8	+13	-5.8	2.2	0.15	0.17	0.23	0.97	0.035	11.9	8.7
005-2	3.00	3.2	10	0.35	4083	969	1032	776	1185	1434	46.8	+1.9	+23	-6.8	3.4	0.19	0.29	0.35	1.17	0.055	11.6	8.5
006-2	2.91	3.1	0	0.40	4551	689	≈0	689	≈0	689	≈0.0	--	≈0	-8.2	1.8	0.15	0.00	0.15	0.00	0.029	11.5	8.3
007-2	2.77	3.1	5	0.40	4539	767	597	712	663	973	37.9	-2.0	-13	-5.1	2.5	0.16	0.15	0.21	0.78	0.040	11.0	8.0
008-2	3.18	3.2	10	0.40	4544	1164	1055	940	1241	1572	42.0	+1.3	+16	-8.7	4.1	0.17	0.27	0.35	0.90	0.066	12.6	9.1
009-2	3.20	3.1	15	0.40	4530	1476	1437	1055	1767	2084	44.1	+3.6	+63	-8.3	4.3	0.23	0.39	0.46	0.97	0.069	12.7	9.3
010-2	3.33	3.1	20	0.40	4589	1915	1428	1314	1992	2389	36.6	+5.2	+104	-13.2	5.7	0.29	0.43	0.52	0.74	0.092	13.1	9.7
022-2	2.39	1.6	10	0.35	4068	1006	824	846	991	1303	39.5	+3.0	+30	-9.0	3.2	0.21	0.25	0.32	0.83	0.052	9.2	6.5
023-2	2.65	3.1	15	0.35	2001	697	637	510	790	940	42.2	+6.4	+51	-19.0	2.0	0.25	0.40	0.47	0.91	0.032	20.9	15.0
024-2	2.55	3.0	5	0.35	5847	1281	624	1221	731	1424	25.9	+1.5	+11	-11.4	3.7	0.21	0.13	0.24	0.49	0.060	6.9	4.9
025-2	2.83	2.9	5	0.15	3934	1633	237	1606	377	1650	8.2	+7.4	+28	-35.7	6.4	0.41	0.10	0.42	0.14	0.103	4.8	3.5
026-2	2.73	3.0	15	0.15	4002	2146	583	1920	1126	2225	15.4	+8.9	+100	-45.2	8.4	0.48	0.28	0.56	0.28	0.135	4.6	3.4
027-2	2.65	3.0	10	0.25	4038	1252	658	1118	871	1417	27.9	+6.4	+56	-15.3	4.4	0.28	0.22	0.35	0.53	0.071	7.4	5.3
028-2	1.45	3.0	5	0.35	4041	1203	356	1167	460	1254	16.5	+3.7	+17	-25.0	5.9	0.29	0.11	0.31	0.30	0.095	5.7	3.9
029-2	1.34	3.0	15	0.35	3991	1895	959	1571	1457	2143	27.8	+7.2	+105	-31.5	8.2	0.39	0.36	0.54	0.53	0.132	5.3	3.8
030-2	1.26	1.5	5	0.35	4022	1267	331	1234	440	1310	14.6	+4.1	+18	-31.6	6.6	0.31	0.11	0.33	0.26	0.106	4.9	3.3
031-2	1.29	3.0	5	0.35	1994	501	228	479	274	552	24.7	+6.9	+19	-22.9	2.0	0.24	0.14	0.28	0.46	0.032	10.2	7.1
7.00-6, 6-PR Tire																						
A-73																						
-011-2	3.25	3.2	0	0.35	2745	404	≈0	404	≈0	404	≈0.0	--	≈0	-5.3	1.5	0.15	0.00	0.15	0.00	0.033	8.9	6.4
012-2	2.94	3.1	0	0.40	2772	397	≈0	397	≈0	397	≈0.0	--	≈0	-5.8	1.2	0.14	0.00	0.14	0.00	0.027	9.1	6.7
013-2	3.15	3.1	0	0.35	2455	301	≈0	201	≈0	301	≈0.0	--	≈0	-4.2	1.2	0.12	0.00	0.12	0.00	0.027	9.6	7.0
014-2	2.90	3.2	5	0.35	2474	417	272	393	308	499	33.0	-0.2	-1	-7.2	1.7	0.16	0.12	0.20	0.65	0.038	8.8	6.4
015-2	3.22	3.2	10	0.35	2476	562	558	456	655	719	44.8	+0.9	+6	-7.9	2.5	0.18	0.27	0.29	0.99	0.056	9.7	7.1
016-2	2.79	3.2	15	0.35	2463	752	726	555	900	1048	44.9	+2.3	+21	-11.2	3.2	0.23	0.37	0.43	0.99	0.071	8.4	6.2
017-2	3.11	3.2	20	0.35	2459	1038	708	752	1020	1259	34.2	+3.7	+38	-15.4	4.2	0.31	0.41	0.51	0.67	0.094	9.4	6.8
018-2	2.76	3.1	5	0.40	2743	534	282	513	333	605	28.0	-1.8	-6	-9.9	1.9	0.18	0.12	0.22	0.53	0.042	8.6	6.2
019-2	2.80	3.2	20	0.40	2773	1174	754	848	1112	1399	32.6	+3.9	+43	-17.1	4.8	0.31	0.41	0.50	0.63	0.107	8.7	6.4
020-2	2.93	3.1	10	0.40	2797	683	581	571	692	909	40.5	≈0	≈0	-8.8	3.2	0.20	0.25	0.32	0.85	0.071	9.0	6.6
021-2	2.80	3.1	15	0.40	2758	970	679	762	908	1187	34.9	+7.8	+25	-13.9	4.1	0.28	0.33	0.43	0.69	0.091	8.7	6.4
6.00-9, 4-PR Tire																						
A-73																						
-032-2	3.04	2.8	5	0.35	2005	267	345	236	364	434	52.1	+4.1	+15	-4.1	0.5	0.12	0.18	0.22	1.29	0.010	12.4	9.0
033-2	2.25	3.0	10	0.35	2010	504	512	408	585	713	45.1	+4.4	+26	-9.1	2.4	0.20	0.29	0.36	1.02	0.047	9.2	6.5
034-2	2.58	3.0	20	0.35	2009	827	682	543	926	1073	39.6	+6.5	+60	-10.6	3.1	0.27	0.46	0.54	0.83	0.060	11.5	8.2
035-2	2.65	3.0	5	0.15	1995	660	207	640	260	691	17.1	+6.2	+16	-17.9	3.9	0.32	0.13	0.35	0.31	0.079	4.7	3.4
036-2	2.47	3.0	15	0.15	1974	1721	348	897	600	1079	18.8	+8.3	+50	-39.7	5.9	0.45	0.30	0.55	0.34	0.114	4.4	3.2
037-2	2.69	3.0	10	0.25	2016	513	472	422	559	700	42.9	+4.6	+26	-8.0	2.7	0.21	0.28	0.35	0.93	0.052	7.9	5.7
038-2	2.74	1.5	15	0.15	1970	1037	293	926	550	1077	15.7	+8.4	+46	-47.6	8.0	0.47	0.28	0.55	0.28	0.155	4.9	3.6
039-2	2.73	3.0	15	0.15	2958	1693	427	1531	829	1741	13.4	+9.2	+76	-50.0	8.6	0.58	0.28	0.59	0.24	0.167	3.2	2.3
040-2	2.78	3.0	15	0.15	1023	351	281	265	364	451	38.9	+7.2	+26	-10.8	2.8	0.26	0.36	0.44	0.81	0.054	9.6	6.9
041-2	4.61	3.0	5	0.35	2022	262	426	224	446	499	58.3	+1.6	+7	-3.2	0.7	0.11	0.22	0.25	1.63	0.014	18.8	13.7
042-2	4.22	3.0	15	0.35	2032	564	799	341	907	969	54.4	+5.0	+45	-5.4	1.2	0.17	0.45	0.48	1.42	0.023	17.1	12.3
043-2	4.22	1.5	5	0.35	2002	232	427	193	460	499	62.2	+1.1	+5	-3.6	0.2	0.10	0.23	0.25	1.84	0.023	17.4	12.6
044-2	4.13	3.1	5	0.35	3064	351	533	302	570	645	57.1	+0.7	+4	-2.7	0.3	0.10	0.19	0.21	1.52	0.006	11.1	8.1

Table 3

Results of Tire Tests in Yuma Sand

Test No.	Penetration Resistance Gradient, G MPa/m	Carriage Velocity v_a m/sec	Turn Angle α deg	Deflection δ/h	Load, W N	Forces Acting on Carriage: Drag P'_T, N	Forces Acting on Carriage: Lateral Force S', N	Forces Acting on Wheel: Towed Force P_T, N	Forces Acting on Wheel: Side Force S, N	Forces Acting on Wheel: Resultant, R N	Resultant Angle ε, deg
					8.50-10, 8-PR Tire						
A-73											
-003-1	0.74	3.0	15	0.35	4073	1735	1304	1338	1711	2172	37.0
004-1	0.82	1.5	5	0.35	4028	1015	479	970	565	1122	25.2
005-1	1.17	1.5	10	0.35	4067	972	1138	759	1294	1500	49.6
006-1	1.33	1.5	10	0.35	4055	908	1154	694	1292	1467	51.8
					6.00-9, 4-PR Tire						
007-1	1.32	1.5	15	0.15	1976	915	438	771	658	1014	25.5
008-1	1.43	2.8	10	0.35	2057	451	620	338	680	759	53.6
009-1	1.87	1.5	15	0.35	2043	564	932	304	1046	1089	58.8
010-1	2.01	1.5	5	0.35	2014	233	398	199	414	459	59.5

Eccentricity e, cm	Trail Moment, M_t m-N	Slip, S %	Sinkage at Towed Point z_T, cm	Towed Force Coefficient P_T/W	Side Force Coefficient S/W	Resultant Coefficient R/W	Lateral Force/Drag $S'/P'_T = \tan \varepsilon$	Sinkage Coefficient at Towed Point z_T/d	Sand Mobility No. N_s
				8.50-10, 8-PR Tire					
+6.4	+109	-23.3	7.3	0.33	0.42	0.53	0.75	0.116	2.9
+3.5	+20	-27.0	5.3	0.24	0.14	0.28	0.47	0.085	3.2
+3.1	+40	-9.2	3.8	0.19	0.32	0.37	1.17	0.061	4.5
+2.9	+37	-8.7	3.9	0.17	0.28	0.36	1.27	0.063	5.1
				6.00-9, 4-PR Tire					
+7.8	+51	-36.2	6.1	0.39	0.33	0.51	0.48	0.118	2.4
+2.8	+19	-9.8	2.6	0.16	0.33	0.37	1.38	0.050	5.7
+3.1	+33	-3.2	1.4	0.15	0.51	0.53	1.65	0.027	7.6
+0.5	+2	-4.2	0.4	0.10	0.21	0.23	1.70	0.008	8.2

Table 4

Tire Data

Design Load, W' N	Deflection δ/h	Unloaded Section Height h , m	Unloaded Width b , m	Unloaded Diameter d , m	Unloaded Inflation Pressure kPa
		8.50-10, 8-PR			
4500	0.40	0.158	0.204	0.621	34.4
6700	0.40	0.161	0.204	0.627	75.8
6900	0.40	0.161	0.204	0.627	76.5
2000	0.35	0.158	0.203	0.625	8.3
2700	0.35	0.159	0.204	0.624	17.2
4000	0.35	0.158	0.204	0.621	37.1
5800	0.35	0.161	0.204	0.627	77.1
4000	0.25	0.162	0.200	0.629	93.0
5800	0.25	0.164	0.208	0.634	150.0
4000	0.15	0.167	0.200	0.633	200.0
5800	0.15	0.165	0.204	0.636	321.0
		7.00-6, 6-PR			
2700	0.40	0.129	0.171	0.449	42.0
6700	0.40	0.133	0.172	0.457	167.0
2400	0.35	0.129	0.171	0.449	44.1
2700	0.35	0.129	0.172	0.449	58.2
5800	0.35	0.133	0.172	0.457	166.0
6700	0.35	0.134	0.173	0.459	193.0
2400	0.15	0.137	0.172	0.466	276.0
		6.00-9, 4-PR			
2000	0.35	0.128	0.159	0.516	28.9
3000	0.35	0.128	0.159	0.516	56.5
1000	0.25	0.128	0.159	0.516	14.5
2000	0.25	0.128	0.159	0.516	57.2
3000	0.25	0.128	0.159	0.516	100.0
4000	0.25	0.128	0.160	0.516	144.5
1000	0.15	0.128	0.159	0.516	52.7
2000	0.15	0.128	0.160	0.516	133.5
3000	0.15	0.128	0.160	0.516	191.5
4000	0.15	0.128	0.163	0.516	281.0

APPENDIX A: NOTATION

b	Tire section width, unloaded
c	Cohesion
C	Cone penetration resistance
C_u	Uniformity coefficient = d_{60}/d_{10}
d	Tire diameter, unloaded
d_{10}	Grain size diameter at 10 percent finer by weight
d_{60}	Grain size diameter at 60 percent finer by weight
D_r	Relative density = $\left[(e_{max} - e_n)/(e_{max} - e_{min})\right] \times 100$
e	Eccentricity of resultant
e_{max}	Void ratio of cohesionless soil in loosest state
e_{min}	Void ratio of cohesionless soil in densest state
e_n	Void ratio of soil in natural state
G	Cone penetration resistance gradient
h	Tire section height, unloaded
ℓ	Length of tire contact area
LL	Liquid limit of cohesive soil
M	Torque input to the axle
M_t	Trail moment
M_{20}	Torque at 20 percent slip
M/Wr_a	Torque coefficient
M_{20}/Wr_a	Torque coefficient at 20 percent slip
N_c	Clay mobility number
N_s	Basic sand mobility number
N'_s	Sand mobility number from tests with mortar sand
P	Net pull
P_T	Towed force acting in plane of wheel
P'_T	Drag acting in direction of travel
P_T/W	Towed force coefficient
P_{20}	Pull at 20 percent slip
P_{20}/W	Pull coefficient at 20 percent slip
PI	Plasticity index of cohesive soil = LL - PL
PL	Plastic limit of cohesive soil

P/W	Pull coefficient
r	Undeflected radius of tire
r_a	Active radius of tire = $r - 0.5$
R	Resultant of force acting in plane perpendicular to the plane of a wheel = $\sqrt{S^2 + P_T^2} = \sqrt{(S')^2 + (P_T')^2}$
R/W	Resultant coefficient
s	Wheel slip = $\left[(v_w - v_a \cos \alpha)/v_w\right] \times 100$
S	Side force acting perpendicular to plane of wheel
S'	Lateral force acting on carriage system perpendicular to direction of travel
S_c	Side force per unit length of tire contact area due to cohesion
S/W	Side force coefficient
S'/P_T'	Lateral force/drag
v_a	Actual translational velocity of carriage system or vehicle
v_w	Peripheral velocity of wheel
W	Actual wheel load measured during a test
W'	Design wheel load
z	Wheel sinkage
z_T	Sinkage at towed point
z_T/d	Sinkage coefficient at towed point
z_{20}	Sinkage at 20 percent slip
z_{20}/d	Sinkage coefficient at 20 percent slip
z/d	Sinkage coefficient
α	Turn angle
δ	Difference between unloaded and loaded tire section heights
δ/h	Tire deflection
ϵ	Resultant angle, formed by direction of travel and direction of resultant
λ_p	Passive earth pressure coefficient

In accordance with ER 70-2-3, paragraph 6c(1)(b), dated 15 February 1973, a facsimile catalog card in Library of Congress format is reproduced below.

Melzer, Klaus-Jurgen
Performance of towed wheels operating in turned mode on soft soils--a pilot study, by Klaus-J. Melzer. Vicksburg, U. S. Army Engineer Waterways Experiment Station, 1976.
1 v. (various pagings) illus. 27 cm. (U. S. Waterways Experiment Station. Miscellaneous paper M-76-17)
Prepared for U. S. Army Materiel Development and Readiness Command, Alexandria, Virginia, under Project 1T062103A046, Task 03.
Includes bibliography.

1. Clays. 2. One-pass performance. 3. Pneumatic tires. 4. Sands. 5. Towed wheels. 6. Traffic tests. 7. Wheels. I. U. S. Army Materiel Development and Readiness Command. (Series: U. S. Waterways Experiment Station, Vicksburg, Miss. Miscellaneous paper M-76-17)
TA7.W34m no.M-76-17